

**SYNTHESIS, CHARACTERIZATION AND EVALUATION OF
NEW PIPERAZINIUM / DIPIPERIDIUM DICATIONIC -
BASED MOLTEN SALTS AND IONIC LIQUIDS AS
CATALYSTS FOR SOME ORGANIC REACTIONS**

LIA ZAHARANI

INSTITUTE FOR ADVANCED STUDIES

UNIVERSITI MALAYA

KUALA LUMPUR

2021

**SYNTHESIS, CHARACTERIZATION AND
EVALUATION OF NEW PIPERAZINIUM /
DIPIPERIDINIUM DICATIONIC - BASED MOLTEN
SALTS AND IONIC LIQUIDS AS CATALYSTS FOR
SOME ORGANIC REACTIONS**

LIA ZAHARANI

**DISSERTATION SUBMITTED IN FULFILMENT OF THE
REQUIREMENTS FOR THE DEGREE OF MASTER OF
PHILOSOPHY**

INSTITUTE FOR ADVANCED STUDIES

UNIVERSITI MALAYA

KUALA LUMPUR

2021

UNIVERSITI MALAYA
ORIGINAL LITERARY WORK DECLARATION

Name of Candidate: LIA ZAHARANI

Matric No: 17221385/1

Name of Degree: Master of Philosophy

Title of Dissertation: Synthesis, characterization and evaluation of new Piperazinium / Dipiperidinium Dicationic - based molten salts and ionic liquids as catalysts for some organic reactions

Field of Study:

I do solemnly and sincerely declare that:

- (1) I am the sole author/writer of this Work;
- (2) This Work is original;
- (3) Any use of any work in which copyright exists was done by way of fair dealing and for permitted purposes and any excerpt or extract from, or reference to or reproduction of any copyright work has been disclosed expressly and sufficiently and the title of the Work and its authorship have been acknowledged in this Work;
- (4) I do not have any actual knowledge nor do I ought reasonably to know that the making of this work constitutes an infringement of any copyright work;
- (5) I hereby assign all and every right in the copyright to this Work to the University of Malaya ("UM"), who henceforth shall be owner of the copyright in this Work and that any reproduction or use in any form or by any means whatsoever is prohibited without the written consent of UM having been first had and obtained;
- (6) I am fully aware that if in the course of making this work I have infringed any copyright whether intentionally or otherwise, I may be subject to legal action or any other action as may be determined by UM.

Candidate's Signature

Date:

Subscribed and solemnly declared before,

Witness's Signature

Date:

Name:

Designation:

ABSTRACT

The new ionic liquids and molten salts including 4,4'-trimethylene-*N,N'*-dipiperidinium sulfate $[\text{TMDPH}_2]^{2+}[\text{SO}_4]^{2-}$, 4,4'-trimethylene-*N,N'*-dipiperidinium chlorosulfonate $[\text{TMDPH}_2]^{2+}2[\text{ClSO}_3]^-$, 1*H*,4*H*-piperazine-dium dichlorosulfonate $[\text{PZH}_2]^{2+}2[\text{ClSO}_3]^-$ were designed and synthesized. The chemical structure elucidation of these ionic liquids and molten salts was performed by 1D NMR, FTIR, and mass spectra. Then, the correct structure was elucidated by COSY experiment and Raman spectroscopy. Some physical properties, thermal behavior, and thermal stability of these ionic liquids and molten salts were determined and reported. The formation of a two-protonic acid salt namely 4,4'-trimethylene-*N,N'*-dipiperidinium sulfate $[\text{TMDPH}_2]^{2+}[\text{SO}_4]^{2-}$, instead of namely 4,4'-trimethylene-*N,N'*-dipiperidinium hydrogensulfate was evidenced by NMR analyses. The catalytic of this ionic liquid was demonstrated in the esterification reaction of *n*-butanol and glacial acetic acid under different conditions. The desired acetate was obtained in 62-88% yield without using a Dean-stark apparatus under optimal conditions. α -Tocopherol (α -TCP), a highly efficient form of vitamin E, was also treated with glacial acetic acid in the presence of the ionic liquid, and *O*-acetyl- α -tocopherol (Ac-TCP) was obtained in 88.4% yield. The formation of 4,4'-trimethylene-*N,N'*-dipiperidinium chlorosulfonate $[\text{TMDPH}_2]^{2+}2[\text{ClSO}_3]^-$ and 1*H*,4*H*-piperazine-dium dichlorosulfonate $[\text{PZH}_2]^{2+}2[\text{ClSO}_3]^-$ was indicated that the chlorosulfonic acid could not act as a sulfonating agent in the reaction with secondary amines like 4,4'-Trimethylenedipiperidine (TMDP) and Piperazine (PZ) probably due to more steric hindrance of the sulfur atom by chlorine and oxygen atoms. Then, the dual solvent-catalyst activity of these ionic liquids was demonstrated for the synthesis of novel triazole-pyrimidines through a one-pot three-component reaction under mild conditions. The arene diazonium saccharin derivatives were initially produced from various

substituted aromatic amines; subsequently, these intermediates were treated with a greener organic iodide for the preparation of the aryl iodide. The arene diazonium saccharin intermediates could be stored in the liquid phase in a refrigerator for a long time with no significant loss activity. The ionic liquids were retrieved and reused several times without reducing their catalytic efficiency.

Universiti Malaya

ABSTRAK

Cecair ionik baru dan garam cair termasuk 4,4'-trimethylene-*N,N'*-dipiperidinium sulfat [TMDPH₂]²⁺[SO₄]²⁻, 4,4'-trimethylene-*N,N'*-dipiperidinium chlorosulfonat [TMDPH₂]²⁺2[ClSO₃]⁻, 1*H,4H*-piperazine-dium dichlorosulfonat [PZH₂]²⁺2[ClSO₃]⁻ dirancang dan disintesis. Penjelasan struktur kimia cecair ionik dan garam lebur ini dilakukan oleh 1D NMR, FTIR, Raman, dan mass spektrum. Kemudian struktur yang betul dijelaskan oleh COZY dan Raman spektrum. Sebilangan sifat fizikal, kelakuan terma, dan kestabilan terma cecair ionik dan garam cair ini ditentukan dan dilaporkan. Pembentukan garam asid dua-proton iaitu 4,4'-trimethylene-*N,N'*-dipiperidinium sulfat [TMDPH₂]²⁺[SO₄]²⁻, bukannya 4,4'-trimethylene-*N,N'*-dipiperidinium hidrogensulfat dibuktikan oleh analisis NMR. Pemangkin cecair ionik ini ditunjukkan dalam reaksi esterifikasi *n*-butanol dan asid asetik glasial dalam keadaan yang berbeza. Asetat yang dikehendaki diperoleh dalam hasil 62-88% tanpa menggunakan alat Dean-stark dalam keadaan optimum. α -Tocopherol (α -TCP), bentuk vitamin E yang sangat efisien, juga dirawat dengan asid asetik glasial dengan adanya cecair ionik, dan *O*-asetil- α -tokoferol (Ac-TCP) diperoleh pada 88,4% hasil. Pembentukan 4,4'-trimethylene-*N,N'*-dipiperidinium chlorosulfonat [TMDPH₂]²⁺2[ClSO₃]⁻ dan 1*H,4H*-piperazine-dium dichlorosulfonat [PZH₂]²⁺ 2[ClSO₃]⁻ menunjukkan bahawa asid klorosulfonik tidak dapat bertindak sebagai agen sulfonating dalam tindak balas dengan amina sekunder seperti 4,4'-Trimethylenedipiperidine (TMDP) dan Piperazine (PZ) mungkin disebabkan oleh penghambatan atom sulfur yang lebih sterik oleh atom klorin dan oksigen. Kemudian, aktiviti pemangkin pelarut ganda dari cecair ionik ini ditunjukkan untuk sintesis triazole-pyrimidin baru melalui reaksi tiga komponen satu periuk dalam keadaan ringan. Derivatif arena diazonium sakarin pada mulanya dihasilkan dari pelbagai amina aromatik yang diganti; seterusnya, perantara ini dirawat dengan iodida organik yang

lebih hijau untuk penyediaan aril iodida. Pengantara arena diazonium sakarin dapat disimpan dalam fasa cecair di dalam peti sejuk untuk waktu yang lama tanpa aktiviti kehilangan yang ketara. Cecair ionik diambil dan digunakan semula beberapa kali tanpa mengurangkan kecekapan pemangkinnya.

Universiti Malaya

ACKNOWLEDGEMENTS

First of all, I would like to express my deepest appreciation to my supervisor, Prof. Mohd Rafie Johan, Dr. Nader Ghaffari Khaligh and Dr. Nor Aliya Hamizi for giving me the valuable opportunity to conduct this research. Their continuing guidance and advice throughout this research are indeed valuable to me.

My heartfelt thanks go to all my friends who have worked with me in Nano Engineering Group Laboratory, Nanotechnology & Catalysis Research Centre, Institute for Advanced Studies, for their support in completing my lab work.

Last but not least, my sincere appreciation goes to my family for their endless prayers and supports in order for me to achieve my goals. To my mother, Muslimah, my father, Ridwan Daud, and my sisters, Putri Maliza, Khairunnisa and Silvia Fadillah, I love you all so much and thank you for your support.

TABLE OF CONTENTS

Page		
Original Literary Work Declaration		ii
Abstract		iii
<i>Abstrak</i>		v
Acknowledgements		vii
Table of Contents		viii
List of Figures		xiv
List of Tables		xix
List of Symbols and Abbreviations		xx
CHAPTER 1	GENERAL INTRODUCTION	
1.1	Background	1
1.2	Problem Statement	5
1.3	Research Objectives	5
1.4	Scope of Thesis	6
CHAPTER 2	LITERATURE REVIEW	
2.1	Catalysis	7
2.2	Structure-Activity Relationship (SAR)	8
2.3	Principles of Green Chemistry	9
2.4	Ionic liquid and Molten	10
2.5	The Simple Process of Synthesis	11
2.6	The Advantages of The Presence Strategy and Methodology of These New Molten and Ionic Liquid Catalysts	12

2.7	Designing Organic Transformation in The New Molten and Ionic Liquid Catalysts	12
2.7.1	Heterocyclic	13
2.7.2	Knoevenagel's Condensation	13
2.7.3	Esterification and Transesterification	14
CHAPTER 3 ARTICLE 1		
3.1	Introduction	16
3.2	Methodology	18
3.2.1	Material and Method	18
3.2.2	The synthesis of 1 <i>H</i> ,4 <i>H</i> -piperazine-diiium dichlorosulfonate [PZH ₂] ²⁺ 2[ClSO ₃] ⁻ in the solid- or liquid-state	19
3.2.3	1 <i>H</i> ,4 <i>H</i> -piperazine-diiium dichlorosulfonate in the liquid-state	19
3.2.4	1 <i>H</i> ,4 <i>H</i> -piperazine-diiium dichlorosulfonate in the solid-state	20
3.3	Results and Discussion	21
3.4.1	Synthesis of 1 <i>H</i> ,4 <i>H</i> -piperazine-diiium dichlorosulfonate [PZH ₂] ²⁺ 2[ClSO ₃] ⁻	21
3.4.2	1D and 2D NMR Spectra of 1 <i>H</i> ,4 <i>H</i> -piperazine-diiium dichlorosulfonate	21
3.4.3	FTIR spectrum of the 1 <i>H</i> ,4 <i>H</i> -piperazine-diiium dichlorosulfonate	23
3.4.4	Raman spectrum of the 1 <i>H</i> ,4 <i>H</i> -piperazine-diiium dichlorosulfonate	25
3.4.5	The physical properties of 1 <i>H</i> ,4 <i>H</i> -piperazine-diiium dichlorosulfonate	27

3.4.6	The thermal behavior of 1 <i>H</i> ,4 <i>H</i> -piperazine-dium dichlorosulfonate	28
3.5	Conclusion	30
CHAPTER 4 ARTICLE 2		
4.1	Introduction	31
4.2	Methodology	33
4.2.1	Typical procedure for the synthesis of 2-amino-4-aryl-7,7-demethyl-5-oxo-5,6,7,8-tetrahydro-4 <i>H</i> -chromene-3-carbonitrie (2a-j)	33
4.2.2	Ethyl 5-amino-7-(4-chlorophenyl)-4,7-dihydro-[1,2,4]triazolo[1,5- α] pyrimidine -6-carboxylate (2a)	33
4.2.3	Ethyl 5-amino-7-(4-bromophenyl)-4,7-dihydro-[1,2,4]triazolo[1,5- α]pyrimidine -6-carboxylate (2b)	33
4.2.4	Ethyl 5-amino-7-(4-nitrophenyl)-4,7-dihydro-[1,2,4]triazolo[1,5- α] pyrimidine -6-carboxylate (2c)	34
4.2.5	Ethyl 5-amino-7-(2-nitrophenyl)-4,7-dihydro-[1,2,4]triazolo[1,5- α] pyrimidine -6-carboxylate (2d)	34
4.2.6	Ethyl 5-amino-7-(4-methoxyphenyl)-4,7-dihydro-[1,2,4]triazolo[1,5- α] pyrimidine-6-carboxylate (2e)	34
4.2.7	Ethyl 5-amino-7-(2-methoxyphenyl)-4,7-dihydro-[1,2,4]triazolo[1,5- α] pyrimidine-6-carboxylate (2f)	35
4.2.8	Ethyl 5-amino-7-(3,4-dimethoxyphenyl)-4,7-dihydro-[1,2,4]triazolo[1,5- α]pyrimidine-6-carboxylate (2g)	35
4.2.9	Ethyl 5-amino-7-(2,4,6-trimethoxyphenyl)-4,7-dihydro-[1,2,4]triazolo[1,5- α]- pyrimidine-6-carboxylate (2h)	35

4.2.10	Ethyl 5-amino-7-(3,4,5-trimethoxyphenyl)-4,7-dihydro-[1,2,4]triazolo[1,5- α]-pyrimidine-6-carboxylate (2i)	36
4.2.11	Ethyl 5-amino-7-(4-(dimethylamino)phenyl)-4,7-dihydro-[1,2,4]triazolo[1,5- α]-pyrimidine-6-carboxylate (2j)	36
4.3	Results and Discussion	36
4.3.1	Dual Solvent-Catalyst Activity of the New IL	36
4.3.2	Easy Separation and Recyclability of the New IL	41
4.4	Conclusion	42
CHAPTER 5 ARTICLE 3		
5.1	Introduction	44
5.2	Methodology	46
5.2.1	Material and Method	46
5.2.2	The synthesis of 4,4'-trimethylene- <i>N,N'</i> -dipiperidinium dichlorosulfonate [TMDPH ₂] ²⁺ 2[ClSO ₃] ⁻	46
5.2.3	The typical procedure for the synthesis of 2-amino-4-aryl-7,7-dimethyl-5-oxo-5,6,7,8-tetrahydro-4H-chromene-3-carbonitrile (2a-j)	46
5.2.4	Physical and spectra data of new dihydro-[1,2,4]triazolo[1,5- α]pyrimidines	47
5.3	Results and Discussion	50
5.3.1	More characterization and correction of the chemical structure	50
5.3.2	Synthesis of 3-amino-1,2,4-triazole using [TMDPH ₂] ²⁺ 2[ClSO ₃] ⁻ as dual solvent-catalyst	55
5.3.3	Easy separation and recyclability of [TMDPH ₂] ²⁺ 2[ClSO ₃] ⁻	59

5.4	Conclusion	60
CHAPTER 6 ARTICLE 4		
6.1	Introduction	61
6.2	Methodology	63
6.2.1	Material and Method	63
6.2.2	Synthesis of [TMDPH ₂] ²⁺ [SO ₄] ²⁻	63
6.2.3	Typical Esterification Procedure	63
6.2.4	Esterification of α-TCP with Glacial Acetic Acid	64
6.3	Results and Discussion	64
6.3.1	Synthesis and the Structure Elucidation of New Ionic Liquid	64
6.3.2	Physical Properties of [TMDPH ₂] ²⁺ [SO ₄] ²⁻	70
6.3.3	Thermal Behaviour of [TMDPH ₂] ²⁺ [SO ₄] ²⁻	70
6.3.4	Esterification of Alcohols and Glacial Acetic Acid Using [TMDPH ₂] ²⁺ [SO ₄] ²⁻ as a Catalyst	73
6.4	Conclusion	80
CHAPTER 7 ARTICLE 5		
7.1	Introduction	81
7.2	Methodology	82
7.2.1	Material and Method	82
7.2.2	Typical procedure for the synthesis of aryl iodide	82
7.3	Results and Discussion	88
7.4	Conclusion	91

CHAPTER 8 CONCLUSION	92
Reference	95
List of Publications	102
Appendixes	104

Universiti Malaya

LIST OF FIGURES

Figure	Caption	Page
3.1	The chemical structure of protonated anti-benzonorbornenol (1^+)	17
3.2	The image of <i>1H,4H</i> -piperazine-dium dichlorosulfonate in the liquid-state	20
3.3	The image of <i>1H,4H</i> -piperazine-dium dichlorosulfonate in the solid-state	20
3.4	Synthesis of <i>1H,4H</i> -piperazine-dium dichlorosulfonate $[PZH_2]^{2+}2[ClSO_3]^-$	21
3.5	Two possible of <i>1H,4H</i> -piperazine-dium dichlorosulfonate $[PZH_2]^{2+}2[ClSO_3]^-$	22
3.6	The FTIR of <i>1H,4H</i> -piperazine-dium dichlorosulfonate $[PZH_2]^{2+}2[ClSO_3]^-$ in liquid state	24
3.7	The Raman of <i>1H,4H</i> -piperazine-dium dichlorosulfonate $[PZH_2]^{2+}2[ClSO_3]^-$ in liquid-state	25
3.8	The Raman of <i>1H,4H</i> -piperazine-dium dichlorosulfonate $[PZH_2]^{2+}2[ClSO_3]^-$ in solid-state	26
3.9	The DSC of <i>1H,4H</i> -piperazine-dium dichlorosulfonate $[PZH_2]^{2+}2[ClSO_3]^-$	29
3.10	The TGA/DTA of <i>1H,4H</i> -piperazine-dium dichlorosulfonate $[PZH_2]^{2+}2[ClSO_3]^-$	30
4.3	Synthesis of 5-amino-7-aryl-4,7-dihydro-[1,2,4]triazolo[1,5- α]pyrimidine-6-carboxylates under optimized reaction conditions.	38
4.4	A schematic reaction mechanism of the synthesis of triazolo[1,5- α]pyrimidines in the presence of $[PZH_2]^{2+}2[ClSO_3]^-$	41
4.5	Catalytic efficiency of recycled $[PZH_2]^{2+}2[ClSO_3]^-$	42
5.1	Two possible structure of new low-viscous ionic liquid.	51
5.2	Illustrated $^1H,^1H$ -COSY correlation in the 4,4'-trimethylene- <i>N,N'</i> -dipiperidinium chlorosulfonate $[TMDPH_2]^{2+}2[ClSO_3]^-$ and $[TMDP(SO_3H)_2]^{2+} 2Cl^-$	53

5.3	The FTIR spectrum of $[\text{TMDPH}_2]^{2+}2[\text{ClSO}_3]^-$	54
5.4	The Raman spectrum of $[\text{TMDPH}_2]^{2+}2[\text{ClSO}_3]^-$	55
5.5	Synthesis of 5-amino-7-(4-chlorophenyl)-4,7-dihydro--[1,2,4]triazole[1,5-a]pyrimidine-6-carboxylate under optimized reaction conditions	57
5.6	Catalytic efficiency of the recycled $[\text{TMDPH}_2]^{2+}[\text{ClSO}_3]^{2-}$	59
6.1	The proposed chemical structures for the new ionic liquid	65
6.2	The image of 4,4'-trimethylene- <i>N,N'</i> -dipiperidine sulfate	65
6.3	FTIR of new ionic liquid (neat)	69
6.4	DSC of new ionic liquid at nitrogen atmosphere	71
6.5	TGA/DTA of new ionic liquid at nitrogen atmosphere	72
6.6	Esterification of various alcohols and glacial acetic acid in the presence of $[\text{TMDPH}_2]^{2+}[\text{SO}_4]^{2-}$	75
6.7	A schematic reaction mechanism of the esterification in the presence of $[\text{TMDPH}_2]^{2+}[\text{SO}_4]^{2-}$	78
6.8	Esterification of α -tocopherol (α -TCP) with glacial acetic acid using $[\text{TMDPH}_2]^{2+}[\text{SO}_4]^{2-}$	79
7.1	The proposed mechanisms for the preparation of aryl iodides using TBN and saccharine	82
7.2	Preparation of aryl iodides using TBN = saccharine, and TEAI	88
A1	^1H NMR spectrum of piperazine in DMSO-d_6	104
A2	^{13}C NMR spectrum of piperazine in DMSO-d_6	104
A3	^1H NMR spectrum of $[\text{PZH}_2]^{2+}2[\text{ClSO}_3]^-$ in liquid state	105
A4	^1H NMR spectrum of $[\text{PZH}_2]^{2+}2[\text{ClSO}_3]^-$ in solid state	105

A5	^{13}C NMR spectrum of $[\text{PZH}_2]^{2+}2[\text{ClSO}_3]^-$ in liquid state	106
A6	^{13}C NMR spectrum of $[\text{PZH}_2]^{2+}2[\text{ClSO}_3]^-$ in solid state	106
A7	^1H NMR spectrum of $[\text{PZH}_2]^{2+}2[\text{ClSO}_3]^-$ liquid-state in DMSO-d_6	107
A8	^1H NMR spectrum of $[\text{PZH}_2]^{2+}2[\text{ClSO}_3]^-$ in D_2O	107
A9	^{13}C NMR spectrum of $[\text{PZH}_2]^{2+}2[\text{ClSO}_3]^-$ in D_2O	108
A10	$^1\text{H}, ^1\text{H}$ -COSY of $[\text{PZH}_2]^{2+}2[\text{ClSO}_3]^-$ in solid-state	108
A.11	$^1\text{N}, ^{13}\text{C}$ -HMBC of $[\text{PZH}_2]^{2+}2[\text{ClSO}_3]^-$ in solid-state.	109
A.12	$^1\text{H}, ^{15}\text{N}$ -HMBC spectra of $[\text{PZH}_2]^{2+}2[\text{ClSO}_3]^-$ in solid-state	109
A.13	^1H NMR and ^{13}C NMR spectrum of Ethyl 5-amino-7-(4-chlorophenyl)-4,7-dihydro-[1,2,4]triazolo[1,5- α] pyrimidine -6-carboxylate (2a)	110
A.14	^1H NMR and ^{13}C NMR spectrum of Ethyl 5-amino-7-(4-bromophenyl)-4,7-dihydro-[1,2,4]triazolo[1,5- α]pyrimidine -6-carboxylate (2b)	111
A.15	^1H NMR and ^{13}C NMR spectrum of Ethyl 5-amino-7-(4-nitrophenyl)-4,7-dihydro-[1,2,4]triazolo[1,5- α] pyrimidine -6-carboxylate (2c)	112
A.16	^1H NMR and ^{13}C NMR spectrum of Ethyl 5-amino-7-(2-nitrophenyl)-4,7-dihydro-[1,2,4]triazolo[1,5- α] pyrimidine -6-carboxylate (2d)	113
A.17	^1H NMR and ^{13}C NMR spectrum of Ethyl 5-amino-7-(4-methoxyphenyl)-4,7-dihydro-[1,2,4]triazolo[1,5- α] pyrimidine-6-carboxylate (2e)	114
A.18	^1H NMR and ^{13}C NMR spectrum of Ethyl 5-amino-7-(2-methoxyphenyl)-4,7-dihydro-[1,2,4]triazolo[1,5- α] pyrimidine-6-carboxylate (2f)	115
A.19	^1H NMR and ^{13}C NMR spectrum of Ethyl 5-amino-7-(3,4-dimethoxyphenyl)-4,7-dihydro-[1,2,4]triazolo[1,5- α]pyrimidine-6-carboxylate (2g)	116
A.20	^1H NMR and ^{13}C NMR spectrum of Ethyl 5-amino-7-(2,4,6-trimethoxyphenyl)-4,7-dihydro-[1,2,4]triazolo[1,5- α] pyrimidine-6-carboxylate (2h)	117

A.21	^1H NMR and ^{13}C NMR spectrum of Ethyl 5-amino-7-(3,4,5-trimethoxyphenyl)-4,7-dihydro-[1,2,4]triazolo[1,5-a]-pyrimidine-6-carboxylate (2i)	118
A.22	^1H NMR and ^{13}C NMR spectrum of Ethyl 5-amino-7-(4-(dimethylamino)phenyl)-4,7-dihydro-[1,2,4]triazolo[1,5-a]-pyrimidine-6-carboxylate (2j)	119
A.33	The ^1H spectrum of $[\text{TMDPH}_2]^{2+}2[\text{ClSO}_3]^-$ in DMSO-d_6	120
A.34	The ^1H and spectrum of $[\text{TMDPH}_2]^{2+}2[\text{ClSO}_3]^-$ in D_2O	120
A.35	The ^1H , ^1H -COSY spectrum of $[\text{TMDPH}_2]^{2+}2[\text{ClSO}_3]^-$	121
A.36	^1H NMR spectrum of new ionic liquid in DMSO-d_6	121
A.37	^1H NMR spectrum of new ionic liquid in D_2O	122
A.38	^{13}C NMR spectrum of new ionic liquid in DMSO-d_6 .	122
A.39	^{13}C NMR spectrum of new ionic liquid in D_2O	123
A.40	^1H , ^1H -COSY spectrum of new ionic liquid	123
A.41	ESI mass spectra of $[\text{TMDPH}_2]^{2+}[\text{SO}_4]^{2-}$ in positive ion (A) and negative ion (B) modes	124
A.42	^1H NMR spectra copies of the aryl iodides (400 MHz, CDCl_3), Iodobenzene (3a)	124
A.43	^1H NMR spectra copies of the aryl iodides (400 MHz, CDCl_3), <i>I-Iodo-4-methoxybenzene</i> (3b)	125
A.44	^1H NMR spectra copies of the aryl iodides (400 MHz, CDCl_3), <i>I-Iodo-4-methylbenzene</i> (3c)	125
A.45	^1H NMR spectra copies of the aryl iodides (400 MHz, CDCl_3), <i>1,3-Dimethyl-2-iodobenzene</i> (3d)	126
A.46	^1H NMR spectra copies of the aryl iodides (400 MHz, CDCl_3), <i>1,3-Diethyl-2-iodobenzene</i> (3e)	126
A.47	^1H NMR spectra copies of the aryl iodides (400 MHz, CDCl_3), <i>1,3-diiodopropyl-2-iodobenzene</i> (3f)	127

A.48	¹ H NMR spectra copies of the aryl iodides (400 MHz, CDCl ₃), <i>I-Chloro-4-iodobenzene (3g)</i>	127
A.49	¹ H NMR spectra copies of the aryl iodides (400 MHz, CDCl ₃), <i>I-Chloro-2-iodobenzene (3h)</i>	128
A.50	¹ H NMR spectra copies of the aryl iodides (400 MHz, CDCl ₃), <i>I-Bromo-4-iodobenzene (3i)</i>	128
A.51	¹ H NMR spectra copies of the aryl iodides (400 MHz, CDCl ₃), <i>I-Iodo-4-nitrobenzene (3j)</i>	129
A.52	¹ H NMR spectra copies of the aryl iodides (400 MHz, CDCl ₃), <i>I-Iodo-2-nitrobenzene (3k)</i>	129
A.53	¹ H NMR spectra copies of the aryl iodides (400 MHz, CDCl ₃), <i>4-(4-iodophenyl)morpholine (3l)</i>	130

LIST OF TABLES

Table	Caption	Page
3.1	Our results of the IR and Raman spectra of the ClSO_3^- anion together with the previous reports	27
4.1	Optimisation of the synthesis of ethyl 5-amino-7-(4-chlorophenyl)-4,7-dihydro-[1,2,4]triazolo[1,5-a]pyrimidine-6-carboxylate	37
5.1	The structure data $[\text{PZH}_2]^{2+}2[\text{ClSO}_3]^-$ in $\text{DMSO}-d_6$	52
5.2	The assignment of the symmetric and asymmetric vibrations of the chlorosulfonate anion	54
5.3	Optimization of the synthesis of ethyl 5-amino-7-(4-chlorophenyl)-4,7-dihydro--[1,2,4]triazole[1,5-a]pyrimidine-6-carboxylate	56
5.4	The one-pot multicomponent synthesis of triazolo [1,5-a]pyrimidines in the presence of $[\text{PZH}_2]^{2+}2[\text{ClSO}_3]^-$ under optimized reaction conditions	58
6.1	The 1D NMR spectrum data of $[\text{TMDPH}_2]^{2+}[\text{SO}_4]^{2-}$ in $\text{DMSO}-d_6$ and D_2O	66
6.2	The calculated LC-ESI-MS data	70
6.3	Optimization of the esterification of <i>n</i> -butanol and glacial acetic acid	74
6.4	Esterification of various alcohols and glacial acetic acid in the presence of $[\text{TMDPH}_2]^{2+}[\text{SO}_4]^{2-}$ under optimized reaction conditions	77
6.5	Catalytic efficiency of five ionic liquid catalysts for the esterification of <i>n</i> -butanol and glacial acetic acid	80
7.1	Some reported reagents and methods for the diazotization-iodination of 2-nitro aniline 1k	84
7.2	Synthesis of aryl iodides through in situ formation of the arene diaonium saccharin intermediates	89

Symbols and Abbreviations	Phrase
σ	conductivity
α -TCP	α -tocopherol
$[\text{PZH}_2]^{2+}2[\text{ClSO}_3]^-$	1 <i>H</i> ,4 <i>H</i> -piperazine-dium dichlorosulfonate
$[\text{TMDPH}_2]^{2+}2[\text{ClSO}_3]^-$	4,4'-trimethylene- <i>N,N'</i> -dipiperidinium chlorosulfonate
$[\text{TMDPH}_2]^{2+}[\text{SO}_4]^{2-}$	4,4'-trimethylene- <i>N,N'</i> -dipiperidinium sulfate
Ac-TCP	O-acetyl- α -tocopherol
CH_2Cl_2	Dichloromethane
CH_3CN	Acetonitrile
CH_2	Methylene
COSY	Correlation Spectroscopy
D_2O	Water deuterium
DMA	<i>N,N</i> -dimethylacetamide
DMAP	(4-dimethylamino)pyridine
DSC	Differential Scanning Calorimeter
DTA	differential thermal analysis
EtOAc	Ethyl Acetate
FTIR	Fourier-transform infrared spectroscopy
GC-MS	Gas Chromatography-Mass Spectrometry
H_2O	Water
H_{eq}	Equatorial hydrogens
H_{ax}	Axial hydrogens
HMBC	Heteronuclear Multiple Bond Correlation
IL	Ionic Liquid

KF	Karl Fisher
LC-ESI-MS	Liquid Chromatography Electrospray ionization- mass spectrometry
LCMS	Liquid Chromatography Mass spectra
NH ₂	Amine
N ₂	Nitrogen
N-H	Natrium Hydrogen
NMR	nuclear magnetic resonance
pK _a	Acid Dissociation Constant
pK _b	Base Dissociation Constant
PZ	Piperazine
Sac-H	Saccharin
S-Cl	Sulfur Chloride
S-O	Sulfur Oxide
SAR	Structure-Activity Relationship
SO ₂	Sulfur dioxide
<i>t</i> -BuOH	tert-Butyl Alcohol
TEAI	Tetraethylammonium Chloride
TGA	thermo gravimetric analysis
TLC	Thin Layer Chromatography
TMDP	4,4'-trimethylenedipiperidine

CHAPTER ONE

GENERAL INTRODUCTION

1.1 Background

Most industrial scales and academic reactions are still strongly reliant on the catalysis process because they use catalysis for all reactions. Catalytic processes will surely play a decisive role in industrial and academic reactions as they provide green and clean processes, less waste, large yield and selective, reusability, easy separation of catalyst, reduce the cost of production, and can transform many molecules (Alvarez, 2020; Valdés, et al, 2019; Zaijun, 2016; Roduner, 2014). The growing demand for catalysts cannot be fulfilled only by natural products and therefore it is necessary to develop powerful computational methods for chemical synthesis. The synthesis will be arranged into new formations by atoms and molecules (Ball, 2015).

The catalytic activity of compounds is related on the chemical structure and functional groups. Therefore, the catalytic activity of catalysts can be depended on we-defined single or multiple catalytically active site of the catalyst whether Lewis base site, Lewis acid site, Brönsted acid site or Brönsted base site (Liew et al, 2020; Muhammad et al, 2020; Cosmas et al, 2018; Siddiqui et al, 2016; Ball, 2014; Roduner 2014), where these processes can be elucidated using infrared (IR), nuclear magnetic resonance (NMR), LCMS and Raman Spectroscopies (Malherbe, 2019). Based on obtained data and informations, new structural modifications can be made to optimize some property or activity. In current work, Piperazine (PZ) and 4,4'-Trimethylenedipiperidine (TMDP) will be selected because they are bifunctional cyclo-aliphatic nitrogen-heterocycle that can be used as Lewis base organic transformations. Those can be modified Brönsted acids by chlorosulfuric acid and sulfuric acid as an alternative sulfonating agent of organic

compounds. Additionally, the N-H functional group can act as a hydrogen bond acceptor or donor in the catalysis process (Ball, 2015).

Designing organic reactions based on the green chemistry principles is a new development in synthesis chemistry. It is an attractive research prospect and offers a safer alternative in green chemistry. The objectives of this green chemistry method and measurement are to achieve cost-effectiveness, broad substrate scope, metal-free, methods, and safe to access relatively sustainable organic reactions (Khaligh et al., 2019). The new molten and ionic liquid catalysts are another attractive area in green chemistry and produce alternative catalysts due to environmental perspectives and their applications in a variety of the organic transformations including three-component reactions and preparation of a series of novel nitrogen heterocyclic, Knoevenagel's condensation, esterification, and transesterification of various alcohol by acetic acid instead of acetic anhydride, and I₂-supported. Application of new molten and ionic liquid catalysts are continuing to grow exponentially in all fields of pure and applied chemistry due to their tenability of properties, and the use of them as catalyst in industry and academic researches. However, energy and green chemistry were key issues for some drawbacks such as the use of toxic and corrosive reagents as well as expensive reactants or catalysts and volatile solvents, non-biodegradable, unrecovered catalysts, generate the metal wastes, a high catalyst loading, conduct the reactions at high temperature for a long reaction time along with a low yield of products and metal-containing catalysts to preparation processes of new molten and ionic liquid catalysts and evaluation of their catalytic efficiency in organic reactions (Ball, 2015; Khaligh et al., 2019; Roduner, 2014).

The presence strategy and methodology of these new molten and ionic liquid catalysts, offer a simple experimental and use as a non-conventional media for the sustainable procedure of organic synthesis, use of commercially available chemical without further separation and purification treatment such as adsorption, filtration, sedimentation, and distillation that can be much more steps and it has some drawback because it uses many of solvents, generated of the waste and reaction time, high temperature. In addition, the simple methodology will be reduced and eliminated the use and generation of toxic and hazardous reagents, good to the excellent yield of the desired products within shorter reaction times, recyclability that could be reused several times with no significant loss of its activity plus thermally stable even at relatively high temperatures (Khaligh et al., 2019; Khaligh et al., 2017). Often, the new molten and ionic liquid catalysts can be removed by water from the organic products using a simple workup and can be concentrated and then directly recharge with new reactants for another run because the organic product can be extracted by nonpolar organic solvent (Khaligh et al., 2018).

The energy efficiency is also an important category in green chemistry development. The current methodology to preparing the new molten and ionic liquid catalysts use an un-conventional method within short reaction times at room temperature and under atmospheric pressure consumes less energy compare to high pressure and conventional thermal process and it will highlight the importance of green energy in organic synthesis. Apart from this, complete or partial recovering of the catalyst and reagents is very important in the industrial processes due to minimization of the waste, as well as lower the requirement of raw material, energy, and waste disposal costs.

The present methods will be combined with spectroscopic and microscopic techniques that allow us to see the chemical structure of the cations and anions which are determined by their physical and chemical properties (Ball, 2015). In addition, the chemical structure of the new molten and ionic liquid catalysts is elucidated by 1D NMR and 2D NMR, FTIR, Raman analyses, and Mass spectra. These facts motivated us to study the chemical structure of the product using ^1H NMR, ^{13}C NMR, ^1H , ^1H -COSY and ^1H , ^{13}C -HMBC Spectra (Akbarzadeh et al, 2020). The physical properties of these new molten and ionic liquid catalysts will be characterized by TGA which important from a technological perspective because it provides other useful data such as chemical phenomena including chemisorption, thermal decomposition, and solid-gas reaction (Khaligh, 2018), thermal behavior will be characterized by DSC, and physical properties by melting point, liquefied, solubility, pH, titrimetry, density, viscosity, conductivity and total water content. This dissertation can be one of the efforts to understand and reveal how the properties relevant to the catalytic activity of new molten and ionic liquid catalysts are encoded by cations and anions of chemical structures. Interestingly, this can be easy and allow the chemist to design and change the structure of cation/anion or functional groups of molten and ionic liquid catalysts which leads to new molten and ionic liquid catalysts with desirable physical and chemical properties and catalytic systems (Khaligh et al., 2019). With this proposed works, it is possible to design new molten and ionic liquid catalysts to cater a desirable physical, chemical and catalytic properties, and also it is possible to study the catalytic efficiency of new molten and ionic liquid catalysts in organic transformation such as nitrogen heterocyclic, Knoevenagel's condensation, esterification and transesterification and I_2 -supported.

1.2 Problem Statement

The preparation processes of new molten and ionic liquid catalysts for organic transformations are sometimes exemplified as the use of expensive chemical and toxic solvents and reagents. Furthermore, some of the reported promoters could not be recovered and recycled. This new molten and ionic liquid catalysts method avoids the use of toxic, volatile, and hazardous reagents and flammable solvents during the reaction and workup, reduce the generation of heavy metal or corrosive waste and acid-free reaction conditions. Moreover, the simple synthesis process under catalyst and solvent-free/less and commercially available, eco-friendly, short reaction times, energy efficiency, good to excellent yields and use the recyclable catalysts instead of using catalysts that contain toxic metals and could not be recycled could play a more important role in large scale and industrial processes. Similarly in the promotion of one-pot multicomponent reactions in the new molten and ionic liquid catalysts instead of using multi-step for preparation of catalysts (Khaligh et al, 2019; Wenda et al, 2011). In addition, the promoter will easily regenerate and could be reused several times with no significant loss of its activity.

1.3 Research Objectives

The objectives of this study are listed as follows:

- a) To synthesize and characterize novel molten salts and ionic liquids.
- b) To investigate physical properties of the molten salts and ionic liquids.
- c) To evaluate performances of the molten salts and ionic liquids as catalysts for esterification, iodination, Knoevenagel's and multicomponent reactions.

1.4 Scope of Thesis

This thesis is organized as follows:

This research work focuses on the design of new molten and ionic liquid and catalytic systems based on intensive updates and technology alert on recent publications, and will be synthesized and characterized of the new molten and ionic liquid catalysts with the simple synthesis process under catalyst and solvent-free/less and commercially available, eco-friendly, short reaction times, low energy consumption, good to excellent yields and use the recyclable catalysts instead of using catalysts that contain toxic metals and could not be recycled. Evaluation of their catalytic efficiency in organic reactions including three-component reactions and preparation of a series of novel nitrogen heterocyclic, Knoevenagel's condensation, esterification and transesterification of various alcohol by acetic acid instead of acetic anhydride and aryl iodide in organic transformations.

CHAPTER TWO

LITERATURE REVIEW

2.1 Catalysis

Catalysis is the acceleration of a slow chemical process by the presence of a foreign material (Ertl, 2009). Catalysis is also a multidisciplinary field that involves physical chemistry, inorganic chemistry, organic chemistry, chemical engineering, and material science. Catalysis is very important in industry and academic reaction because they use catalysis for all reactions and catalysts cannot be fulfilled only by nature products and therefore it needs to develop a chemical synthesis process. Moreover, the employment of catalysts in organic synthesis also offers other interesting advantages, thus opening the door to the improvement of the selectivity of a selected process, the tolerance to potentially degradable or sensitive functional groups, the enantiomeric excess (Alvarez, 2020).

Catalysis has been always assisted by the accumulated knowledge and basic principles of physical chemistry, solid-state chemistry and tools for characterizing what is happening in the reaction (Ball, 2015). The main characteristics of a good catalyst are activity and selectivity, reproducibility, thermal and mechanical stability, and the capacity for easy regeneration.

- (a) Activity: the catalyst activity is related to the nature, the number, strength, and spatial arrangement of the chemical bonds.
- (b) Selectivity: the selectivity is the high yield of a particular product that is the capacity of the catalyst to conduct the conversion of the reactants in one particular path.

- (c) Stability: the stability indicates that the catalyst properties will not noticeably change during the catalytic process.
- (d) Reproducibility: the reproducibility is related to the consistency of its properties in different sets of production lots.

2.2 Structure-Activity Relationship (SAR)

Structure-Activity Relationship is a method used in the prediction of the chemical and chemical activity relationship as a function of structural and molecular information of a compound (Muhammad et al, 2020; Cosmas et al, 2018). SAR involves elucidating the details of one or more such relationships such as infrared (IR), nuclear magnetic resonance (NMR), LCMS, and Raman Spectroscopies and using that information to make new structural modifications to optimize some property or activity. SAR aims to identify which functional groups are important for activity, thus, employs few methods to aid in its activity, including: alter, remove or mask a functional group and test the analog for activity.

The active site, there are 4 types of active sites:

- (a) Lewis base site, can be defined as a site on which acid is chemically adsorbed and also it is capable of providing an electron pair.
- (b) Lewis acid site, can be defined as a site on which a base is chemically adsorbed and also it is capable of taking an electron pair.
- (c) Brönsted acid site, has a propensity to give a proton, and
- (d) Brönsted base site, tends to receive a proton.

Acid catalysis is one of the most common types of catalysis in the modification of base with strong acid as an alternative sulfonating agent of organic compounds. Protonation by Brønsted acids polarizes the system and leads to a new electron distribution in the protonated species, which activates the molecule and may induce the breaking of existing bonds and the formation of new bonds (Roduner, 2014).

2.3 Principles of Green Chemistry

The current trend in the design of novel catalysts and process is a new development in green chemistry. It is an attractive research prospect and offers a safer alternative in green chemistry. Furthermore, some basic principles of green chemistry, e.g.:

- (a) Use of non-toxic, non-hazardous reagents and solvents for the preparation of catalysts, reactions, and workups,
- (b) Conduct the reaction under solvent-free conditions,
- (c) Reduce the generation of hazardous waste during catalyst preparations, reactions, and workups,
- (d) Utilize a very small amount of catalysts, and
- (e) Use the recyclable organocatalysts instead of using toxic metal-containing and non-recyclable catalysts.

Non-basic principles of green chemistry:

- (a) Exist two or more preparative steps that increase the preparation cost,
- (b) Use of toxic, flammable, or volatile solvents,
- (c) Use expensive, toxic, or non-reusable catalyst,
- (d) Tedious workup, and
- (e) Generation of toxic, hazardous, or corrosive waste.

2.4 Ionic liquid and Molten Salt

Three types of liquid systems, including molten salts, ionic liquid and liquid metals. Molten salts are ionic liquids with melting points above 100°C and have been employed in numerous fields like synthesis, catalysis, and separation.

Ionic liquids and molten are a vital topic in organic chemistry and has been employed in a broad range of sectors, product, and processes. The current trend in catalyst research is to design greener catalysts and eco-friendly technologies, as well as directing the activities towards sustainability and investigating the catalytic activity under realistic conditions regarding temperature and pressure.

In recent years more increased attention has been paid to the dual solvent-catalyst efficiency of ionic liquids and molten in the organic synthesis due to their diverse properties including low volatility and vapor pressure, high to excellent thermal and chemical stability, and tunable and designable polarity and properties (Khaligh et al, 2019). Easy separation of the organic products and recyclability of ionic liquids and molten are accounted as notable merits of ionic liquid and molten in the most organic transformations, which lead to avoiding the generation of metal-containing waste, and the minimizing of toxic, volatile, and flammable organic waste (Mihankhah et al, 2019; Khaligh et al, 2018).

Design and development of new ionic liquid and molten and their applications in various organic transformations have been widely studied as solvents and/or catalysts in organic synthesis, primarily due to their distinct properties, including low volatility and vapor pressure, and good to high thermal and chemical stability. The polarity and physical properties of the ionic liquid are tunable and designable by the judicial choice of cations

or anions, which is the most prominent feature of ionic liquid and molten. Furthermore, the easy separation of organic product from and recyclability of ionic liquid and molten are seen as other notable merits of ionic liquid and molten applications in most organic transformation. These advantages lead to avoiding the generation of metal-containing waste and minimizing the use of toxic volatile, and flammable organic solvents. The viscosity of ionic liquid and molten is very important for their application in organic synthesis as a solvent because most of the ionic liquid and molten are very viscous, which would result in the less efficient mass transfer of reactants.

2.5 The Simple Process of Synthesis

The presence of simple process and methodology include short reaction time, wide substrate scope, use of a metal-free catalyst and green solvents, and simple work-up process, safe, cost-effective. All use reagents commercially available and inert to moisture and air, reduces waste generation, energy consumption, low cost of raw material, good porosity and high surface area, excellent recyclability, high density, and waste disposal costs.

According to the principles of green chemistry, the methodology is performed without separation and purification in the current ionic liquid and molten, which avoids the use of solvents and reduces the generation of waste. Furthermore, an improvement in energy efficiency is due to shorter reaction times and the performance of reaction at room temperature, and also by the planetary ball milling process at ambient and neat conditions.

The presence strategy and methodology can act as a green solvent and acid catalyst due to low viscosity and acid functionality. The product will be simply extracted

and the ionic liquid and molten will be retrieved several times without reducing its catalytic efficiency.

2.6 The Advantages of The Presence Strategy and Methodology of These New Molten and Ionic Liquid Catalysts

The Presence strategy and methodology of these new molten and ionic liquid catalysts have advantages such as simple experimental and sustainable procedure, avoid the use of toxic and volatile organic solvents, simple work-up, solvent-free conditions, and recyclability, high yields of the desired products within short reaction times at room temperature and atmospheric pressure consumes less energy compared to high pressure and conventional thermal process, easy separation of product and catalyst, and low catalyst loading, as well as avoids the generation of heavy metal and corrosive waste.

2.7 Designing Organic Transformation in The New Molten and Ionic Liquid Catalysts

Applications of new molten and ionic liquid catalysts are continuing to grow exponentially in all fields of pure and applied chemistry due to their chemical tenability and they can be suitable solvents for spectroscopic measurement. In this perspective, designing organic transformations in the new molten and ionic liquid catalysts media is another attractive area in green chemistry including three-component reactions and preparation of a series of novel nitrogen heterocyclic, esterification of various alcohol by acetic acid instead of acetic anhydride.

2.7.1 Heterocyclic

The different heterocyclic catalysts based on acid, base, metal and enzymes have been extensively studied due to a broad range of biological and pharmaceutical activities, including anticancer, antioxidant, antiparasitic, antimicrobial, antibacterial, antiproliferative and anti-tubulin, anti-HIV, anti-fungal properties such as Triazolopyrimidines that constitute an influential class of bicyclic nitrogen heterocycles. Triazolopyrimidines are often prepared through a one-pot three-component condensation of aryl aldehydes, active methylene compounds, and aminotriazoles in the presence of a catalytic system because of their electron-donating groups. (Liew et al, 2020; Fischer, 2007).

2.7.2 Knoevenagel's Condensation

Knoevenagel's condensation has been broadly studied to investigate the catalytic activity of the organo-catalyst such as 4,4'-Trimethylenedipiperidine (TMDP), Piperazine, (4-Dimethylamino)Pyridine (DMAP), Pyrazine, Pyridine, etc. for the one-pot multi-component synthesis.

4,4'-Trimethylenedipiperidine (TMDP), Piperazine, (4-Dimethylamino)Pyridine (DMAP), Pyrazine, Pyridine etc., as organocatalyst or aromatic nitrogen-containing organic base which is commercially available and easy to handle, high thermal stability and good solubility in water, high recyclability make it an attractive organocatalyst, bearing Lewis base sites and acceptor-donor hydrogen bonding groups, for mechanochemistry, and also were employed to promote a solid phase one-pot three-component reaction under mild and cost-and energy-effective conditions. Further research is currently being formed for other organic transformations in the presence of these organic bases.

These organocatalysts containing Lewis base sites having acceptor-donor hydrogen bonding functional groups, and high porosity could play a vital role in the promotion of the one-pot multi-component condensation in the solid-phase synthesis. The nitrogen atom of these organic bases and their derivatives can attack as a nucleophile to the central atom of chlorosulfonic acid or sulfuric acid due to more steric hindrance of the sulfur atom and nitrogen atom as well as basicity of organic base.

Designing and development of easy separable and recyclable heterogeneous organocatalysts are highly demanded, which can be used in the catalytic amount and greener conditions which showed potential applications in anionic and cationic dyes adsorption, gas absorbent, removal of the toxic metal ions, detection of nitroaromatic explosives. It has been gained significant importance in catalytic applications due to its cost-effective synthesis, cheap starting materials, microporosity, good thermal and chemical stabilities, and a high density of amine functional groups and triazine moieties.

2.7.3 Esterification and Transesterification

Esterification is an eco-friendly solvent and/or catalyst in a variety of reactions such as thermal and chemical stability, low vapor pressure, and recoverability (Przypis et al., 2020; Dorosz et al., 2020). The catalytic activity of this ionic liquid and molten will be demonstrated in the esterification reaction of various alcohols by glacial acetic acid instead of acetic anhydride under different conditions.

The catalytic activity of the new ionic liquid and molten will be studied for the direct esterification of various carboxylic acids instead of acid anhydride and alcohols under obtained optimal reaction conditions is still one of the exciting research topics. Therefore, it is required to develop an efficient and greener methodology to overcome

some drawbacks and achieve a suitable balance between the economic and ecological aspects of production.

Ester is a product from the reaction of esterification that is a natural and synthetic ester that has been utilized in different fields, including pharmaceuticals, perfumes, flavors, cosmetics, adhesives, detergents, solvents, plasticizers, lubricants, electronic materials, and daily and fine chemicals, diluents, etc. (Malkar et al., 2020; Otera et al., 2009; Siengalewicz et al., 2014). Low molecular mass ester has been widely found in fragrances and essential oil (Baser et al., 2010), pheromones (Kartika et al., 2015) and imparts pleasant fruity odor are isobutyl formate (raspberry), n-propyl acetate (pear), methyl butyrate (apple), ethyl butyrate (pineapple), isobutyl propionate (rum), isoamyl acetate (banana), benzyl acetate (peach), octyl acetate (orange) and methyl salicylate (wintergreen) (Malkar et al., 2020). The carboxylic acid ester can be synthesized using various chemical reactants, catalysts, and reaction media. Although numerous papers have appeared for the esterification reaction, the development of an efficient synthesis of a carboxylic acid ester using carboxylic acids instead of acid anhydride is still an exciting research topic.

The esterification will be carried out at different conditions and four parameters, including catalyst type and loading, the mole ratio of alcohol and acetic acid, temperature, and reaction time will be varied to find the optimal conditions.

CHAPTER THREE

ARTICLE 1

STRUCTURAL ELUCIDATION, SPECTROSCOPIC ANALYSES, AND
PHYSICAL PROPERTIES OF 1*H*,4*H*-PIPERAZINE-DIUM
DICHLOROSULFONATE

3.1 Introduction

Chlorosulfonic acid has been used as an alternative sulfonating agent of organic compounds after sulfuric acid and sulfur trioxide (Qureshi et al, 2009; Janosik et al, 2005; Guan et al, 2005). Chlorosulfonic acid was applied as catalyst (Kotharkar et al, 2006) and an electrophilic olefin cyclization agent in the organic reactions (Palomino et al, 2003). It was also used to improve the catalytic activity of various catalyst (Zhang et al, 2014; Yadav et al, 2004). The crystal structure of only two compounds containing chlorosulfonate anion, $\text{NO}^+\text{SO}_3\text{Cl}^-$ and the protonated anti-benzonorbornenol (1^+) $\text{SO}_3\text{Cl}^-\text{CH}_2\text{Cl}_2$ (Figure 3.1) (Laube, 2004), were reported in the literature. *N*-methyl-2-pyrrolidonium chlorosulfonate was prepared and used as a sulfonating agent for one-pot synthesis of δ -sultones (Rad et al, 2016). We became interested to study the reaction of chlorosulfonic acid with aliphatic and aromatic nitrogen-containing organic bases when, contrary to previously reported data in the literature, we observed different spectroscopic data and physical properties for the obtained product.

In our opinion, it seems unlikely that the nitrogen atom of above-mentioned organic bases like piperazine and its derivatives can attack as a nucleophile to the central atom of chlorosulfonic acid due to more steric hindrance of the sulfur atom and nitrogen atom as well as basicity of organic bases. Therefore, we begin our research to find the

answer to the following question “Does chlorosulfonic acid act a strong acid or sulfonating agent in the reaction with aliphatic and aromatic nitrogen-containing organic bases?” and in pursuit of our studies (Khaligh et al, 2018), herein, we indicate that piperazine and chlorosulfonic acid can participate in an acid-base reaction to form 1*H*,4*H*-piperazine-dium dichlorosulfonate $[PZH_2]^{2+}2[ClSO_3]^-$ as a new ionic liquid containing chlorosulfonate anion.

The new ionic liquid was obtained liquid-state and solid-state when the reaction was conducted in dichloromethane and acetonitrile as a solvent, respectively. It seems that a change of dichloromethane into acetonitrile can result in a dramatic change in packing and symmetry of 1*H*,4*H*-piperazine-dium dichlorosulfonate $[PZH_2]^{2+}2[ClSO_3]^-$. Their structure was characterized by 1D and 2D NMR and mass spectrum. Furthermore, IR and Raman spectra of liquid- and solid-state of pure 1*H*, 4*H*-piperazine-dium dichlorosulfonate were studied. Assignments were made for IR and Raman peaks, and the differences between our results and previous report on the IR and Raman assignments for the frequencies are discussed.

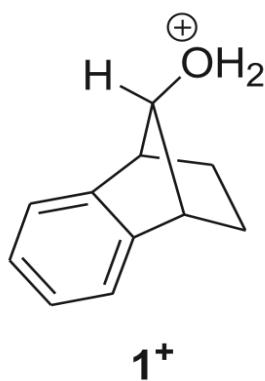


Figure 3.1: The chemical structure of protonated anti-benzonorbornenol (1⁺)

3.2 Methodology

3.2.1 Material and Method

Unless specified, all chemicals were analytical grade and purchased from Merck, Aldrich, and Fluka Chemical Companies and used without further purification. Products were characterized by their physical constant and IR, NMR, and elemental analysis.

The purity determination by TLC using silica gel SIL G/UV 254 plates. The FT-IR spectra were recorded on a Perkin Elmer 781 Spectrophotometer using KBr pellets for solid and neat for liquid samples in the range of 4000-400 cm^{-1} . Raman spectra were recorded using Renishaw InVia Raman Spectroscopy in the range of 3200-100 cm^{-1} with 785 nm laser source wavelength. In all the case, the ^1H and ^{13}C NMR spectra were recorded with Bruker Avance III 600 MHz instruments. All chemical shifts are quoted in parts per million (ppm) relative to TMS using a deuterated solvent. Micro-analyses were performed on a Perkin-Elmer 240-B microanalyzer. Melting points were recorded on a Buchi B-545 apparatus in open capillary tubes. The mass spectra of the products were recorder using an Agilent 6560 iFunnel Q-TOF LC-MS instruments. The density was determined using a Mettler Toledo DM45 Deltarange Density meter, and the calibration was performed using doubly distilled and degassed water and dried air at atmospheric pressure. The viscosity was measured using a Brookfield DV-III Ultra Viscometer.

DSC curves were obtained with the use of a DSC-Mettler Toledo DSC 822e calorimeter. The measurement was performed in aluminium pans with a pierced lid with a sample mass 9.24 mg under a dry nitrogen atmosphere (10 mL min^{-1}). Dynamic scans were performed at a heating rate of $10 \text{ }^\circ\text{C min}^{-1}$ in two temperature cycles at a range of 30-300 and 30-500 $^\circ\text{C}$. TGA/DTA curves were obtained with the use of a Mettler Toledo TGA/SDRA 851e. All measurements were performed in an Al_2O_3 crucible with a sample

mass of 10.65 mg under a nitrogen atmosphere (10 mL min^{-1}). Dynamic scans were performed at heating rate of $10 \text{ }^\circ\text{C min}^{-1}$ in the temperature range of $30\text{-}800 \text{ }^\circ\text{C}$. The purity and yield of the products were determined using GC-MS on an Agilent 6890GC/5973MSD analysis instrument under 70 eV conditions. The conductivity (σ) was measured using a Mettler Toledo Seven Easy conductivity meter. The total water content was recorded by Karl Fisher (KF) titration using a Metrohm 831 kF *coulometer*. The conditions of temperature, pressure and drying time were 90°C , 65 mbar and 10 h, respectively. The pH was measured using a pH meter F-71, LAQUA-HORIBA Scientific.

3.2.2 Synthesis of 1*H*,4*H*-piperazine-dium dichlorosulfonate $[\text{PZH}_2]^{2+}2[\text{ClSO}_3]^-$ in the solid- or liquid-state

The neat chlorosulfonic acid (3.0 ml, 40 mmol) was dropwise added to piperazine (1.72 g, 20 mmol) in dry CH_2Cl_2 (20 mL) or CH_3CN (20 mL) at ice bath. The reaction mixture was stirred at room temperature for overnight which led to the formation of two phases. The upper phases was decanted, and excess of solvent was removed under reduced pressure. The residue was washed three times with CH_2Cl_2 or CH_3CN and isolated 6.128 g of colorless viscous liquid (yield 96%) and 6.064 g of white solid (yield 95%) (Figures 3.2 and 3.3).

3.2.3 1*H*,4*H*-piperazine-dium dichlorosulfonate $[\text{PZH}_2]^{2+}2[\text{ClSO}_3]^-$ in the liquid-state

Colorless viscous liquid; ^1H NMR (600 MHz, DMSO-d_6) δ 9.11 (s, 4H), 3.34 (s, 8H) ppm; ^{13}C NMR (150 MHz, DMSO-d_6) δ 40.54 ppm.

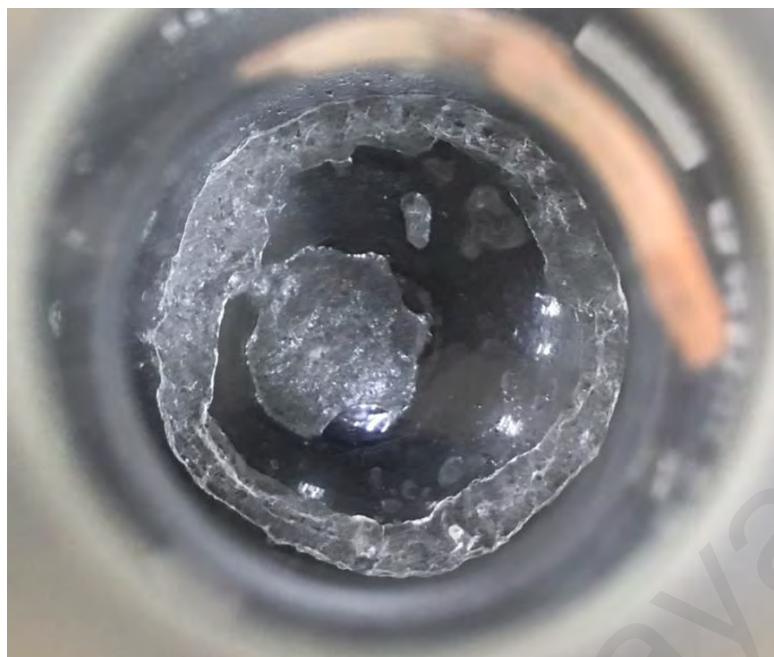


Figure 3.2: The image of 1*H*,4*H*-piperazine-dium dichlorosulfonate in the liquid-state

3.2.4 1*H*,4*H*-piperazine-dium dichlorosulfonate [PZH₂]²⁺2[ClSO₃]⁻ in the solid-state

White solid, melting point 290-291 °C; ¹H NMR (600 MHz, DMSO-d₆) δ 9.12 (s, 4H), 3.34 (s, 8H) ppm; ¹³C NMR (150 MHz, DMSO-d₆) δ 40.44 ppm.



Figure 3.3: The image of 1*H*,4*H*-piperazine-dium dichlorosulfonate in the solid-state

3.3 Results and Discussion

3.4.1 Synthesis of 1*H*,4*H*-piperazine-dium dichlorosulfonate [PZH₂]²⁺2[ClSO₃]⁻

1*H*,4*H*-piperazine-dium dichlorosulfonate [PZH₂]²⁺2[ClSO₃]⁻ was prepared through the dropwise addition of two equivalents of neat chlorosulfonic to a solution of piperazine in CH₂Cl₂ or CH₃CN. Then, the reaction mixture was stirred at room temperature overnight (Figure 3.4).

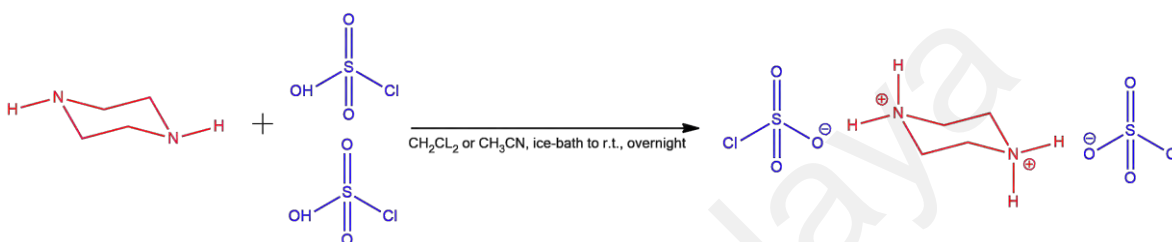


Figure 3.4: Synthesis of 1*H*,4*H*-piperazine-dium dichlorosulfonate [PZH₂]²⁺ 2[ClSO₃]⁻

The product was a colorless viscous liquid and white solid in dichloromethane and acetonitrile, respectively; which their structures were characterized by 1D and 2D NMR, mass, FTIR, and Raman Spectra. The C₄H₁₁N₂ was detected by a positive mode of LC-ESI-MS at *m/z* 87.0918 and 87.0916 as well as C₄H₁₂CIN₂O₃S⁺ at *m/z* 203.0252 and 203.0253 for solid and liquid state of 1*H*,4*H*-piperazine-dium dichlorosulfonate, respectively.

3.4.2 1D and 2D NMR Spectra of 1*H*,4*H*-piperazine-dium dichlorosulfonate [PZH₂]²⁺2[ClSO₃]⁻

The ¹H NMR of piperazine in DMSO-*d*₆ showed one singlet at 2.59 and one broad singlet centered at 2.04 at ratio 8 to 2 which are assigned to four methylene groups in piperazine ring and protons of two >NH moieties, respectively. Four carbons of piperazine ring are also displayed at 47.41 ppm (see Figures A.1 and A.2).

It was indicated that an internal salt is often formed when an amine group is present in the molecule containing sulfonic acid moiety, and hydrogens of amine and sulfonic acid groups observed as a broad singlet at ca. 8.3 ppm (Zhang et al 2014). We proposed that the reaction of piperazine and chlorosulfonic acid in dichloromethane or acetonitrile can afford two structures (I) and (II) (Figure 3.5).

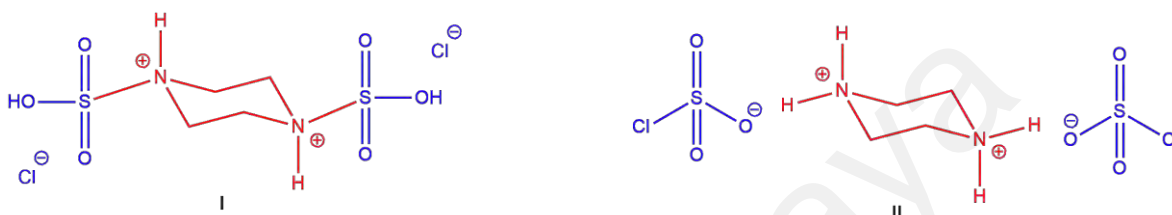
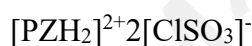


Figure 3.5: Two possible of 1*H*,4*H*-piperazine-dium dichlorosulfonate



The ^1H NMR spectra of the 1*H*,4*H*-piperazine-dium dichlorosulfonate $[\text{PZH}_2]^{2+}2[\text{ClSO}_3]^-$ exhibited only two singlet peaks in a ratio 2:1 for eight protons $>\text{CH}_2$ at 3.34 ppm and the four protons of $>\text{NH}_2$ at 9.11 ppm and 9.12 ppm in liquid and solid-state, respectively. The ^{13}C NMR spectrum showed one peak for four identical carbons at 40.44 and 40.54 ppm in liquid and solid-state, respectively (Figs. A.3- A.6). The inaccurate integration ratios are due to an exchange labile proton between the residual water in $\text{DMSO-}d_6$ and $[\text{PZH}_2]^{2+}2[\text{ClSO}_3]^-$.

The ^1H NMR spectrum of $[\text{PZH}_2]^{2+}2[\text{ClSO}_3]^-$ in liquid state showed the presence of water as two peaks, a singlet at 3.67 ppm corresponding to H_2O and triplet at 7.12 ppm in $\text{DMSO-}d_6$ corresponding to hydrogen coupling with ^{14}N nucleus with a coupling constant of 51.1 Hz (Figure A.7).

The spectrum of 1*H*,4*H*-piperazine-dium dichlorosulfonate in D₂O also confirms the exchangeable and labile nature of the protons at 9.11 ppm or 9.12 ppm for the liquid and solid-states (Figure A.8). The eight inert protons and four carbons of piperazine ring were observed at 3.52 ppm and 40.34 ppm in ¹H NMR and ¹³C NMR spectrum of [PZH₂]²⁺2[ClSO₃]⁻ in D₂O (Figures A.8 and A.9).

As shown in Figure A.10, a correlation between the protons of >NH₂⁺ at 9.12 ppm and CH₂ groups at 3.34 ppm is observed in ¹H,¹H-COSY spectrum of [PZH₂]²⁺2[ClSO₃]⁻ which approves the structure (II). The same correlation was detected in ¹H,¹H-COSY spectrum of [PZH₂]²⁺2[ClSO₃]⁻ in liquid state.

Also, the correlations of protons with carbon and nitrogen atoms of piperazinium ring are observed in ¹H,¹³C- and ¹H,¹⁵N-HMBC spectrum of [PZH₂]²⁺2[ClSO₃]⁻ (Figs. A.11 and A.12). The 1D and 2D NMR spectrum results suggested that the 1*H*,4*H*-piperazine-dium ring with stable chair conformation interconverts rapidly at room temperature and two set of protons including ammonium and methylene moieties are in an identical environment and exhibit identical chemical shift due to nitrogen atom and ring inversion.

3.4.3 FTIR spectrum of the 1*H*,4*H*-piperazine-dium dichlorosulfonate [PZH₂]²⁺2[ClSO₃]⁻

The presence of chlorosulfonate anion and the confirmation of structure (II) are further supported by Raman and IR spectroscopy. The infrared spectra of 1*H*,4*H*-piperazine-dium dichlorosulfonate [PZH₂]²⁺2[ClSO₃]⁻ is shown in Figure 3.6. The contribution of

the ClSO^- ion was identified by comparison with the infrared spectra of other salts of same anions (Waddington et al, 1960). The spectra contained a few strong bands at 418, 441, 458 and 578 cm^{-1} , and strong bands at 770, 887, 996, 1099, 1135, and 1377 cm^{-1} , respectively. The bands at 441 cm^{-1} , 574 cm^{-1} , and 770 cm^{-1} were assigned to the S-Cl stretching, SO_2 bending, and S-O stretching modes, respectively (Erben et al, 2003). The medium intensity band at 1653 cm^{-1} and two relatively sharp bands at 1610 and 1587 cm^{-1} , which are due to the deformation vibration modes of $>\text{NH}_2^+$ groups in 1*H*,4*H*-piperazine-dium ring and are characteristic of secondary amine salts (Heacock et al, 1956). Two bands at 2982 and 3134 cm^{-1} are assigned to methylene groups in 1*H*,4*H*-piperazine-dium ring and two peaks at 3447 and 3390 cm^{-1} can be attributed to NH_2^+ moieties groups. It is also worth mentioning that peaks at 2475, 2615, and 2741 cm^{-1} are assigned to N-H stretch bond and their shifting from approximately 3000 cm^{-1} to thus region is due to the increase of the hydrogen bonding strength (Heacock et al, 1956).

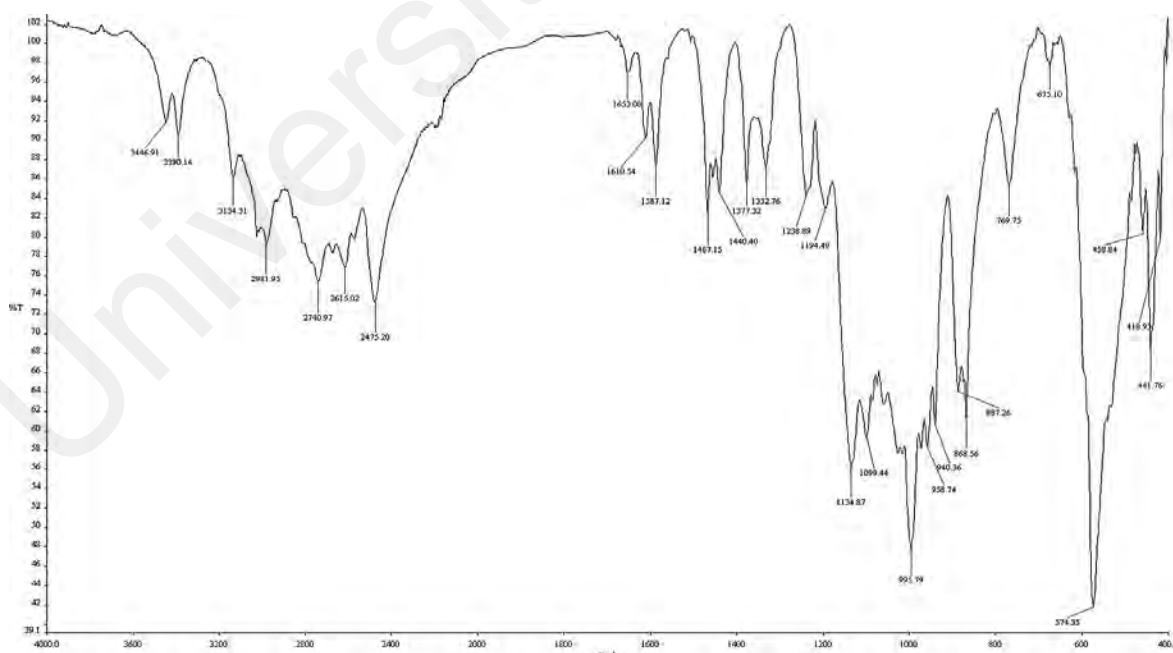


Figure 3.6: The FTIR of 1*H*,4*H*-piperazine-dium dichlorosulfonate $[\text{PZH}_2]^{2+}2[\text{ClSO}_3]^-$ in liquid state.

3.4.4 Raman spectrum of the 1*H*,4*H*-piperazine-dium dichlorosulfonate [PZH₂]²⁺2[ClSO₃]⁻

Raman spectrum of 1*H*,4*H*-piperazine-dium dichlorosulfonate was studied to confirm of the presence of chlorosulfonate anion and ionic structure (II) (Figures 3.7 and 3.8). By comparison with the S-Cl frequencies in chlorosulfonic acid, NaSO₃Cl and KSO₃Cl in DMSO (Gillespie et al, 1962), it appears that bands at 420 and 438 cm⁻¹ can be assigned to the S-Cl frequency in [PZH₂]²⁺2[ClSO₃]⁻.

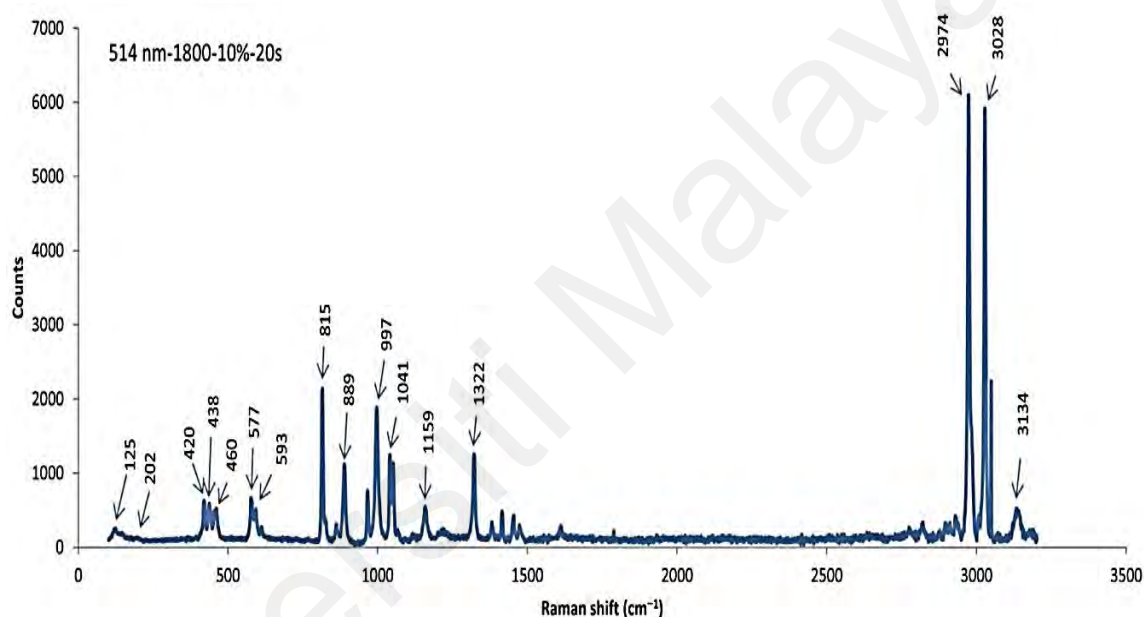


Figure 3.7: The Raman of 1*H*,4*H*-piperazine-dium dichlorosulfonate [PZH₂]²⁺2[ClSO₃]⁻ in liquid-state

Gillespie and Robinson studied the Raman spectra of NaSO₃Cl in dimethyl sulfoxide, while Stufkens and Gerding investigated the Raman spectra of chlorosulfonic acid and sodium chlorosulfonate in acetic acid and *N,N*-dimethylacetamide (DMA). It is well documented that the solvent such as *N,N*-dimethylacetamide (DMA) can form the strong interaction with the chlorine of the ClSO₃⁻ and cause the change in polarization, and some disturbing occurs in the presence of solvent. Although Stufkens and Gerding characterized the lowest band (312 cm⁻¹) in the Raman spectrum of HSO₃Cl in acetic acid

as the $\delta(\text{S-Cl})-\nu_6(\text{E})$, and Gillespie and Robinson mentioned 220 cm^{-1} band for this vibrational frequency, the cm^{-1} band was not observed in Raman spectra of $\text{NO}\cdot\text{SO}_3\text{Cl}$ in the solid and molten salt state (Stufkens et al, 2010)]. Our results are exhibited together with those of Paul (Paul et al 1969), Waddington (Waddington et al, 1960), Gillespie (Gillespie et al, 1962) and Stufkens (Stufkens et al, 1970) in Table 3.1.

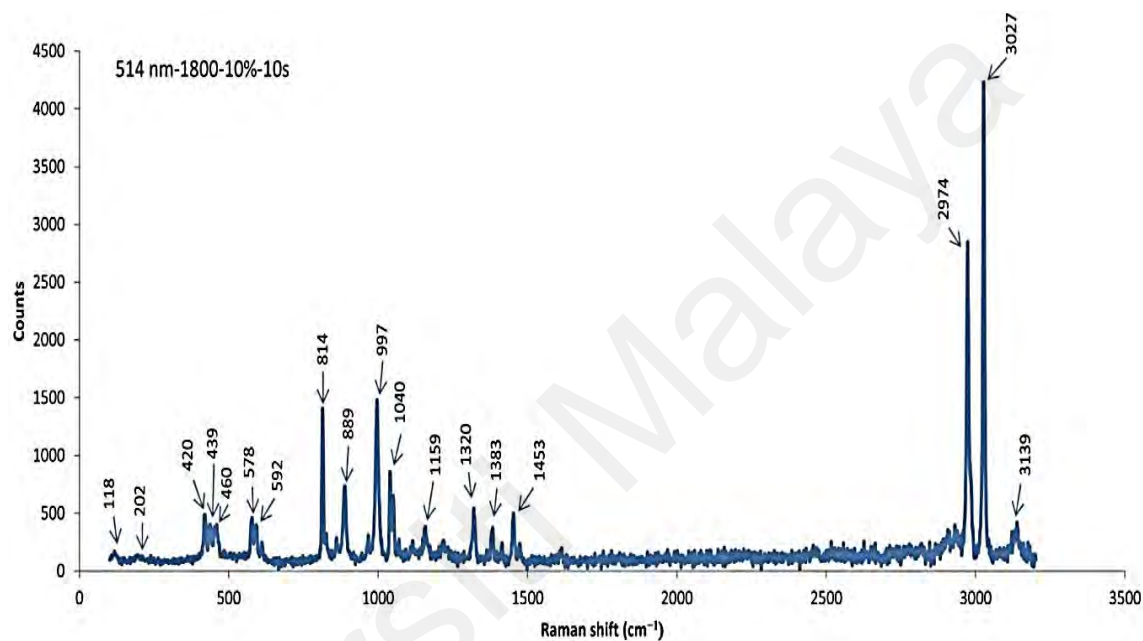


Figure 3.8: The Raman of $1H,4H$ -piperazine-dium dichlorosulfonate $[\text{PZH}_2]^{2+}2[\text{ClSO}_3]^-$ in solid-state

Although the depolarized band of the S-Cl wag at 202 cm^{-1} for liquid- and solid-state of $1H,4H$ -piperazine-dium dichlorosulfonate, were very weak in our Raman spectra, the bands at $420\text{-}460\text{ cm}^{-1}$ were polarized and assigned as the S-Cl stretch $\nu_3(\text{A})$ (Figs. 5 and 6) (Gillespie et al, 1962; Steger et al, 1967).

Table 3.1: Our results of the IR and Raman spectra of the ClSO_3^- anion together with the previous reports

Waddington	Paul	Gillespie	Stufkens	Our results		Approximate description	Assignment
(IR >500 cm^{-1})		Raman		FTIR (>450 cm^{-1})	Raman		
1044	1044	1050	1042	996,1135	1040 ^a , 1041 ^b	ν_s (SO_3)	ν_1 (A ₁)
565	562	535	601	574	577 ^a , 578 ^b	δ_s (SO_3)	ν_2 (A ₁)
540	540	416	381	419, 442	420 ^{a,b} , 438 ^a , 439 ^b	ν (S-Cl)	ν_3 (A ₁)
1275	1250	1195	1300	1135, 1332	1159 ^{a,b} , 1322 ^a , 1320 ^b	ν_{as} (SO_3)	ν_4 (E)
583	580	585	553	574	588, 613	δ_{as} (SO_3)	ν_5 (E)
-	-	220	312	-	202 ^{a,b}	δ (S-Cl)	ν_6 (E)

^a Liquid-state of 1*H*,4*H*-piperazine-dium dichlorosulfonate

^b Solid-state of 1*H*,4*H*-piperazine-dium dichlorosulfonate

3.4.5 The physical properties of 1*H*,4*H*-piperazine-dium dichlorosulfonate $[\text{PZH}_2]^{2+}2[\text{ClSO}_3]^-$

$[\text{PZH}_2]^{2+}2[\text{ClSO}_3]^-$ in liquid-state showed no crystallization even at low temperature (-4 °C). The density of liquid-state was recorded 1.12 g/mL at 27.00 ± 0.02 °C. The viscosity of $[\text{PZH}_2]^{2+}2[\text{ClSO}_3]^-$ in liquid-state was determined 18.2 ± 0.02 mPa s (cP) at 27.00 ± 0.02 °C under ambient pressure. The ionic conductivity (σ) of neat $[\text{PZH}_2]^{2+}2[\text{ClSO}_3]^-$ in the liquid-state was measured 1.91 mS cm^{-1} at 25 °C. The total water content of $[\text{PZH}_2]^{2+}2[\text{ClSO}_3]^-$ in solid- and liquid-state were determined 0.24 ± 0.02 wt %, respectively by Karl Fisher titration using a Metrohm 831 kF coulometer in conditions of ambient humidity and temperature. The conditions of temperature, pressure and drying time were 100 °C, 80 mbar and 12 h, respectively. The pH of several 0.01 M solutions of $[\text{PZH}_2]^{2+}2[\text{ClSO}_3]^-$ in solid- and liquid-state were recorded 1.9 ± 0.1 at 27 ± 1 °C, respectively. One of the more interesting properties of new ionic compound was its solubility. Although $[\text{PZH}_2]^{2+}2[\text{ClSO}_3]^-$ was soluble in water, dimethyl sulfoxide, and acetonitrile it was immiscible with methanol, ethanol, ethyl acetate, and *n*-hexane. The

solubility of internal salts is very dependent on the possibilities of stabilizing the crystal by internal hydrogen bonding, and upon the pK_a or pK_b of any ionizable moieties. This unusual solubility can be very useful for the organic synthesis including the increase of recyclability of catalyst, and the reducing toxic waste generation through the separation of organic products by a simple workup.

3.4.6 The thermal behavior of 1*H*,4*H*-piperazine-dium dichlorosulfonate $[PZH_2]^{2+}2[ClSO_3]^-$

The thermal behavior of $[PZH_2]^{2+}2[ClSO_3]^-$ is displayed as a differential scanning calorimetry (DSC) plot in two cycles at temperature ranges of 30-300 and 30-500°C in Figure 3.9 in a nitrogen atmosphere and over a temperature range of 30-300°C, two sharp endothermic peaks were recorded on the DSC curve of $[PZH_2]^{2+}2[ClSO_3]^-$, and no exothermic peak was observed. The first peak is likely due to the melting point of $[PZH_2]^{2+}2[ClSO_3]^-$ which began at 31.7°C and ended at 70.5°C, with a latent heat of fusion of 30.4 J g⁻¹. The second endothermic sharp peak was observed in the range of 138.8-160.3°C and centred at 147.7°C, which was assigned to the dehydration and degassing of the IL, supported by the thermogravimetric/differential thermal analyses (TGA/DTA) results, with a latent heat of evaporation of 59.2 J g⁻¹. The second cycle at a temperature range of 30-500°C showed a sharp peak with an onset and en-point at 303.7 and 369.4°C, respectively. The maximum temperature of this peak at 356.6°C was assigned as the boiling point-decomposition of $[PZH_2]^{2+}2[ClSO_3]^-$ due to an appreciable loss of weight, a remarkable change in heat capacity of the sample, and an exothermic baseline shift. The latent heat of evaporation-decomposition of the IL is 616.6 J g⁻¹.

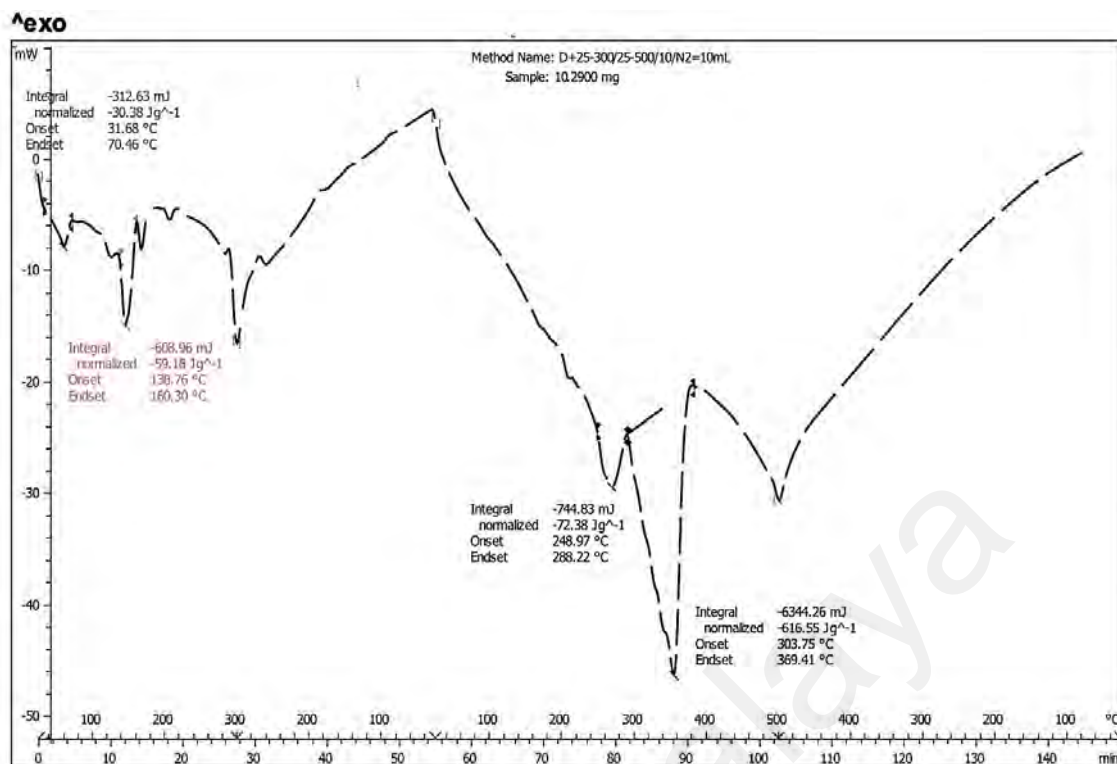


Figure 3.9: The DSC of 1*H*,4*H*-piperazine-dium dichlorosulfonate $[\text{PZH}_2]^{2+}2[\text{ClSO}_3]^-$

Figure 3.10 displays a TGA/DTA curve of $[\text{PZH}_2]^{2+}2[\text{ClSO}_3]^-$ in a temperature range from 30 to 800°C under nitrogen atmosphere. Three peaks are visible on the DTA curve, and $[\text{PZH}_2]^{2+}2[\text{ClSO}_3]^-$ started to decompose at 295°C, and its thermal decomposition is mainly completed at 345°C, which is in good agreement with the result of DSC. The first peak is observed to be below 200°C, centered at 138°C, with a maximum mass loss of 13.8%. This is attributed to the content of inherent moisture and the physically adsorbed solvent in $[\text{PZH}_2]^{2+}2[\text{ClSO}_3]^-$. The second and the third peaks showed a maximum mass loss of 47.0 and 32.5 at 250-320 and 320-345°C, respectively, which is related to the total decomposition of $[\text{PZH}_2]^{2+}2[\text{ClSO}_3]^-$. The DSC and TGA/DTA results showed that $[\text{PZH}_2]^{2+}2[\text{ClSO}_3]^-$ is thermally stable up to 250°C probably owing to the strong electrostatic attractions between piperazine-1,4-dium and chlorosulfonate in the structure of $[\text{PZH}_2]^{2+}2[\text{ClSO}_3]^-$

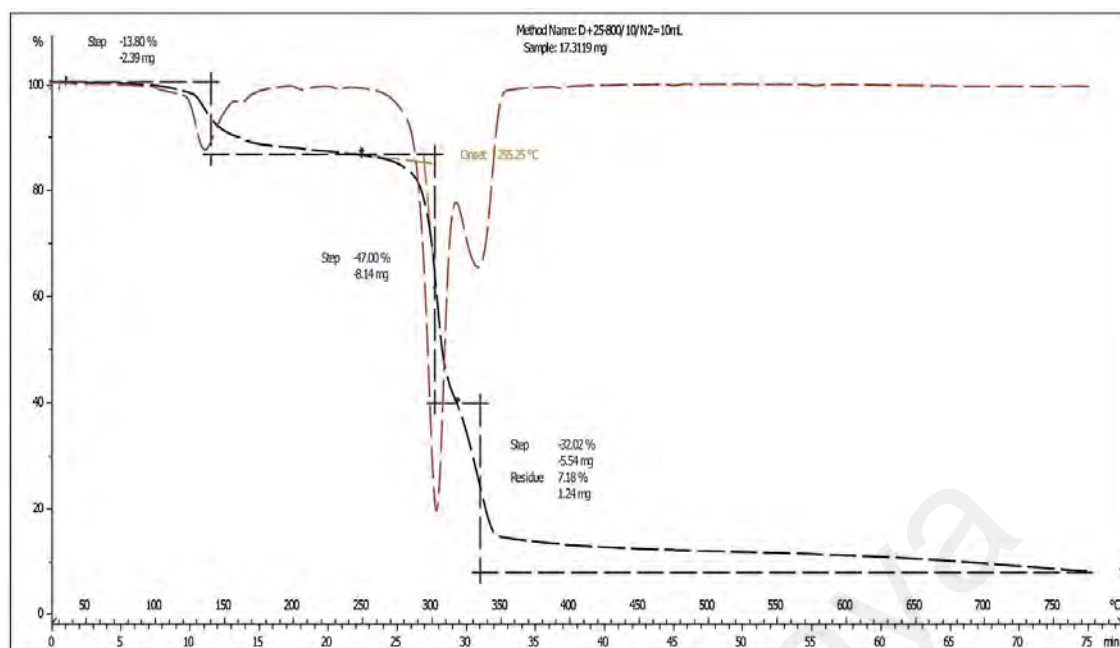


Figure 3.10: The TGA/DTA of 1*H*,4*H*-piperazine-dium dichlorosulfonate $[\text{PZH}_2]^{2+}2[\text{ClSO}_3]^-$

3.5 Conclusion

In summary, a novel mono-core dicationic salt-containing chlorosulfonate counterion was prepared in a pure solid and liquid state and its structure was characterized by 1D and 2D NMR, Mass spectra. The physical properties such as density and viscosity and pH of the aqueous solutions of new ionic liquid were determined. The correct structure was elucidated by COSY analysis, which was supported by Raman study. The FTIR and Raman spectra of pure liquid and solid state $[\text{PZH}_2]^{2+}2[\text{ClSO}_3]^-$ were studied and our assignments for IR and Raman peaks were compared with previous reports in the literature for chlorosulfonate anion. The lowest band in Raman spectrum of $[\text{PZH}_2]^{2+}2[\text{ClSO}_3]^-$ solid- or liquid-state was found at 418 cm^{-1} frequency which is assigned to S-Cl stretch. The band S-Cl wag is depolarized and was weakly observed at 206 and 203 cm^{-1} frequencies in Raman spectra of both solid- and liquid-state of 1*H*,4*H*-piperazine-dium dichlorosulfonate. A combination of the S-Cl stretches and the S-Cl wag was attributed to 675 cm^{-1} frequencies in FTIR.

CHAPTER FOUR

ARTICLE 2

SYNTHESIS OF NEW DIHYDRO-[1,2,4]TRIAZOLO[1,5- α]PYRIMIDE
SCAFFOLDS] USING 1*H*,4*H*-PIPERAZINE-DIUM DICHLOROSULFONATE

4.1 Introduction

In recent years, the design and development of new ionic liquids (ILs) and their applications have been widely studied as solvents and/or catalysts in organic synthesis, primarily due to their distinct properties, including low volatility and vapor pressure, and good to high thermal and chemical stability. The polarity and physical properties of ILs are tunable and designable by judicious choice of cations or anions, which is the most prominent feature of ILs (Khaligh et al, 2019). Furthermore, the easy separation of organic products from and recyclability of ILs are seen as other notable merits of IL applications in most organic transformations. These advantages lead to avoiding the generation of metal-containing waste and minimizing the use of toxic, volatile, and flammable organic solvents (Mihankhah et al, 2018; Khaligh et al, 2018; Khaligh et al, 2019).

Triazolo-pyrimidines constitute an influential class of bicyclic nitrogen heterocycles. They have been extensively studied due to their broad range of biological and pharmaceutical activities (Oukoloff et al, 2019), including anticancer (Zhang et al, 2007), antiparasitic (Esteban et al, 2019), antimicrobial (Abd et al, 2020), antibacterial (Wang et al, 2015), antiproliferative and anti-tubulin (Yang et al, 2019), anti-HIV (Huang et al, 2015), and anti-fungal (Chen et al, 2008) properties. Triazolo[1,5- α]pyrimidines are often prepared through a one-pot three-component condensation of aryl

aldehydes, active methylene compounds, and aminotriazoles in the presence of catalytic system. Due to their biological and pharmaceutical properties, extensive studies have been reported to access new substituted triazolo[1,5- α]pyrimidines (Fizer et al, 2016). Each reported method has merits and limits/disadvantages. Some disadvantages include the a) high cost of catalyst preparation due to two or more preparative steps which leads to the generation of more waste, b) use of toxic, volatile, and/or highly flammable solvents, c) use of expensive, toxic, and non-recyclable catalysts, d) tedious and time-consuming workup, and e) generation of toxic waste. Therefore, the design and development of safe and greener processes as well as inexpensive, non-toxic, and recyclable catalysts are highly demanded.

In continuing our research on the synthesis of new ILs and their applications in various organic transformations as the solvent and/or catalyst, we designed and synthesized a new IL. Two structures were proposed for the new IL, in which the structure of 1*H*,4*H*-piperazine-dium dichlorosulfonate ($[\text{PZH}_2]^{2+}2[\text{ClSO}_3]^-$) was confirmed by 1D and 2D NMR, FT-IR, Raman, and mass spectrum analysis. Furthermore, the dual solvent-catalyst activity of the new IL was demonstrated for the synthesis of new dihydro[1,2,4]triazolo[1,5 α]pyrimidine scaffolds.

4.2 Methodology

General materials, characterizations and methodology refers to 3.2.1.

4.2.1 Typical procedure for the synthesis of 2-amino-4-aryl-7,7-demethyl-5-oxo-5,6,7,8-tetrahydro-4*H*-chromene-3-carbonitrie (2a-j)

A mixture of aromatic aldehyde (0.20 mmol), ethyl cyanoacetate (23.39 mg, 0.022 mL, 0.21 mmol), and 3-amino-1,2,4-triazole (16.82 mg, 0.21 mmol) was stirred in 0.5 mL of $[\text{PZH}_2]^{2+}2[\text{ClSO}_3]^-$ at 35°C for appropriate reaction times. After completion of the reaction, the product was extracted by EtOAc (5 x 5 mL). The crude product was purified by recrystallization from ethanol after removal of EtOAc by rotary evaporator at reduced pressure.

4.2.2 Ethyl 5-amino-7-(4-chlorophenyl)-4,7-dihydro-[1,2,4]triazolo[1,5- α]pyrimidine -6-carboxylate (2a)

Compound **2a** was obtained as a white solid, melting point 190-191°C; δ_{H} (400 MHz, DMSO- d_6) 8.83 (s, 2H), 8.41 (s, 1H), 8.07 (d, J 8.6, 2H), 7.66 (d, J 8.6, 2H), 6.56 (s, 1H), 5.65 (s, 1H), 4.31 (q, J 7.2, 2H), 1.30 (t, J 7.2, 3H). δ_{C} (100 MHz, DMSO- d_6) 161.6, 153.6, 143.1, 138.0, 132.4, 130.2, 129.4, 115.4, 103.2, 62.44, 51.7, 14.0. Anal. Calc. for $\text{C}_{14}\text{H}_{14}\text{ClN}_5\text{O}_2$: C 52.59, H 4.41, N 21.90. Found: C 52.57, H 4.45, N 21.87%.

4.2.3 Ethyl 5-amino-7-(4-bromophenyl)-4,7-dihydro-[1,2,4]triazolo[1,5- α]pyrimidine -6-carboxylate (2b)

Compound **2b** was obtained as a white solid, melting point 184-185°C; δ_{H} (400 MHz, DMSO- d_6) 8.68 (s, 2H), 8.42 (s, 1H), 7.98 (d, J 8.6, 2H), 7.83-7.80 (d, J 1.6 and 8.6, 2H), 6.43 (s, 1H), 5.63 (s, 1H), 4.36 (q, J 7.2, 2H), 1.30 (t, J 7.2, 3H). δ_{C} (100 MHz, DMSO-

*d*₆) 161.6, 153.8, 140.0, 132.4, 132.4, 130.5, 127.1, 115.4, 103.4, 62.4, 52.0, 14.0. Anal. Calc. for C₁₄H₁₄BrN₅O₂: C 46.17, H 3.87, N 19.23. Found: C 46.14, H 3.91, N 19.21%.

4.2.4 Ethyl 5-amino-7-(4-nitrophenyl)-4,7-dihydro-[1,2,4]triazolo[1,5-*a*]pyrimidine -6-carboxylate (2c)

Compound **2c** was obtained as a white solid, melting point 197-198°C; δ_{H} (400 MHz, DMSO-*d*₆) 8.85 (s, 1H), 8.53 (s, 2H), 8.04 (d, *J* 8.2, 1H), 7.63 (d, *J* 8.6 2H), 6.61 (s, 1H), 5.64 (s, 1H), 4.34 (q, *J* 7.2, 2H), 1.34 (t, *J* 7.2, 3H). δ_{C} (100 MHz, DMSO-*d*₆) 163.6, 152.9, 143.2, 139.2, 132.5, 130.5, 128.2, 115.3, 103.2, 62.3, 51.8, 14.0. Anal. Calc. for C₁₄H₁₄N₆O₄: C 50.91, H 4.27, N 25.44. Found: C 50.88, H 4.32, N 25.47%.

4.2.5 Ethyl 5-amino-7-(2-nitrophenyl)-4,7-dihydro-[1,2,4]triazolo[1,5-*a*]pyrimidine -6-carboxylate (2d)

Compound **2d** was obtained as a white solid, melting point 183-184°C; δ_{H} (400 MHz, DMSO-*d*₆) 8.83 (s, 1H), 8.55 (s, 2H), 8.32 (d, *J* 8.2, 1H), 7.97-7.91 (m, 2H), 7.84 (t, *J* 7.6, 1H), 6.61 (s, 1H), 4.35 (q, *J* 7.0, 2H), 1.33 (t, *J* 7.0 3H). δ_{C} (100 MHz, DMSO-*d*₆) 160.9, 154.9, 147.2, 141.2, 134.7, 132.5, 130.5, 128.2, 125.2, 114.2, 107.4, 62.7, 52.0, 13.9. Anal. Calc. for C₁₄H₁₄N₆O₄: C 50.91, H 4.27, N 25.44. Found: C 50.86, H 4.33, N 25.41%.

4.2.6 Ethyl 5-amino-7-(4-methoxyphenyl)-4,7-dihydro-[1,2,4]triazolo[1,5-*a*]pyrimidine-6-carboxylate (2e)

Compound **2e** was obtained as a white solid, melting point 187-188°C; δ_{H} (400 MHz, DMSO-*d*₆) 8.57 (s, 1H), 8.07 (d, *J* 8.8, 2H), 7.13 (d, *J* 8.8, 2H), 6.43 (s, 1H, NH), 5.22 (s, 1H, CH), 4.28 (q, *J* 7.0, 2H), 3.85 (s, 3H), 1.28 (t, *J* 7.0 3H). δ_{C} (100 MHz, DMSO-*d*₆)

163.5, 162.3, 154.4, 137.1, 133.5, 123.9, 116.2, 114.9, 98.5, 62.0, 55.7, 51.7, 14.0. Anal. Calc. for C₁₅H₁₇N₅O₃: C 57.13, H 5.43, N 22.21 Found: C 57.08, H 5.47, N 22.24%.

4.2.7 Ethyl 5-amino-7-(2-methoxyphenyl)-4,7-dihydro-[1,2,4]triazolo[1,5- α]pyrimidine-6-carboxylate (2f)

Compound **2f** was obtained as a white solid, melting point 205-206°C; δ_{H} (400 MHz, DMSO-*d*₆) 8.54 (s, 1H), 8.35 (s), 8.12 (d, *J* 7.8, 1H), 7.64-7.59 (m, 1H), 7.20-7.17 (m, 1H), 7.13-7.09 (m, 1H), 6.37 (s, 1H), 5.65 (s, 1H), 4.30 (q, *J* 7.0, 2H), 3.87 (s, 3H), 1.29 (t, *J* 7.0, 3H). δ_{C} (100 MHz, DMSO-*d*₆) 161.9, 158.8, 148.9, 140.6, 135.5, 128.4, 120.7, 119.7, 115.6, 112.1, 102.1, 62.3, 56.0, 51.7, 13.9. Anal. Calc. for C₁₅H₁₇N₅O₃: C 57.13, H 5.43, N 22.21 Found: C 57.11, H 5.45, N 22.18%.

4.2.8 Ethyl 5-amino-7-(3,4-dimethoxyphenyl)-4,7-dihydro-[1,2,4]triazolo[1,5- α]pyrimidine-6-carboxylate (2g)

Compound **2g** was obtained as a white solid, melting point 190-191°C; δ_{H} (400 MHz, DMSO-*d*₆) 8.45 (s, 2H), 8.23 (s, 1H), 7.72 (s, 1H), 7.69 (dd, *J* 8.6 and 1.6, 1H), 7.14 (d, *J* 8.4, 1H), 6.38 (s, 1H), 5.21 (s, 1H), 4.30 (q, *J* 7.0, 2H), 3.88 (s, 3H), 3.80 (s, 3H), 1.3 (t, *J* 7.0, 3H). δ_{C} (100 MHz, DMSO-*d*₆) 162.4, 154.6, 153.6, 148.8, 131.1, 126.8, 124.0, 116.3, 113.0, 111.9, 98.6, 62.0, 56.0, 55.5, 52.0, 14.0. Anal. Calc. for C₁₆H₁₉N₅O₄: C 55.64, H 5.55, N 20.28 Found: C 55.61, H 5.58, N 20.24%.

4.2.9 Ethyl 5-amino-7-(2,4,6-trimethoxyphenyl)-4,7-dihydro-[1,2,4]triazolo[1,5- α]pyrimidine-6-carboxylate (2h)

Compound **2h** was obtained as a white solid, melting point 206-207°C; δ_{H} (400 MHz, DMSO-*d*₆) 8.61 (s, 2H), 8.26 (s, 1H), 6.65 (s, 1H), 6.31 (s, 2H), 5.71 (s, 1H), 4.25 (d, *J*

7.0, 2H), 3.86 (s, 3H), 3.84 (s, 6H), 1.26 (t, *J* 7.0, 3H). δ_C (100 MHz, DMSO-*d*₆) 165.8, 163.1, 160.8, 146.7, 140.0, 115.6, 103.2, 102.1, 91.0, 61.8, 55.8, 55.6, 51.4, 14.0. Anal. Calc. for C₁₇H₂₁N₅O₅: C 54.39, H 5.64, N 18.66 Found: C 54.42, H 5.59, N 18.61%.

4.2.10 Ethyl 5-amino-7-(3,4,5-trimethoxyphenyl)-4,7-dihydro-[1,2,4]triazolo[1,5-*a*]-pyrimidine-6-carboxylate (2i)

Compound **2i** was obtained as a white solid, melting point 211-212°C; δ_H (400 MHz, DMSO-*d*₆) 8.62 (s, 2H), 8.27 (s, 1H), 6.66 (s, 1H), 6.43 (s, 2H), 5.61 (s, 1H), 4.29 (q, *J* 7.0, 2H), 3.82 (s, 3H), 3.80 (s, 6H), 1.28 (t, *J* 7.0, 3H). δ_C (100 MHz, DMSO-*d*₆) 167.4, 165.8, 160.8, 141.7, 130.0, 105.6, 102.1, 91.0, 62.0, 55.8, 51.4, 14.0. Anal. Calc. for C₁₇H₂₁N₅O₅: C 54.39, H 5.64, N 18.66 Found: C 54.41, H 5.57, N 18.69%.

4.2.11 Ethyl 5-amino-7-(4-(dimethylamino)phenyl)-4,7-dihydro-[1,2,4]triazolo[1,5-*a*]-pyrimidine-6-carboxylate (2j)

Compound **2j** was obtained as a yellow solid, melting point 181-182°C; δ_H (400 MHz, DMSO-*d*₆) 8.36 (s, 2H), 8.06 (s, 1H), 7.92 (d, *J* 9.0, 2H), 6.81 (d, *J* 9.0, 2H), 6.27 (s, 1H), 5.21 (s, 1H), 4.24 (q, *J* 7.0, 2H), 3.05 (s, 6H), 1.25 (t, *J* 7.0, 3H). δ_C (100 MHz, DMSO-*d*₆) 163.4, 154.1, 153.7, 137.2, 133.7, 118.3, 117.5, 111.6, 92.0, 61.4, 52.6, 40.1, 14.1. Anal. Calc. for C₁₇H₂₁N₅O₅: C 58.52, H 6.14, N 25.59. Found: C 58.48, H 6.19, N 25.56%.

4.3 Results and Discussion

4.3.1 Dual Solvent-Catalyst Activity of the New IL

Initially, the condensation of 4-chlorobenzaldehyde (**1a**), ethyl cyanoacetate, and 3-amino-1,2,4-triazole were chosen as a model reaction. A few spots were detected by TLC,

along with the aldehyde spot, when the model reactants were stirred in ethanol as solvent at 35°C which showed complete conversion and ethyl 5-amino-7-(4-chlorophenyl)-4,7-dihydro-[1,2,4]triazolo[1,5-a]pyrimidine-6-carboxylate (**2a**) was isolated in 32% yield after workup and recrystallization from hot ethanol (Table 4.1, entry 2). A notable improvement was observed when the amount of $[\text{PZH}_2]^{2+}2[\text{ClSO}_3]^-$ was increased to 0.5 mL (Table 4.1, entries 3 and 4). The model reaction was then carried out in the presence of $[\text{PZH}_2]^{2+}2[\text{ClSO}_3]^-$ as the reaction medium and catalyst which led to 82% yield after 2 h (Table 4.1, entry 5). The shorter reaction times resulted in lower yields of the desired product (Table 4.1, entries 6 and 7). A remarkable decrease in yield was observed when the model reaction was conducted in water as a solvent, which is probably due to the limited solubility of reactants in the aqueous medium. Based on the results mentioned above, we selected entry 5 in Table 4.1 as the optimal experimental conditions.

Table 4.1: Optimization of the synthesis of ethyl 5-amino-7-(4-chlorophenyl)-4,7-dihydro-[1,2,4]triazolo[1,5-a]pyrimidine-6-carboxylate

Entry ^A	Vol. $[\text{PZH}_2]^{2+}2[\text{ClSO}_3]^-$ [mL]	Solvent	Reaction time [h]	Yield [%] ^B
1	0.0	EtOH	2.0	— ^C
2	0.02	EtOH	2.0	32
3	0.1	EtOH	2.0	52
4	0.5	EtOH	2.0	76
5	0.5	Neat	2.0	82 ^D
6	0.5	Neat	1.0	62
7	0.5	Neat	1.5	78
8	0.5	Deionized water	2.0	64

^AReaction conditions: 4-chlorobenzaldehyde (**1a**) (70.3 mg, 0.5 mmol), ethyl cyanoacetate (0.053 mL, 0.5 mmol), and 3-amino-1,2,4-triazole (42.0 g, 0.5 mmol), solvent (1.0 mL), reaction temperature 35°C.

^BIsolated yield.

^CMixture of products and incomplete conversion.

^DThe chosen optimal conditions.

The substrate scope of the current application of $[\text{PZH}_2]^{2+}2[\text{ClSO}_3]^-$ as a dual solvent-catalyst was demonstrated for the preparation of 5-amino-7-aryl-4,7-dihydro [1,2,4]triazolo[1,5-*a*]pyrimidine-6-carboxylate derivatives through the condensation of various substituted aromatic aldehydes **1a-j**, ethyl cyanoacetate, and 3-amino-1,2,4-triazole under optimized reaction conditions (Figure 4.3).

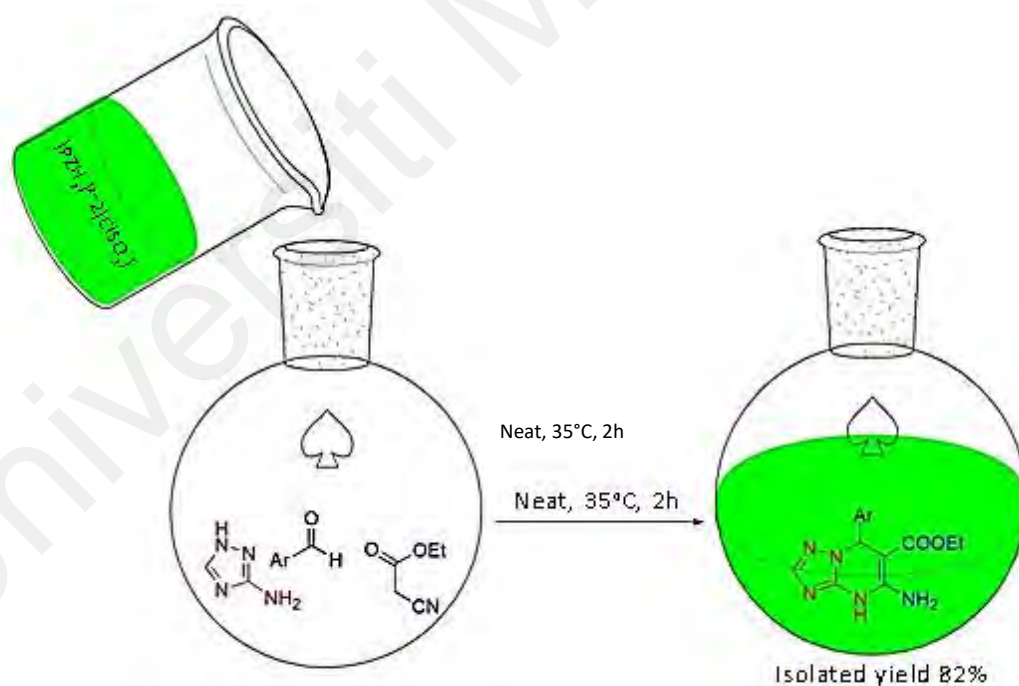
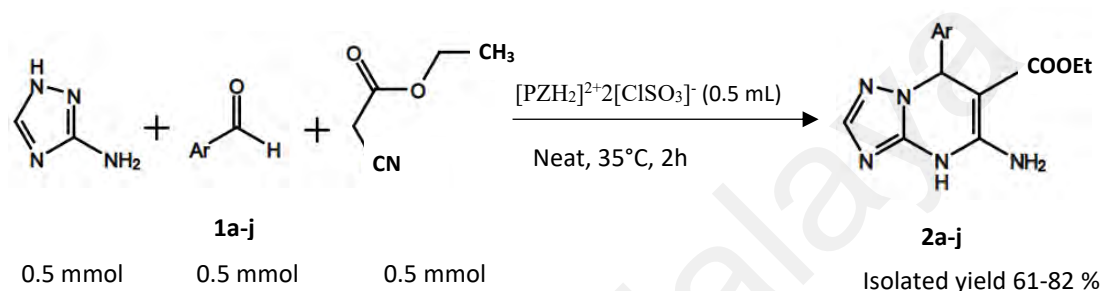


Figure 4.3: Synthesis of 5-amino-7-aryl-4,7-dihydro-[1,2,4]triazolo[1,5-*a*]pyrimidine-6-carboxylates under optimized reaction conditions.

A variety of aromatic aldehydes bearing electron-withdrawing or donating substituents were examined under optimized reaction conditions. The functional groups such as methoxy, nitro, and halides were tolerated without the formation of any by-products (Table 4.2). The nature and position of substituents of the aromatic aldehyde demonstrated a significant influence on the yields and reaction times. When electron-withdrawing groups were on aromatic aldehydes, the reactions were completed within the shorter reaction times and offered higher yields than electron-donating substituents in the same positions (Table 4.2, entries 1-4 and 10).

The aromatic aldehydes with electron-withdrawing groups at the *para*-position afforded higher yields than the electron-donating groups at the same positions (Table 4.2, entries 1-3, 5, 7-9). Furthermore, the substituents at the *para*-position of the aromatic aldehydes gave higher yields than the same substituents at the *meta*- or *ortho*-positions (Table 4.2, entries 3-6). 4-(Dimethylamino)benzaldehyde afforded a low yield (61 %) under optimal conditions, which could be attributed to the inductive and resonance effect of the dimethylamino group (Table 4.2, entry 10). All products were characterized by melting point, ^1H and ^{13}C NMR spectra, and elemental analysis (see Figures A.13 – A.22).

The above mentioned results demonstrate the dual solvent-catalyst efficiency of $[\text{PZH}_2]^{2+}2[\text{ClSO}_3]^-$ for the synthesis of triazolo[1,5-*a*]pyrimidines as a typical one-pot multicomponent reaction.

According to the proposed mechanism, both aldehyde and ethyl cyanoacetate can be initially activated by $[\text{PZH}_2]^{2+}2[\text{ClSO}_3]^-$ through hydrogen bond formation (Figure 4.4). Intermediate **IV** is formed through a nucleophilic attack of ethyl cyanoacetate to the activated aldehyde. The Knoevenagel intermediate **V** is formed via dehydration of

the intermediate **IV**. $[\text{PZH}_2]^{2+}2[\text{ClSO}_3]^-$ can promote the dehydration step as a dehydrating agent (Zhang et al, 2007). The $[\text{PZH}_2]^{2+}2[\text{ClSO}_3]^-$ activates 3-amino-1,2,4-triazole, which reacts with the Knoevenagel intermediate **V** and affords the intermediate **VI**. Finally, an intramolecular cyclisation gives the triazolo[1,5-*a*]-pyrimidine.

Table 4.2: The one-pot multicomponent synthesis of triazolo[1,5-*a*]pyrimidines in the presence of $[\text{PZH}_2]^{2+}2[\text{ClSO}_3]^-$ under optimized reaction conditions

Entry ^A	Aldehydes 1a-j	Product Triazolo[1,5- <i>a</i>]pyrimidines 2a-j	Reaction time [min]	Yield [%] ^B
1	1a , Ar = 4-Cl-C ₆ H ₄ ⁻	2a	120	82
2	1b , Ar = 4-Br-C ₆ H ₄ ⁻	2b	120	80
3	1c , Ar = 4-NO ₂ -C ₆ H ₄ ⁻	2c	115	82
4	1d , Ar = 2-NO ₂ -C ₆ H ₄ ⁻	2d	130	70
5	1e , Ar = 4-(CH ₃ O)-C ₆ H ₄ ⁻	2e	145	75
6	1f , Ar = 2-(CH ₃ O)-C ₆ H ₄ ⁻	2f	145	70
7	1g , Ar = 3,4-(CH ₃ O)-C ₆ H ₃ ⁻	2g	140	73
8	1h , Ar = 2,4,6-(CH ₃ O) ₃ -C ₆ H ₂ ⁻	2h	165	70
9	1i , Ar = 3,4,5-(CH ₃ O) ₃ -C ₆ H ₂ ⁻	2i	140	71
10	1j , Ar = 4-(CH ₃) ₂ N-C ₆ H ₄ ⁻	2j	170	61

^AReaction conditions: various aldehydes **1a-j** (0.5 mmol), ethyl cyanoacetate (0.5 mmol), 3-amino-1,2,4-triazole (0.5 mmol), 1 mL of $[\text{PZH}_2]^{2+}2[\text{ClSO}_3]^-$, reaction temperature 35°C.

^BIsolated yield.

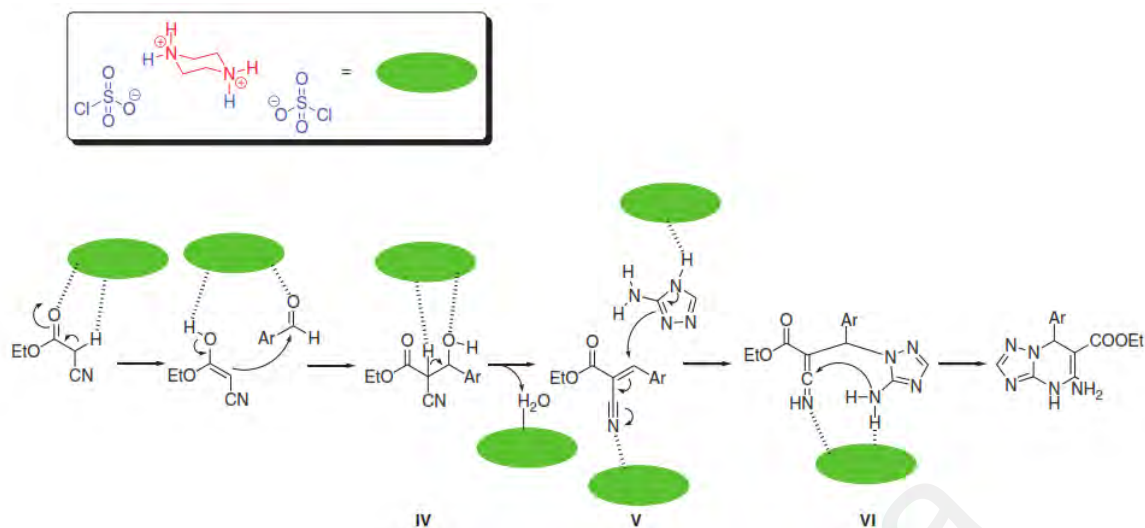


Figure 4.4: A schematic reaction mechanism of the synthesis of triazolo[1,5-a]pyrimidines in the presence of $[PZH_2]^{2+}2[ClSO_3]^-$

A large scale experiment was investigated by the condensation 7.0 g of 4-chlorobenzaldehyde (**1a**) with ethyl cyanoacetate and 3-amino-1,2,4-triazole in 5 mL of $[PZH_2]^{2+}2[ClSO_3]^-$ under optimized reaction conditions. The desired product **2a** was isolated in 76 % yield after 2 h.

4.3.2 Easy Separation and Recyclability of the New IL

The products were separated via extraction by ethyl acetate after completion of the reaction. After removing ethyl acetate at a reduced pressure by rotary evaporation, pure products were obtained by recrystallizing from ethanol. The new IL was dried under vacuum and was used for the next run. The results demonstrated that the recovered IL could be reused up to 10 times without significant loss in efficiency and afforded **2a** in the range of 82-76 % isolated yield (Figure 4.5).

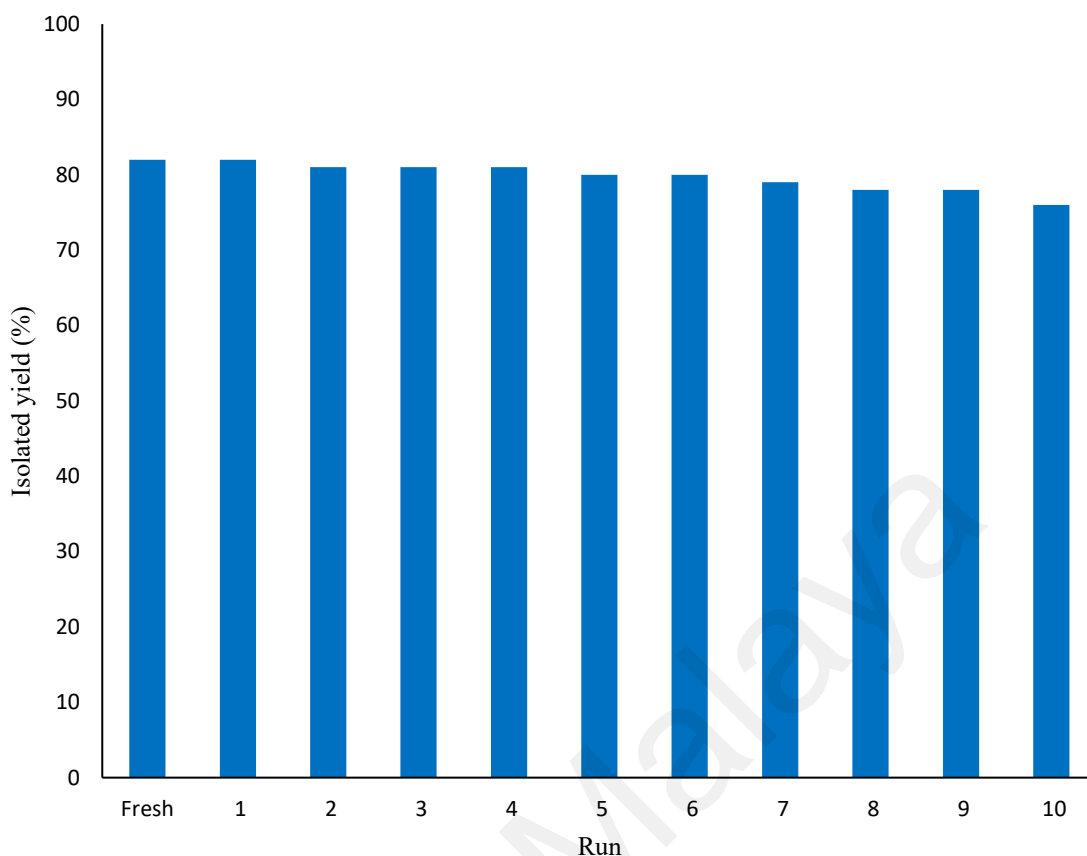


Figure 4.5: Catalytic efficiency of recycled $[\text{PZH}_2]^{2+}2[\text{ClSO}_3]^-$

4.4 Conclusion

In conclusion, a novel ionic liquid containing chlorosulfonate anions was designed and synthesized. The structure elucidation of this ionic liquid was conducted by 1D and 2D NMR, FT-IR, Raman, and mass spectra analysis. The prominent physical properties of this ionic liquid were measured and reported. The nucleophilic attack of the nitrogen atom of the piperazine ring to the central atom of chlorosulfonic acid seems unlikely, primarily due to steric hindrance of the sulfur atom by chlorine and oxygen atoms. Hence, the piperazine and chlorosulfonic acid formed structure **II** through an acid-base reaction. The dual-solvent-catalyst efficiency of $[\text{PZH}_2]^{2+}2[\text{ClSO}_3]^-$ was demonstrated to promote a one-pot three-component reaction under mild conditions. The current protocol has advantages such as being a relatively simple and sustainable procedure, giving a high

yield of the desired products at 35°C, it avoids the use of toxic and volatile organic solvents, requires a simple workup, and allows recyclability of the IL. All mentioned merits will lead to reducing heavy metal and corrosive waste generation. Further research on the investigation of properties and applications of $[\text{PZH}_2]^{2+}2[\text{ClSO}_3]^-$ is underway in our laboratory.

Universiti Malaya

CHAPTER FIVE

ARTICLE 3

THE STRUCTURE ELUCIDATION OF NEW IONIC LIQUID AND ITS
APPLICATION FOR THE SYNTHESIS OF A SERIES OF NOVEL
TRIAZOLO[1,5- α]PYRIMIDINE SCAFFOLDS

5.1 Introduction

New catalysts and processes have been designed and introduced to follow some basic principles of green chemistry such as use less toxic and less volatile reagents and solvents during the reaction and workup, conduct the reaction in the absence of solvent, reduce the generation of the hazardous waste, utilize a small amounts of catalysts, and use the recyclable organocatalysts instead of using toxic metal-containing and non-recyclable catalysts (Tanaka et al, 2000; Wenda et al, 2011).

Triazolo-pyrimidines constitute a significant class of bicyclic heterocycles containing nitrogen which have been broadly synthesized and reported due to a wide range of biological and pharmaceutical activities (Oukoloff et al, 2019) such as anticancer (Zhang et al 2007), antiparasitic (Esteban et al, 2019), antimicrobial (Abd et al, 2020), antibacterial (Wang et al, 2015), antiproliferative and antitubulin (Yang et al, 2019), anti-HIV (Huang et al, 2015), and anti-fungal (Chen et al, 2008). Triazolo [1,5- α]pyrimidine derivatives are often synthesized through a one-pot multicomponent condensation of aryl aldehydes, aminotriazoles, and compounds bearing an active methylene moiety, and in the presence of a catalytic system. Extensive studies have been reported to access a broad range of the substituted triazolo [1,5- α]pyrimidine (Fischer, 2007). Very recently, the bismuth loaded on fluorapatite ($\text{Bi}_2\text{O}_3/\text{FAp}$) was used for the preparation of 1,2,4-triazolo

[1,5- α]pyrimidine scaffolds in ethanol at room temperature (Kerru et al, 2020). The methods have merits and certain limits/disadvantages. Some disadvantages are including (a) exist two or more preparative steps that increase the preparation cost, (b) use of toxic, flammable, or volatile solvents, (c) use of expensive, toxic, or non-reusable catalysts, (d) tedious workup, and ϵ generation of toxic, hazard, or corrosive waste. Furthermore, the preparation of the pharmaceutical and medicine products using Lewis acids is not appropriate due to their high toxicity (Rao et al, 2007). Also, some of substituents such as methoxy, nitro, cyano, as well as heterocycle aldehydes containing nitrogen and sulfur atoms, or coordination of their acidic sites (Hirunsit et al, 2018). Moreover, most of Lewis acids require an activation step before application. Therefore, the designing and development of easy separable and recyclable heterogeneous organocatalyst are highly demanded. Which can be used in the catalytic amount and greener conditions.

Recently, the synthesis of new ionic liquid (IL) named 4,4'-trimethylene-*N,N'*-sulfonic acid-dipiperidinium chloride was reported by our group. New low-viscose IL was characterized and successfully applied as an efficient catalyst for the synthesis of 4*H*-pyrans (Khaligh et al, 2019). Herein, the chemical structure of this IL is corrected regarding 1D NMR and 2D NMR, especially by $^1\text{H}, ^1\text{H}$ -COSY. The existence of chlorosulfonate anion in new IL was supported by the frequencies in FTIR and Raman Spectra, which were in good agreement with previous reports for chlorosulfonate anion in the literature. Also, the dual solvent-catalyst activity of new IL, as an extension of solvent and catalytic efficiency of new IL, was demonstrated for the synthesis of a series of novel dihydro-[1,2,4] triazolo [1,5- α]pyrimidine scaffolds under mild conditions.

5.2 Methodology

5.2.1 Material and Method

General materials, characterizations and methodology refers to 3.2.1.

5.2.2 The synthesis of 4,4'-trimethylene-*N,N'*-dipiperidinium dichlorosulfonate [TMDPH₂]²⁺2[ClSO₃]⁻

The neat chlorosulfonic acid (3.0 ml, 40 mmol) was dropwise added to 4,4'-trimethylene-dipiperidine (4.21 g, 20 mmol) in dry CH₂Cl₂ (20 mL). The reaction mixture was stirred at room temperature for overnight, which led to the formation of two phases. The upper phases were decanted, the residue was washed with CH₂Cl₂ (3 x 5 mL), and excess of solvent was removed under reduced pressure. The resulting ionic liquid was isolated 8.34 g (94%) as a low-viscous pale-yellow liquid.

5.2.3 The typical procedure for the synthesis of 2-amino-4-aryl-7,7-dimethyl-5-oxo-5,6,7,8-tetrahydro-4*H*-chromene-3-carbonitrile (2a-j)

A mixture of aromatic aldehyde (0.5 mmol), ethyl cyanoacetate (0.053 mL, 0.5 mmol), and 3-amino-1,2,4-triazole (42 mg, 0.5 mmol) was stirred in 1.0 mL of [TMDPH₂]²⁺2[ClSO₃]⁻ at room temperature for appropriate reaction times. After completion, the products were extracted with ethyl acetate (3 x 5 mL). The organic layers were combined and dried over anhydrous Na₂SO₄. The solvent was evaporated under vacuum after filtration. The pure products were obtained by recrystallization from ethanol. The residue IL was also dried into an oven at 50 °C for 4 h and used in the next runs.

5.2.4 Physical and spectra data of new dihydro-[1,2,4]triazolo[1,5- α]pyrimidines

Ethyl 5-amino-7-(4-chlorophenyl)-4,7-dihydro-[1,2,4]triazolo [1,5- α]pyrimidine-6-carboxylate (**2a**)

0.147 g of white solid (92%), m.p. 190-191 °C; ^1H NMR (400 MHz, DMSO- d_6) δ 8.83 (s, 2H), 8.41 (s, 1H) 8.07 (d, $J = 8.6$ Hz, 2H), 7.66 (d, $J = 8.6$ Hz, 2H), 6.56 (s, 1H), 5.65 (s, 1H), 4.31 (q, $J = 7.2$ Hz, 2H), 1.30 (t, $J = 7.2$ Hz, 3H) ppm; ^{13}C NMR (100 MHz, DMSO- d_6) δ 161.6, 153.6, 143.1, 138.0, 132.4, 130.2, 129.4, 115.4, 103.2, 62.44, 51.7, 14.0 ppm; Anal. Calcd. For $\text{C}_{14}\text{H}_{14}\text{ClN}_5\text{O}_2$: C, 52.59; H, 4.41; N, 21.90; Found: C, 52.57; H, 4.45; N, 21.87.

Ethyl 5-amino-7-(4-bromophenyl)-4,7-dihydro-[1,2,4]triazolo[1,5- α]pyrimidine -6-carboxylate (**2b**)

0.166 g of white solid (91%), m. p. 184-185°C; ^1H (400 MHz, DMSO- d_6) δ 8.68 (s, 2H), 8.42 (s, 1H), 7.81 (d, $J = 8.6$, 2H), 6.43 (s, 1H), 5.63 (s, 1H), 4.36 (q, $J = 7.2$, 2H), 1.30 (t, $J = 7.2$ Hz, 3H) ppm. ^{13}C NMR (100 MHz, DMSO- d_6) δ 161.6, 153.8, 140.0, 132.4, 132.4, 130.5, 127.1, 115.4, 103.4, 62.4, 52.0, 14.0 ppm; Anal. Calc. for $\text{C}_{14}\text{H}_{14}\text{BrN}_5\text{O}_2$: C, 46.17; H 3.87; N, 19.23; Found: C, 46.14; H, 3.91; N, 19.21.

Ethyl 5-amino-7-(4-nitrophenyl)-4,7-dihydro-[1,2,4]triazolo[1,5- α] pyrimidine -6-carboxylate (**2c**)

0.155 g of white solid (94%), m. p. 197-198°C; ^1H NMR (400 MHz, DMSO- d_6) δ 8.85 (s, 1H), 8.53 (s, 2H), 8.04 (d, $J = 8.2$ Hz, 1H), 7.63 (d, $J = 8.2$ Hz, 2H), 6.61 (s, 1H), 5.64 (s, 1H), 4.34 (q, $J = 7.2$ Hz, 2H), 1.34 (t, $J = 7.2$ Hz, 3H) ppm. ^{13}C NMR (100 MHz, DMSO- d_6) δ 163.6, 152.9, 143.2, 139.2, 132.5, 130.5, 128.2, 115.3, 103.2, 62.3, 51.8, 14.0 ppm; Anal. Calc. for $\text{C}_{14}\text{H}_{14}\text{N}_6\text{O}_4$: C, 50.91; H, 4.27; N, 25.44; Found: C, 50.88; H, 4.32; N, 25.47.

Ethyl 5-amino-7-(2-nitrophenyl)-4,7-dihydro-[1,2,4]triazolo[1,5-*a*] pyrimidine -6-carboxylate (**2d**)

0.137 g of white solid (83%), m. p. 183-184°C; ¹H NMR (400 MHz, DMSO-*d*₆) δ 8.83 (s, 1H), 8.55 (s, 2H), 8.32 (d, *J* = 8.2 Hz, 1H), 7.97-7.91 (m, 2H), 7.84 (t, *J* = 7.6 Hz, 1H), 6.61 (s, 1H), 5.63 (s, 1H), 4.35 (q, *J* = 7.0 Hz, 2H), 1.33 (t, *J* = 7.0 Hz, 3H) ppm. ¹³C NMR (100 MHz, DMSO-*d*₆) δ 160.9, 154.9, 147.2, 141.2, 134.7, 132.5, 130.5, 128.2, 125.2, 114.2, 107.4, 62.7, 52.0, 13.9; Anal. Calc. for C₁₄H₁₄N₆O₄: C, 50.91; H, 4.27; N, 25.44; Found: C, 50.86; H, 4.33; N, 25.41.

Ethyl 5-amino-7-(4-methoxyphenyl)-4,7-dihydro-[1,2,4]triazolo[1,5-*a*] pyrimidine-6-carboxylate (**2e**)

0.136 g of white solid (86%), m. p. 187-188°C; ¹H NMR (400 MHz, DMSO-*d*₆) δ 8.57 (s, 2H), 8.31 (s, 1H), 8.07 (d, *J* = 8.8 Hz, 2H), 7.13 (d, *J* = 8.8 Hz, 2H), 6.43 (s, 1H, NH), 5.22 (s, 1H, CH), 4.28 (q, *J* = 7.0 Hz, 2H), 3.85 (s, 3H), 1.28 (t, *J* = 7.0 Hz, 3H) ppm. ¹³C NMR (100 MHz, DMSO-*d*₆) δ 163.5, 162.3, 154.4, 137.1, 133.5, 123.9, 116.2, 114.9, 98.5, 62.0, 55.7, 51.7, 14.0 ppm; Anal. Calc. for C₁₅H₁₇N₅O₃: C, 57.13; H, 5.43; N, 22.21; Found: C, 57.08; H, 5.47; N 22.24.

Ethyl 5-amino-7-(2-methoxyphenyl)-4,7-dihydro-[1,2,4]triazolo[1,5-*a*] pyrimidine-6-carboxylate (**2f**)

0.126 g of white solid (80%), m. p. 205-206°C; ¹H NMR (400 MHz, DMSO-*d*₆) δ 8.54 (s, 1H), 8.35 (s), 8.12 (d, *J* = 7.8 Hz, 1H), 7.64-7.59 (m, 1H), 7.20-7.17 (m, 1H), 7.13-7.09 (m, 1H), 6.37 (s, 1H), 5.65 (s, 1H), 4.30 (q, *J* = 7.0 Hz, 2H), 3.87 (s, 3H), 1.29 (t, *J* = 7.0 Hz, 3H) ppm. ¹³C NMR (100 MHz, DMSO-*d*₆) δ 161.9, 158.8, 148.9, 140.6, 135.5, 128.4, 120.7, 119.7, 115.6, 112.1, 102.1, 62.3, 56.0, 51.7, 13.9 ppm; Anal. Calc. for C₁₅H₁₇N₅O₃: C, 57.13; H, 5.43; N, 22.21; Found: C, 57.11; H, 5.45; N, 22.18.

Ethyl 5-amino-7-(3,4-dimethoxyphenyl)-4,7-dihydro-[1,2,4]triazolo[1,5- α]pyrimidine-6-carboxylate (**2g**)

0.147 g of white solid (85%), m. p. 190-191°C; ^1H NMR (400 MHz, DMSO- d_6) δ 8.45 (s, 2H), 8.23 (s, 1H), 7.72 (s, 1H), 7.69 (dd, $J = 8.6$ and 1.6 Hz, 1H), 7.14 (d, $J = 8.4$, 1H), 6.38 (s, 1H), 5.21 (s, 1H), 4.30 (q, $J = 7.0$ Hz, 2H), 3.88 (s, 3H), 3.80 (s, 3H), 1.3 (t, $J = 7.0$, 3H) ppm. ^{13}C NMR (100 MHz, DMSO- d_6) δ 162.4, 154.6, 153.6, 148.8, 131.1, 126.8, 124.0, 116.3, 113.0, 111.9, 98.6, 62.0, 56.0, 55.5, 52.0, 14.0 ppm. Anal. Calc. for $\text{C}_{16}\text{H}_{19}\text{N}_5\text{O}_4$: C, 55.64; H, 5.55; N, 20.28; Found: C, 55.61; H, 5.58; N, 20.24.

Ethyl 5-amino-7-(2,4,6-trimethoxyphenyl)-4,7-dihydro-[1,2,4]triazolo[1,5- α]pyrimidine-6-carboxylate (**2h**)

0.150 g of white solid (80%), m. p. 206-207°C; ^1H NMR (400 MHz, DMSO- d_6) δ 8.61 (s, 2H), 8.26 (s, 1H), 6.65 (s, 1H), 6.31 (s, 2H), 5.71 (s, 1H), 4.25 (d, $J = 7.0$ Hz, 2H), 3.86 (s, 3H), 3.84 (s, 6H), 1.26 (t, $J = 7.0$ Hz, 3H) ppm. ^{13}C NMR (100 MHz, DMSO- d_6) δ 165.8, 163.1, 160.8, 146.7, 140.0, 115.6, 103.2, 102.1, 91.0, 61.8, 55.8, 55.6, 51.4, 14.0 ppm; Anal. Calc. for $\text{C}_{17}\text{H}_{21}\text{N}_5\text{O}_5$: C, 54.39; H, 5.64; N, 18.66; Found: C, 54.42; H, 5.59; N, 18.61.

Ethyl 5-amino-7-(3,4,5-trimethoxyphenyl)-4,7-dihydro-[1,2,4]triazolo[1,5- α]pyrimidine-6-carboxylate (**2i**)

0.157 g of white solid (84%), m. p. 211-212°C; ^1H NMR (400 MHz, DMSO- d_6) δ 8.62 (s, 2H), 8.27 (s, 1H), 6.66 (s, 1H), 6.43 (s, 2H), 5.61 (s, 1H), 4.29 (q, $J = 7.0$ Hz, 2H), 3.82 (s, 3H), 3.80 (s, 6H), 1.28 (t, $J = 7.0$ Hz, 3H) ppm. ^{13}C NMR (100 MHz, DMSO- d_6) δ 167.4, 165.8, 160.8, 141.7, 130.0, 105.6, 102.1, 91.0, 62.0, 55.8, 51.4, 14.0 ppm; Anal. Calc. for $\text{C}_{17}\text{H}_{21}\text{N}_5\text{O}_5$: C, 54.39; H, 5.64; N, 18.66; Found: C, 54.41; H, 5.57; N, 18.69.

Ethyl 5-amino-7-(4-(dimethylamino)phenyl)-4,7-dihydro-[1,2,4]triazolo[1,5-*a*]-pyrimidine -6-carboxylate (**2j**)

0.119 g of yellow solid (73%), m. p. 181-182°C; ¹H NMR (400 MHz, DMSO-*d*₆) δ 8.36 (s, 2H), 8.06 (s, 1H), 7.92 (d, *J* = 9.0 Hz, 2H), 6.81 (d, *J* = 9.0 Hz, 2H), 6.27 (s, 1H), 5.21 (s, 1H), 4.24 (q, *J* = 7.0 Hz, 2H), 3.05 (s, 6H), 1.25 (t, *J* = 7.0 Hz, 3H) ppm. ¹³C NMR (100 MHz, DMSO-*d*₆) δ 163.4, 154.1, 153.7, 137.2, 133.7, 118.3, 117.5, 111.6, 92.0, 61.4, 52.6, 40.1, 14.1 ppm; Anal. Calc. for C₁₇H₂₁N₅O₅: C, 58.52; H, 6.14; N, 25.59; Found: C, 58.48; H, 6.1

5.3 Results and Discussion

5.3.1 More characterization and correction of the chemical structure

Chlorosulfonic acid has been used as an alternative sulfonating agent of organic compounds after sulfuric acid and sulfur trioxide (Qureshi et al, 2009; Bakker et al, 1999; Janosik et al, 2006; Guan et al, 2005). Chlorosulfonic acid was applied as a catalyst (Shitole et al, 2016; Kotharkar et al 2006) and an electrophilic olefin cyclization agent in the organic reactions (Linares et al, 2003). It was also used to improve the catalytic activity of various catalysts (Zhang et al 2014; Yadav et al, 2004).

The treatment of 4,4'-trimethylene-dipiperidine [TMDP] with two equivalents of neat chlorosulfonic acid afforded a low-viscous ionic liquid, which was reported and characterized. In continuing our study on the solvent and catalyst activity of new ionic liquid, we decided to investigate two possible functions of chlorosulfonic acid in the reaction with TMDP as a strong acid or sulfonating agent (Figure 5.1). The nucleophilic attack of the nitrogen atom of the piperidine rings of TMDP to the central atom of chlorosulfonic acid seems unlikely due to more steric hindrance of the sulfur atom by

chlorine and oxygen atoms. Therefore, we proposed two possible structures for new ionic liquid; the chlorosulfonic acid can act as a sulfonating agent or strong acid, which leads to structure (I) or (II), respectively. Further studies were performed to elucidate the correct structure of new ionic liquid by the detailed ^1H , ^1H -COSY, Mass, FTIR, and Raman spectra analyses.

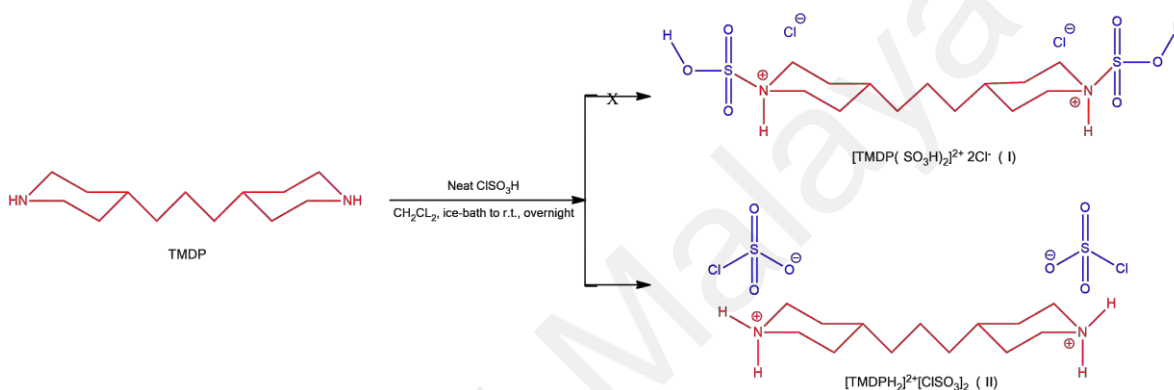


Figure 5.1: Two possible structure of new low-viscous ionic liquid.

In the ^1H NMR spectrum of new ionic liquid, two relatively broadened pseudo-singlets centered at 8.46 and 8.17 ppm were attributed to the acidic hydrogen of piperidinium rings (see Figure A.33). Due to the magnetic anisotropy of piperidinium ring bonds for chair conformation, the chemical shifts at 8.46 were assigned to the acidic hydrogens at the equatorial position, and the axial counterparts were displayed at 8.17 ppm (Belhocine et al, 2015). The lower field position of these acidic hydrogens relative to that of TMDP indicated that they are not involved in a strong intramolecular hydrogen bonding. As shown in Figure 3, peaks at 8.46 and 8.17 disappeared entirely in D_2O due to hydrogen exchange with the deuterium of heavy water.

A doublet at 3.22 ppm with a J coupling of 12.4 Hz was assigned to the equatorial hydrogens (H_{eq}) of C-2, C-2', C-6, and C-6' and their axial counterpart (H_{ax}) appeared as an apparent quartet at 2.82 ppm with a J coupling of 12.4 Hz. The H_{eq} of C-3, C-3', C5, and C-5' with a J coupling of 11.3 Hz were detected at 1.77 ppm as an apparent doublet. The H_{ax} of C-4 and C-4' was seen at 1.53 – 1.46 ppm as a broadened multiplet, and another multiplet at 1.28 – 1.17 pm was assigned to the H_{ax} of C-3, C-3', C-5 and C-5' together with six protons of the three-carbon spacer. The 1H NMR spectrum of $[TMDPH_2]^{2+}2[ClSO_3]^-$ showed the presence of water as two peaks, a singlet at 3.93 ppm corresponding to H_2O and triplet at 7.12 ppm in $DMSO-d_6$ corresponding to hydrogen coupling with ^{14}N nucleus with a coupling constant of 51.1 Hz. This observation proved that the exchange rate between H_2O and HDO is slow on the NMR timescale for this ionic compound in $DMSO-d_6$ (See Figure A.34) (Table 5.1).

Table 5.1: The structure data of $[TMDPH_2]^{2+}2[ClSO_3]^-$ in $DMSO-d_6$.

Atom	δ_H (ppm)	J (Hz)	δ_C (ppm)
$NH^+(eq)$	8.46	be s	-
$NH^+(ax)$	8.17	br s	-
CH-2, CH-2', CH-6, and CH-6'(eq)	3.22	d, 12.4	43.5
CH-2, CH-2', CH-6, and CH-6'(ax)	2.82	q, 12.4	43.5
CH-3, CH-3', CH-5, and CH-5'(eq)	1.77	d, 11.3	28.5
CH-3, CH-3', CH-5, and CH-5'(ax)	1.28-1.17	m	28.5
CH-4 and CH-4'	1.52-1.45	m	35.6
$CH_2-\alpha$	1.28-1.17	m	32.9
$CH_2-\beta$	1.28-1.17	m	22.7

As seen in $^1\text{H}, ^1\text{H}$ -COSY spectra of $[\text{TMDPH}_2]^{2+}2[\text{ClSO}_3]^-$ (See Figure 5.4), the signals at 8.48 and 8.17 ppm exhibited the correlations with themselves and H_{eq} and H_{ax} of C2, C2', C6, C6' at 3.22 ppm and 2.82 ppm. In our previous work, weak signals were assigned to the correlations of acidic protons of N-SO₃H moieties with H_{ax} and H_{eq} of C2, C2', C6, C6' and acidic hydrogen of the piperidinium rings, while they could not be strongly correlated through five bonds bearing oxygen, sulfur, and nitrogen atoms (Figure A.35).

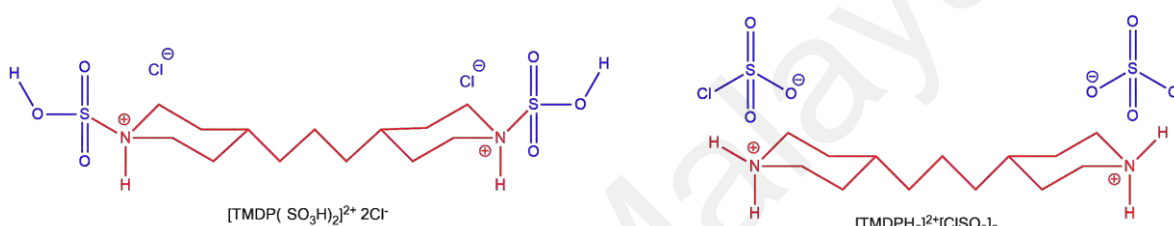
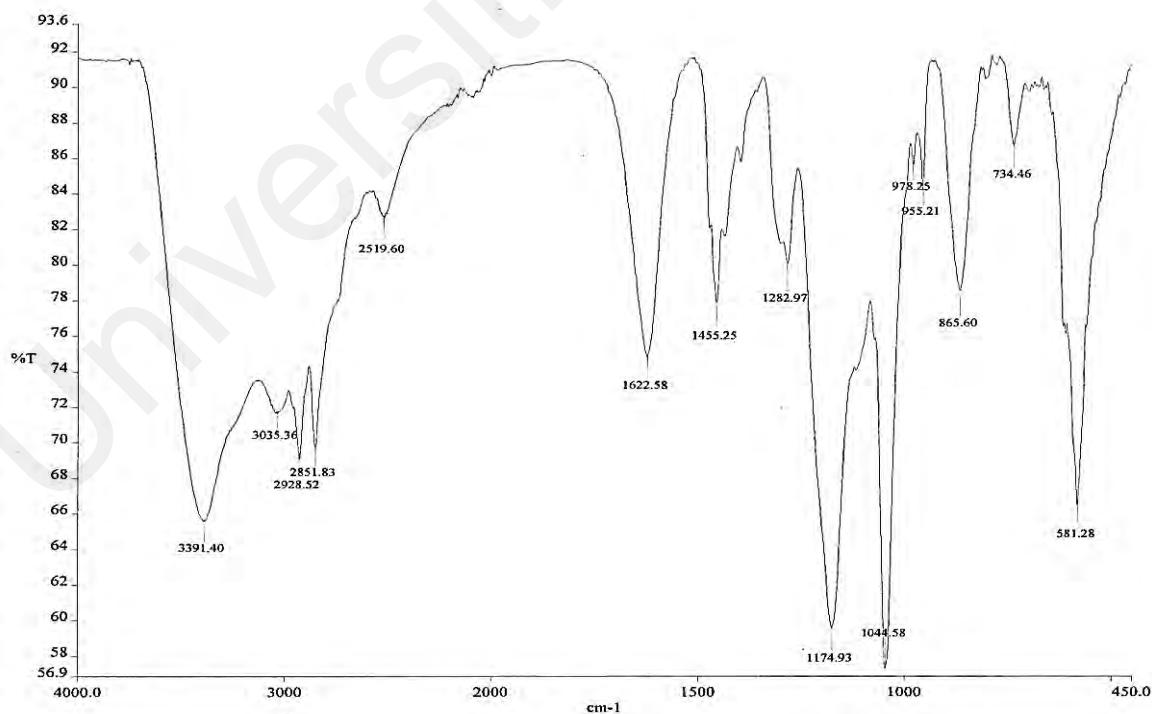


Figure 5.2: Illustrated $^1\text{H}, ^1\text{H}$ -COSY correlation in the 4,4'-trimethylene-*N,N'*-dipiperidinium chlorosulfonate $[\text{TMDPH}_2]^{2+}2[\text{ClSO}_3]^-$ and $[\text{TMDP}(\text{SO}_3\text{H})_2]^{2+} 2\text{Cl}^-$.

The tetrahedral structure of chlorosulfonate anion (ClSO_3^-) belongs to the C_{3v} point group, and it should show six Raman and FTIR active vibration modes including three symmetric vibrations viz. symmetric vibrations: an SO_3 symmetric stretch, an S-Cl stretch, an SO_3 symmetric bend, and three asymmetric vibrations e.g., an SO_3 asymmetric stretch, an S-Cl wag (or ClSO_3 deformation), and an SO_3 asymmetric bend. The current assignments and those of previous reports are given in Table 2. The FTIR data of $[\text{TMDPH}_2]^{2+}2[\text{ClSO}_3]^-$ are similar to the Waddington and Klanberg data of $[\text{Me}_4\text{N}]^+[\text{ClSO}_3]^-$ (See Figure 5.3). The lowest bands in the Raman spectrum of new ionic liquid were found at 440 and 193 cm^{-1} which are assigned to S-Cl stretch and wag, respectively (See Figure 5.4).

Table 5.2: The assignment of the symmetric and asymmetric vibrations of the chlorosulfonate anion.

Approximate description	Frequency (cm-1) in Raman and FTIR							FTIR	Raman
	Waddington	Paul	Gillespie	Ciruna	Steger	Stufkens	Our work		
	[25]	[26]	[27]	[28]	[29]	[30]			
	(FTIR 400-500 cm-1)		Raman (3200-100 cm-1)						
SO ₃ sym. stretch	1044	1044	1050	1035 – 1077	1062	1042	1044	1040	
S-Cl stretch	535	562	416	376 – 417	392	381	488	440	
SO ₃ sym. bend	565	540	535	529 – 554	600, 640	601	610	799	
SO ₃ asym. Stretch	1275	1250	1195	1240 – 1270	1250 – 1312	1300	1320	1255	
SO ₃ asym. bend	585	580	585	566 – 599	531 – 559	553	578	581	
S-Cl wag (or ClSO ₃ deformation)	-	-	220	229 – 251	220	312	-	193	

Figure 5.3: The FTIR spectrum of [TMDPH₂]²⁺2[ClSO₃]⁻

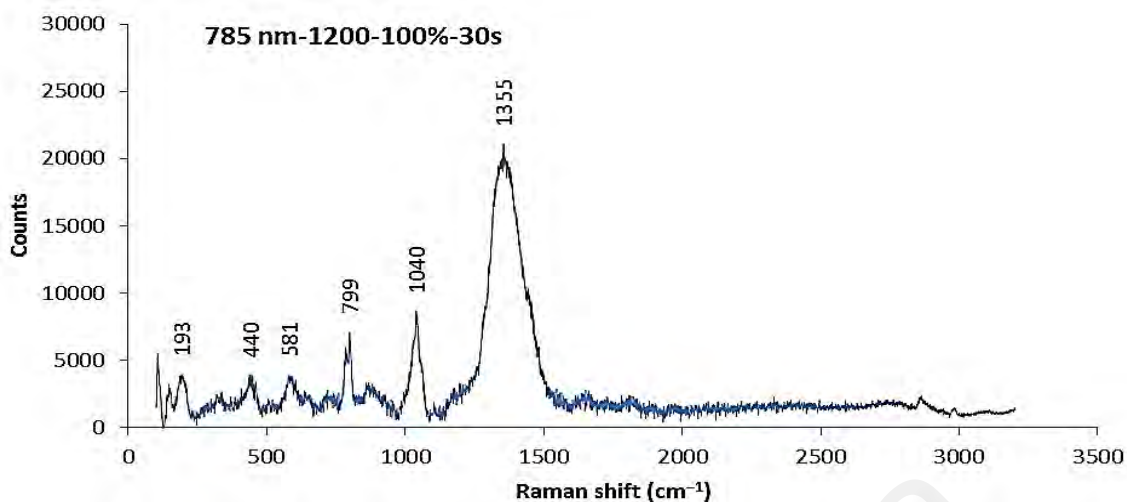


Figure 5.4: The Raman spectrum of $[\text{TMDPH}_2]^{2+}2[\text{ClSO}_3]^-$

The mass spectrum of $[\text{TMDPH}_2]^{2+}2[\text{ClSO}_3]^-$ showed $[\text{TMDPH}]^+$ at m/z 211.2169 in positive mode by LC-ESI-MS analysis. Based on the mentioned spectra analysis results, we indicated that the nucleophilic attack of the nitrogen atom of the piperazine rings of TMDP to the central atom of chlorosulfonic acid seems unlikely due to more steric hindrance of the sulfur atom by chlorine and oxygen atoms. Thus, chlorosulfonic acid could not act as a sulfonating agent in the reaction with secondary amines like TMDP, *i.e.*, TMDP and chlorosulfonic acid as a weak base and strong acid, respectively, participate in an acid-base reaction to form $[\text{TMDPH}_2]^{2+}2[\text{ClSO}_3]^-$. Further studies are conducting in our group for the synthesis of the other pure organic chlorosulfonate salts and the investigation of the FTIR and Raman spectra.

5.3.2 Synthesis of 3-amino-1,2,4-triazole using $[\text{TMDPH}_2]^{2+}2[\text{ClSO}_3]^-$ as dual solvent-catalyst

Initially, the condensation of the 4-chlorobenzaldehyde (**1a**), ethyl cyanoacetate, and 3-amino-1,2,4-triazole were chosen as a model reaction. A few spots were detected on TLC together with aldehyde spot when the model reactants were stirred in ethanol as solvent at room temperature for 2 h (Table 5.3, entry 1). Then, a catalytic amount of

$[\text{TMDPH}_2]^{2+}2[\text{ClSO}_3]^-$ was added to the reaction in ethanol at room temperature which showed complete conversion and ethyl 5-amino-7-(4-chlorophenyl)-4,7-dihydro-[1,2,4]triazole[1,5-a]pyrimidine-6-carboxylate (**2a**) was isolated in 62% yield after workup and recrystallization from hot ethanol (Table 5.3, entry 2). A notable improvement was observed when the amount of $[\text{TMDPH}_2]^{2+}2[\text{ClSO}_3]^-$ was increased (Table 5.3, entry 3).

Table 5.3: Optimization of the synthesis of ethyl 5-amino-7-(4-chlorophenyl)-4,7-dihydro--[1,2,4]triazole[1,5-a]pyrimidine-6-carboxylate.^a

Entry	Amount of Solvent [TMDPH ₂] ²⁺ [ClSO ₃] ⁻ ₂ (mL)	Reaction time (h)	Yield (%)	
1	0.0	EtOH	2.0	Mixture of products and incomplete conversion
2	0.2	EtOH	2.0	62
3	0.4	EtOH	2.0	86
4	0.4	Neat	2.0	86
5	0.8	Neat	2.0	92^c
6	0.8	Neat	1.0	74
7	0.8	Neat	1.5	88
8	0.8	Di. water	4.0	64

^a Reaction conditions: 4-chlorobenzaldehyde (**1a**) (70.3 mg, 0.5 mmol), ethyl cyanoacetate (0.053 mL, 0.5 mmol), and 3-amino-1,2,4-triazole (42.0 g, 0.5 mmol), solvent (1.0 mL), room temperature.

^b Isolated yield.

^c The chosen optimal conditions.

No change in yield was observed when the reaction was conducted in the absence of ethanol (Table 5.3, entry 4). Therefore, the model reaction was carried out in the presence of $[\text{TMDPH}_2]^{2+}2[\text{ClSO}_3]^-$ as a catalyst and the reaction medium, which led in a

92% yield after 2 h (Table 5.3, entry 5). The shorter reaction times results in lower yields of the desired product (Table 5.3, entries 6 and 7). A significant increase in yield was observed even after longer reaction time when the model reaction was performed in water as a solvent, which can be probably due to limited solubility of reactants in the aqueous medium (Table 5.3, entry 8). Based on the results mentioned above, we selected entry 5 in Table 3 as the best experimental conditions.

The substrate scope of the current application of $[\text{TMDPH}_2]^{2+}2[\text{ClSO}_3]^-$ as dual solvent-catalyst was demonstrated for the preparation of 5-amino-7-(4-chlorophenyl)-4,7-dihydro--[1,2,4]triazole[1,5-a]pyrimidine-6-carboxylate through the condensation of various substituted aromatic aldehydes **1 (a-j)**, ethyl cyanoacetate, and 3-amino-1,2,4-triazole under optimized reaction conditions (Figure 5.5).

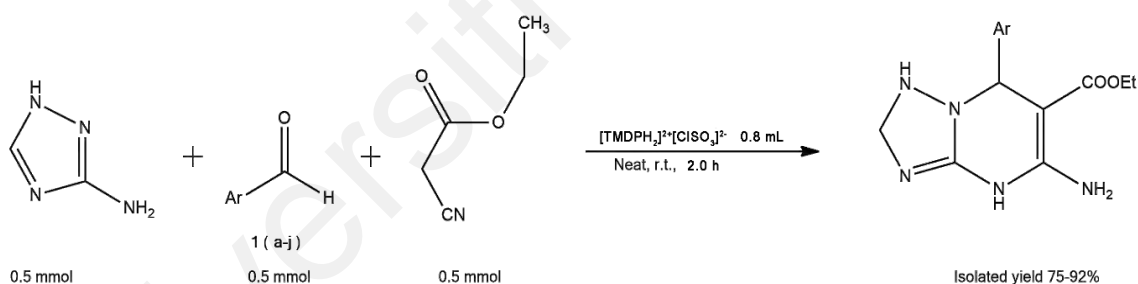


Figure 5.5: Synthesis of 5-amino-7-(4-chlorophenyl)-4,7-dihydro-[1,2,4]triazole[1,5-a]pyrimidine-6-carboxylate under optimized reaction conditions.

A variety of aromatic aldehydes bearing electron-withdrawing or -donating substituents were examined under optimized reaction conditions. The functional groups such as methoxy, nitro, and halides were tolerated without the formation of any by-products (Table 5.4). The nature and position of substituents on the aromatic aldehydes showed a significant influence on the yields and reaction times. The electron-withdrawing groups gave a higher yield within shorter reaction times than electron-donating

substituents in identical positions (Table 5.4, entries 1-4 and 10). The aromatic aldehydes with electron-withdrawing groups at the *para*-position afforded higher yield than electron-donating groups at the same position (Table 5.4, entries 1-3, 5, 7-9). Furthermore, the substituents at the *para*-position of the aromatic aldehydes gave higher yields than the same substituents at the *meta*- or *ortho*- positions (Table 5.4, entries 3-6). 4-(dimethylamino)benzaldehyde afforded a low yield (73%) under optimal conditions that could be attributed to the inductive and resonance effect of the dimethylamino group (Table 5.4, entry 10). All products were characterized by melting point, ^1H and ^{13}C NMR spectra, and elemental analysis.

Table 5.4: The one-pot multicomponent synthesis of triazolo [1,5-*a*]pyrimidines in the presence of $[\text{TMDPH}_2]^{2+}2[\text{ClSO}_3]^-$ under optimized reaction conditions.^a

Entry	Aldehydes 1(a-j)	Triazolo [1,5- <i>a</i>]pyrimidines	Reaction time (min)	Yield (%) ^b	Melting point (°C)
1	1a , 4-Cl-C ₆ H ₄ ⁻	3a	120	92	190-191
2	1b , 4-Br-C ₆ H ₄ ⁻	3b	120	91	184-185
3	1c , 4-NO ₂ -C ₆ H ₄ ⁻	3c	105	94	197-198
4	1d , 2-NO ₂ -C ₆ H ₄ ⁻	3d	120	83	183-184
5	1e , 4-(CH ₃ O)-C ₆ H ₄ ⁻	3e	135	86	187-188
6	1f , 2-(CH ₃ O)-C ₆ H ₄ ⁻	3f	135	80	205-206
7	1g , 3,4-(CH ₃ O)-C ₆ H ₃ ⁻	3g	120	85	190-191
8	1h , 2,4,6-(CH ₃ O) ₃ - 1a , C ₆ H ₂ ⁻	3h	150	80	206-207
9	1i , 3,4,5-(CH ₃ O) ₃ -C ₆ H ₂ ⁻	3i	120	84	211-212
10	1j , 4-(CH ₃) ₂ N-C ₆ H ₄ ⁻	3j	150	73	181-182

^a Reaction conditions: various aldehydes 1 (a-j) (0.5 mmol), ethyl cyanoacetate (0.5 mmol), 3-amino-1,2,4-triazole (0.5 mmol), $[\text{TMDPH}_2]^{2+}2[\text{ClSO}_3]^-$ (0.8 mL), room temperature.

^b Isolated yield.

Above mentioned results demonstrates the dual solvent-catalyst efficiency of $[\text{TMDPH}_2]^{2+}2[\text{ClSO}_3]^-$ for the synthesis of triazolo [1,5-a]pyrimidines as a typical one-pot multicomponent reaction. Also, a large-scale experiment was studied by the condensation 7.0 g of 4-chlorobenzaldehyde with ethyl cyanoacetate and 3-amino-1,2,4-triazole in 5 mL of $[\text{TMDPH}_2]^{2+}2[\text{ClSO}_3]^-$ under optimized reaction conditions. The desired product **3a** was isolated in 92% yield after 2 h.

5.3.3 Easy separation and recyclability of $[\text{TMDPH}_2]^{2+}2[\text{ClSO}_3]^-$

The products were separated via extraction by ethyl acetate after completion of the reaction. The extractions were combined and dried over anhydrous Na_2SO_4 . The ethyl acetate was evaporated at a reduced pressure by the rotary evaporator, which gave the pure products in 73-92% yield. The residue IL was also dried into an oven at 50 °C for 4 h and used in the next runs. The yields and reaction times of **2a** were range 92-88% and 120-130 min, respectively, when the model reaction was conducted by the recovered IL for five runs (Figure 5.6).

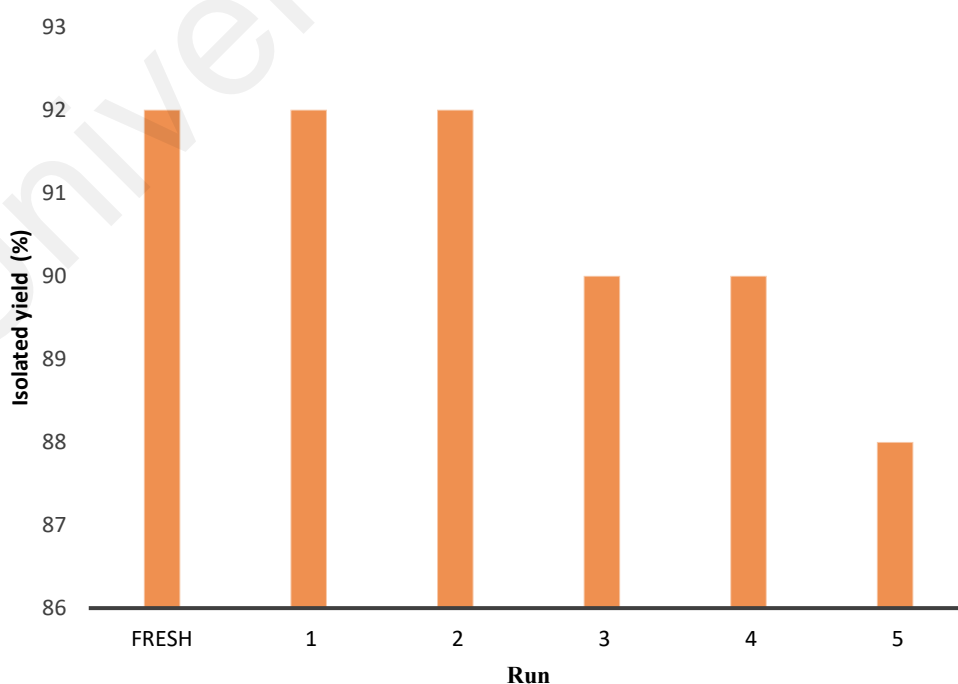


Figure 5.6: Catalytic efficiency of the recycled $[\text{TMDPH}_2]^{2+}2[\text{ClSO}_3]^-$

5.4 Conclusion

In conclusion, the chemical structure of novel bis-core dicationic TMDP salt-containing chlorosulfate counterion was elucidated by 1D NMR and COSY analysis. Further supports of the corrected structure were obtained by the detailed FTIR and Raman analysis. The lowest bands in the Raman spectrum of new ionic liquid were found at 440 and 193 cm^{-1} , which are assigned to S-Cl stretch and wag, respectively. Our results showed that the nucleophilic attack of the nitrogen atom of the piperidine rings of TMDP to the central atom of chlorosulfonic acid seems unlikely due to more steric hindrance of the sulfur atom by chlorine and oxygen atoms.; thus, the TMDP and chlorosulfonic acid participate in an acid-base reaction to form $[\text{TMDPH}_2]^{2+}2[\text{ClSO}_3]^-$. Furthermore, $[\text{TMDPH}_2]^{2+}2[\text{ClSO}_3]^-$ was employed to promote the one-pot three-component reaction under mild conditions, which afforded the desired products in 73-94% isolated yield within 120-150 min. the current work approved the dual solvent-catalyst efficiency of $[\text{TMDPH}_2]^{2+}2[\text{ClSO}_3]^-$ as a recyclable ionic liquid. Furthermore, the current protocol has the advantages such as simple experimental and sustainable procedure, high yield of the desired products within short reaction times at room temperature; avoid the use of toxic and volatile organic solvents, simple workup, and recyclability of IL which all as mentioned merits will cause to minimize the generation of heavy metal and corrosive waste. A new application of $[\text{TMDPH}_2]^{2+}2[\text{ClSO}_3]^-$ in the one-pot multicomponent reactions as dual solvent-catalyst has highlighted the importance of low viscous binuclear ionic liquids in organic synthesis and we hope that further research in new applications of $[\text{TMDPH}_2]^{2+}2[\text{ClSO}_3]^-$ will be presented in future with promising results.

CHAPTER SIX

ARTICLE 4

**SYNTHESIS, CHARACTERISATION, AND DETERMINATION OF
PHYSICAL PROPERTIES OF NEW TWO-PROTONIC ACID IONIC LIQUID
AND ITS CATALYTIC APPLICATION IN THE ESTERIFICATION**

6.1 Introduction

Catalysis is a vital topic in organic chemistry, and has been employed in a broad range of sectors, products, and processes. The current trend in catalysis research is to design greener catalysts and eco-friendly technologies, as well as directing the activities towards sustainability and investigating the catalytic activity under realistic conditions regarding temperature and pressure.

Natural and synthetic esters have been utilized in different fields, including pharmaceuticals, perfumes, flavors, cosmetics, adhesives, detergents, solvents, plasticizers, lubricants, electron materials, and daily and fine chemicals, etc. Low molecular mass esters have been widely found in fragrances and essential oils and pheromones (Kartika et al, 2004).

The carboxylic acid esters can be synthesized using various chemical reactants, catalysts, and reaction media. Although numerous papers have appeared for the esterification reaction, the development of an efficient synthesis of carboxylic acid esters using carboxylic acids instead of acid anhydride is still an exciting research topic.

The Fischer esterification is the conventional and most common process for the esterification (Keogh et al, 2019). The catalytic esterification has been reported using various catalysts (Keogh et al, 2019); nonetheless, there are some drawbacks, for example

- (a) Use of excessive reagents and dehydration agents or Dean Stark apparatus,
- (b) Use of expensive, toxic, or especially substrates bearing acid or base sensitive groups,
- (c) Limited substrate-scope, especially substrates bearing acid or base sensitive groups,
- (d) Use of an activated carboxylic acid together with a stoichiometric base,
- (e) The generation of a large amount of waste during the process,
- (f) Use of non-recyclable catalysts and inactivation of catalytic sites, and
- (g) A tedious process for the preparation of catalysts, and the separation and purification of products.

Therefore, it is required to develop an efficient and greener methodology to overcome some drawbacks and achieve a suitable balance between the economic and ecological aspects of production. Due to the outstanding properties of ionic liquids (ILs), such as thermal and chemical stability, low vapor pressure, and recoverability, they have been extensively employed as an eco-friendly solvent and/or catalyst in a variety of reactions, such as esterification (Hernandes et al, 2015; Hallett et al, 2011; Przepis et al, 2020; Matuszek et al, 2014; Ciappe et al, 2013). In continuing our previous works on 4,4'-trimethylenedipiperidine (TMDP) (Khaligh et al, 2019), the synthesis of a new IL was designed and carried out through stirring TMDP and sulfuric acid (98%) in CH_2Cl_2 . The chemical structure of the new ionic liquid ($[\text{TMDPH}_2][\text{SO}_4]$) was characterized by FT-IR, 1D NMR, 2D NMR, and mass analysis. The existence of a sulfate anion, instead of hydrogen sulfate, was evidenced by detailed ^1H NMR analyses. The physical properties

of the new IL have been determined and are reported herein. The catalytic activity of the new IL was studied for the direct esterification of various carboxylic acids and alcohols under obtained optimal reaction conditions.

6.2 Methodology

6.2.1 Material and Method

General materials, characterizations and methodology refers to 3.2.1.

6.2.2 Synthesis of $[\text{TMDPH}_2]^{2+}[\text{SO}_4]^{2-}$

A flask containing a solution of 4,4'-trimethylene-dipiperidine (4.21 g, 20 mmol) in dry CH_2Cl_2 (20 mL) was cooled to a low temperature by an ice bath. Sulfuric acid (98%, 1.840 g mL^{-1}) (1.1 mL, ~20 mmol) was added drop wise to the solution at low temperature (ice bath). Two phases were formed after stirring at room temperature overnight. The upper phase was removed by decantation, and the pale-yellow sticky residue was washed with CH_2Cl_2 (3 x 10 mL). After evaporation of excess solvent under reduced pressure, the resulting IL was obtained as a pale-yellow sticky solid. The IL could be crystallized from methanol.

6.2.3 Typical Esterification Procedure

Glacial acetic acid (0.60 g, 0.572 mL, 10 mmol), *n*-butanol (9.694 g) 11.968 mL, 13 mmol), $[\text{TMDPH}_2]^{2+}[\text{SO}_4]^{2-}$ (0.308 g, 1.0 mmol), and cyclohexane (1.157 g, 15 mL) were taken into a 25 mL three necked flask. The flask was equipped with a manifold and a condenser. After an appropriate reaction time (4h), a liquid bi-phase formed in the flask. The liquid phase $[\text{TMDPH}_2]^{2+}[\text{SO}_4]^{2-}$ was isolated after removing the product and water

by separating funnel and drying in a vacuum oven at 50 °C overnight before being tested for reusability.

6.2.4 Esterification of α -TCP with Glacial Acetic Acid

α -tocopherol (α -TCP) (20 mmol), glacial acetic acid (30 mmol), and $[\text{TMDPH}_2]^{2+}[\text{SO}_4]^{2-}$ (0.616 g) were mixed and stirred at 60 °C under N_2 atmosphere for 2 h in a 100 mL round bottom flask covered with tin foil. Liquid chromatography-mass spectrometry was utilized to determine the purity and yield of O-acetyl- α -tocopherol (Ac-TCP) using vitamin E acetate (96% Sigma-Aldrich) as an external standard. The identification of Ac-TCP was performed by comparison of its NMR data with the reference compound (Baker et al, 1991). The yield of Ac-TCP was also calculated based on a reported equation in the literature (Mihankhah et al, 2018).

6.3 Results and Discussion

6.3.1 Synthesis and the Structure Elucidation of New Ionic Liquid

TMDP was treated with one and two equivalent(s) of sulfuric acid to investigate the two possible chemical structures of the new IL that could be formed by an acid-base reaction of TMDP bearing two piperidine rings and sulfuric acid as a two-protonic acid (Figure 6.1).

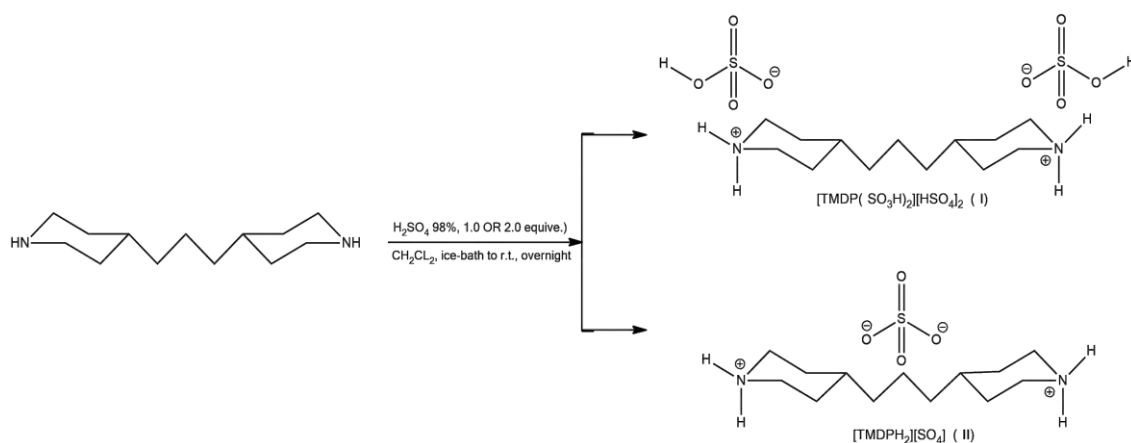


Figure 6.1: The proposed chemical structures for the new ionic liquid

Drop wise addition of two equivalents of sulfuric acid (98%) into a solution of TMDP in dichloromethane in an ice-bath and then stirring the mixture at room temperature overnight afforded a pale yellow sticky solid. The pale yellow crystals were obtained from methanol through crystallization (mp 74-75 °C) (see Figure 6.2). Further studies, including FT-IR, 1D and 2D NMR, and mass spectrometry, were conducted to find the chemical structure of the new IL.

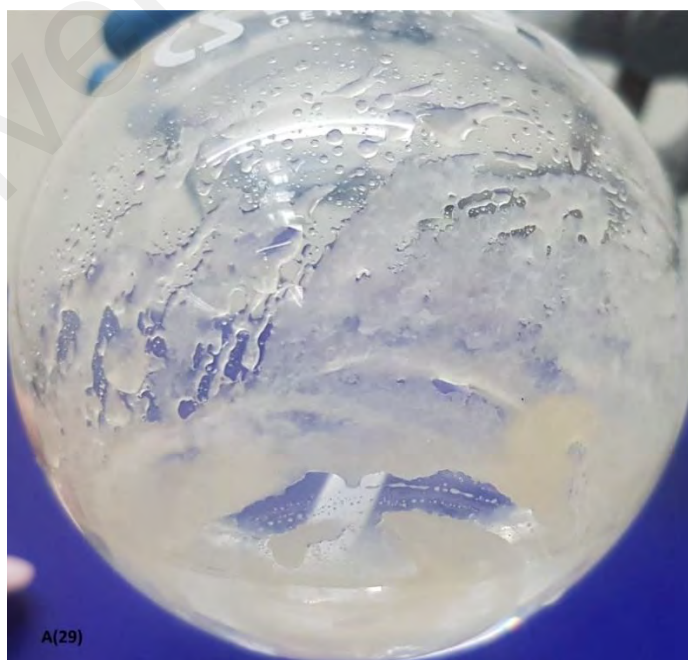
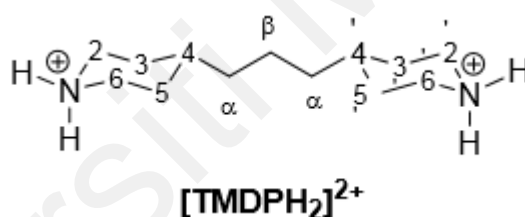


Figure 6.2: The image of 4,4'-trimethylene-*N,N'*-dipiperidine sulfate

The ^1H NMR spectrum of new IL showed two pseudo-singlet peaks at 8.46 and 8.17 ppm. Regarding the magnetic anisotropy of the chair conformation of two piperidium rings, these protons were attributed to the protons at the equatorial and axial positions of $>\text{NH}_2^+$, respectively (see Figure A.36) (Belhocine et al, 2015). The presence of acidic protons on nitrogen atoms at a downfield position showed that intramolecular hydrogen bonding in the new IL was weakened. The chemical shift and coupling constant of the equatorial and axial hydrogens (H_{eq} and H_{ax}) of the two piperidinium rings as well as protons of the three-carbon spacer are given for the new IL in DMSO- d_6 and D_2O in Table 6.1. The observation of a singlet and a triplet signal at 3.63 and 7.15 ppm corresponding to H_2O and hydrogen coupling with ^{14}N nucleus, respectively.

Table 6.1: The 1D NMR spectrum data of $[\text{TMDPH}_2]^{2+}[\text{SO}_4]^{2-}$ in DMSO- d_6 and D_2O



Atom	DMSO- d_6		D $_2$ O			
	δ_{H} [ppm]	J [Hz]	δ_{C} [ppm]	δ_{H} [ppm]	J [Hz]	δ_{C} [ppm]
$\text{NH}^+(\text{eq})$	8.46	br s	-	-	br s	-
$\text{NH}^+(\text{ax})$	8.17	br s	-	-	br s	-
CH-2, CH-2', CH-6, and CH-6' (<i>eq</i>)	3.23	d, 12.1	43.57	3.29	d, 12.8	44.15
CH-2, CH-2', CH-6, and CH-6' (<i>ex</i>)	2.82	dd, 11.5 and 22.6	43.57	2.85	td, 2.5 and 12.9	44.15

CH-3, CH-3', CH-5, and CH-5' (<i>eq</i>)	1.77	D, 13.2	28.57	1.83	d, 14.0	28.37
CH-3, CH-3', CH-5, and CH-5' (<i>ex</i>)	1.26-1.18	M	28.57	1.27-1.17	m	28.37
CH-4 and CH-4'	1.53-1.43	M	35.64	1.53-1.46	m	34.97
CH ₂ - α	1.26-1.18	M	32.95	1.27-1.17	m	32.76
CH ₂ - β	1.26-1.18	M	22.76	1.27-1.17	m	22.29

As one can see in Figure A.37, the protons of $>\text{NH}_2^+$ disappeared in D_2O due to fast hydrogen exchange with the deuterium of D_2O . The carbons of new IL are detected at 43.57, 35.64, 32.95, 28.57, and 22.76 ppm and 44.15, 34.97, 32.76, 28.37, 22.29 ppm in $\text{DMSO-}d_6$ and D_2O , respectively (see Figure A.38 and A.39). The 2D COSY spectra of new IL displayed correlations between the acidic protons of NH_2^+ at 8.46 and 8.17 ppm with the equatorial and axial protons of C2, C2', C6, C6' at 3.23 and 2.82 ppm, respectively (see Figure A.40). The reaction of TMDP and sulfuric acid was also carried out in CH_2Cl_2 at a ratio of 1:1 at room temperature overnight, which gave a white solid. The ^1H and ^{13}C NMR spectra of the TMDP and sulfuric acid at a ratio of 11:1 were recorded in $\text{DMSO-}d_6$. One and two equivalent(s) of sulfuric acid (98%) was then directly added to the NMR tube containing TMDP and sulfuric acid at a ratio of 1 : 1 in $\text{DMSO-}d_6$, and ^1H NMR spectra were recorded.

The single peak of water at 3.92 ppm moved to the downfield region, and a broadened multiplet and singlet signal were observed at 4.45 – 4.43 and 6.96 ppm, respectively. The ^{13}C NMR spectra showed negligible shifts before and after adding sulfuric acid. The ^1H NMR spectrum of sulfuric acid was also investigated, which showed

a relatively sharp singlet at 7.13 ppm in DMSO-*d*₆. The ¹H NMR spectrum of new IL did not show any peaks at a region of 4.38 – 5.25. Moreover, no sharp or broadened peak was detected at a range of 4.0 to 8.5 ppm and above 9.5 ppm. Therefore, the existence of excess sulfuric acid or formation of an acidic anion, namely hydrogen sulfate, could be excluded.

The infrared spectrum of new IL is shown in Figure 6.3. The broadened peak at 3407 cm⁻¹ can be attributed to the N-H vibration mode at the >NH₂⁺ groups. Two bands at 3034, 2923, and 1321 cm⁻¹ were assigned to the symmetric, antisymmetric stretching vibrational, and wagging mode of methylene groups in the piperidinium rings, respectively. All absorption peaks at a range of 2848 to 2524 cm⁻¹ were assigned to the N-H stretching band and their shift towards this region are probably due to the strong interactions between >NH₂⁺ and the sulfate anion through hydrogen bonding (Heacock et al, 1956). The deformation vibration modes of >NH₂⁺ at 1616 and 1462 cm⁻¹ are characteristic of secondary amine salts (Heacock et al, 1956). The asymmetric and symmetric SO₂ stretching vibrations appeared at 1215, 1151, and 1029 cm⁻¹, respectively. The sharp bands at 877 and 577 cm⁻¹, as well as a medium band at 487 cm⁻¹, were assigned to the S-O stretching modes and SO₂ bending, respectively (Erben et al, 2003).

Table 6.2: The calculated LC-ESI-MS data

Cation or anion species	Calcd.	Found	Error (%)
$[M + EtOH + NH_4]^+$	318.2757	318.3014	0.008
$[M + EtOH + CO_2 + NH_4]^+$	274.2858	274.2753	0.004
$[M + H + SO_4 + CH_3OH]^-$	339.1954	339.2005	0.002

Based on our results, structure II was demonstrated for the new IL evidencing it to be $[TMDPH_2]^{2+}[SO_4]^{2-}$, and indicated that complete deprotonation of the sulfuric acid likely occurs by TMDP under our reaction conditions.

6.3.2 Physical Properties of $[TMDPH_2]^{2+}[SO_4]^{2-}$

The bulk amount of $[TMDPH_2]^{2+}[SO_4]^{2-}$ could be liquefied at ~ 110 °C in an oil bath (mp 74-75 °C). The ionic conduction value (σ) of new IL was 1.82 ± 0.04 mS sm^{-1} at 85 °C. The total water content of $[TMDPH_2]^{2+}[SO_4]^{2-}$ was determined 0.18 ± 0.02 wt-% under ambient humidity and temperature. Although $[TMDPH_2]^{2+}[SO_4]^{2-}$ was soluble in water, dimethyl sulfoxide, methanol, and acetic acid, it was immiscible with ethanol, acetonitrile, ethyl acetate, acetone, chloroform, dichloromethane, and n-hexane at room temperature.

6.3.3 Thermal Behaviour of $[TMDPH_2]^{2+}[SO_4]^{2-}$

The thermal behavior of $[TMDPH_2]^{2+}[SO_4]^{2-}$ was investigated by a differential scanning calorimetry (DSC) plot in two cycles over temperature ranges of 30-300 and 30-500 °C (see Figure 6.4). DSC of pure TMDP has been previously reported in the literature (Khaligh et al, 2019), and it displays two sharp and one broad endothermic peak centered at 58, 110, and 332 °C. The peaks at 52.2 and 332.5 °C were attributed to the melting point and boiling points of TMDP, respectively. The second endothermic broad peak at a range of 76-157 °C was attributed to desorption of trapped moisture in TMDP.

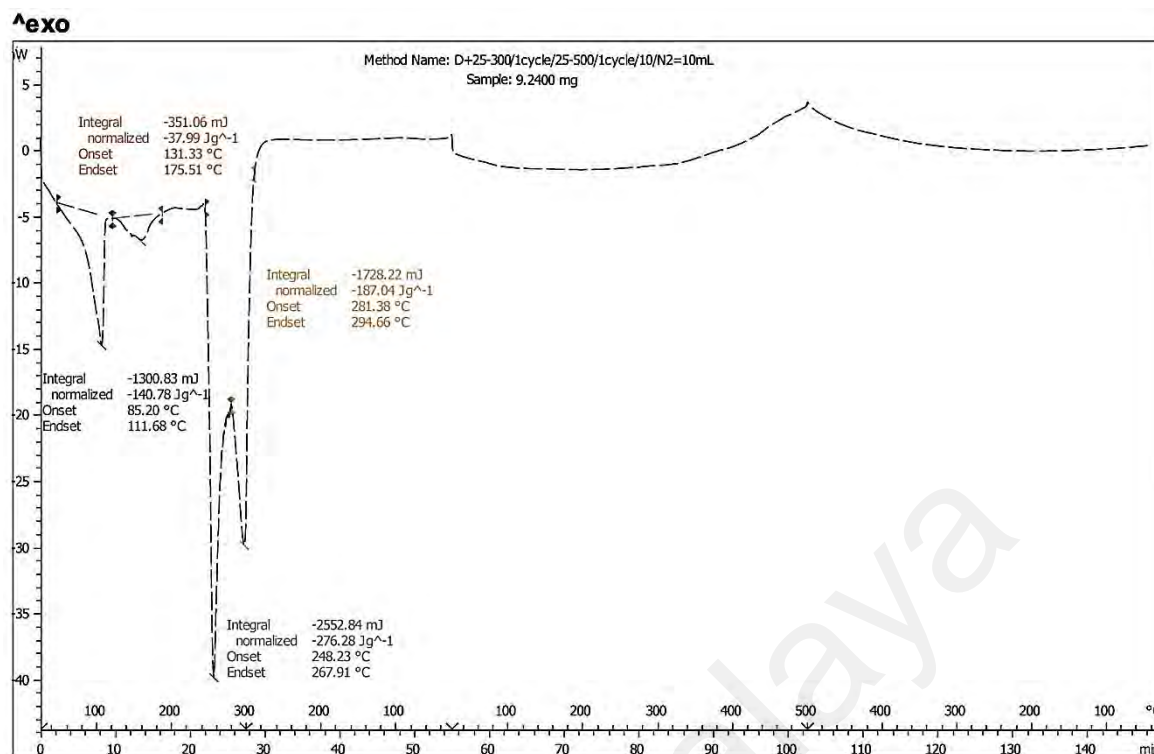


Figure 6.4: DSC of new ionic liquid at nitrogen atmosphere

Under a nitrogen atmosphere and at a range of 30-300 °C, three sharp and one weak endothermic peak(s) were displayed on the DSC curve of $[\text{TMDPH}_2]^{2+}[\text{SO}_4]^{2-}$, and no exothermic peak was observed. The first sharp peak was assigned to the melting point of the IL which began at 85.2 °C and ended at 111.7 °C with a latent heat of fusion of 140.8 J g⁻¹, which was in good agreement with the obtained melting point achieved using an open capillary tube in a Buchi B545 apparatus (mp 74-75 °C). The second endothermic sharp peak was observed in the range 131.3-175.5 °C centred at 160.2 °C, which was assigned to the boiling point decomposition of $[\text{TMDPH}_2]^{2+}[\text{SO}_4]^{2-}$ due to an appreciable loss of weight, a remarkable change in heat capacity of the sample, and an exothermic baseline shift. The latent heat of evaporation and decomposition of the $[\text{TMDPH}_2]^{2+}[\text{SO}_4]^{2-}$ were 276.3 and 187.0 J g⁻¹, respectively. There was no exothermic and endothermic peak in the second cycle at a range of 30-500 °C, which supports the evaporation/decomposition of the $[\text{TMDPH}_2]^{2+}[\text{SO}_4]^{2-}$ below 300 °C in the first cycle.

Moreover, the thermal stability of $[\text{TMDPH}_2]^{2+}[\text{SO}_4]^{2-}$ was studied in a temperature range from 30 to 800 °C under a nitrogen atmosphere through thermogravimetric analysis/differential thermal analysis (TGA/DTA) (see Figure 6.5).

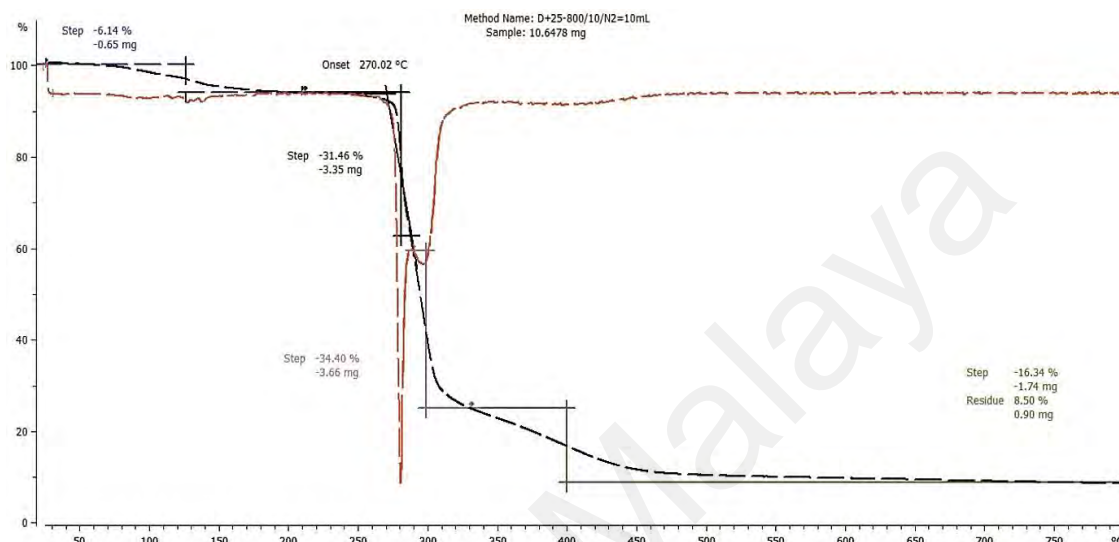


Figure 6.5. TGA/DTA of new ionic liquid at nitrogen atmosphere

Three peaks were observed on the DTA curve, and $[\text{TMDPH}_2]^{2+}[\text{SO}_4]^{2-}$ started to decomposed at 270 °C, which was in good agreement with the result of DSC. The thermal decomposition was mainly completed at 450 °C. The first peak was observed below 200 °C with a maximum mass loss of 6.1 %; this loss was related to the removal and evaporation of the trapped and adsorbed moisture in $[\text{TMDPH}_2]^{2+}[\text{SO}_4]^{2-}$. The second and third peaks showed a maximum mass loss of 31.5 and 34.4 % at 250-290 and 290-330 °C, respectively, which were related to the total decomposition of $[\text{TMDPH}_2]^{2+}[\text{SO}_4]^{2-}$. The DSC and TGA/DTA results showed that $[\text{TMDPH}_2]^{2+}[\text{SO}_4]^{2-}$ is thermally stable up to 270 °C, probably owing to the strong electrostatic attractions between the piperidinium cations and the sulfate anion in the structure of the $[\text{TMDPH}_2]^{2+}[\text{SO}_4]^{2-}$.

6.3.4 Esterification of Alcohols and Glacial Acetic Acid Using $[\text{TMDPH}_2]^{2+}[\text{SO}_4]^{2-}$ as a Catalyst

Initially, the esterification of *n*-butanol (**1e**) and acetic acid was chosen as a model reaction. The influence of four parameters, including the amount of $[\text{TMDPH}_2]^{2+}[\text{SO}_4]^{2-}$, the ratio of *n*-butanol to acetic acid, temperature, and reaction time were studied to find the optimized reaction conditions. As the results show in Table 6.3, the yield of esterification increased with an increase in the catalyst loading, and the highest yield was observed with 10 mol-% of the catalyst (Table 6.3, entries 1-4). The most effective molar ratio of *n*-butanol to glacial acetic acid was 1.3 at 60 °C within 4 h (Table 6.3, entries 5-8).

A significant improvement in the yield was observed when the model reaction was carried out at higher temperatures up to 90 °C; however, no change occurred in yield at a higher temperature (100 °C) (Table 6.2, entries 9-12). A shorter or longer reaction time of about 4 h resulted in lower yields of the desired product (Table 6.3, entries 13-15), which can probably be due to the reversibility of the esterification process. Based on our results, entry 11 in Table 6.3 was selected as the best experimental conditions, i.e., 10 mol-% catalyst, 1.3 : 1.0 molar ratio of *n*-butanol to acetic acid, 85 °C, and 4 h reaction time.

Table 6.3: Optimization of the esterification of *n*-butanol and glacial acetic acid

Entry	[TMDPH ₂] ²⁺ [SO ₄] ²⁻ [mol-%]	Molar ratio of <i>n</i> - butanol to acetic acid	Temp. [°C]	Reaction time [h]	Yield ^A [%]
1	-	1.0 : 1.0	60	4.0	12
2	5	1.0 : 1.0	60	4.0	34
3	10	1.0 : 1.0	60	4.0	42
4	15	1.0 : 1.0	60	4.0	42
5	10	1.1 : 1.0	60	4.0	52
6	10	1.2 : 1.0	60	4.0	58
7	10	1.3 : 1.0	60	4.0	68
8	10	1.4 : 1.0	60	4.0	68
9	10	1.3 : 1.0	65	4.0	72
10	10	1.3 : 1.0	75	4.0	78
11 ^B	10	1.3 : 1.0	85	4.0	88
12	10	1.3 : 1.0	100	4.0	88
13	1.0	1.3 : 1.0	85	2.0	54
14	1.0	1.3 : 1.0	85	6.0	81
15	1.0	1.3 : 1.0	85	8.0	75

^AGC yield.^BThe chosen optimal conditions.

The catalytic activity of $[\text{TMDPH}_2]^{2+}[\text{SO}_4]^{2-}$ was demonstrated for the esterification of other alcohols and glacial acetic acid under optimized reaction conditions (Figure 6.6).

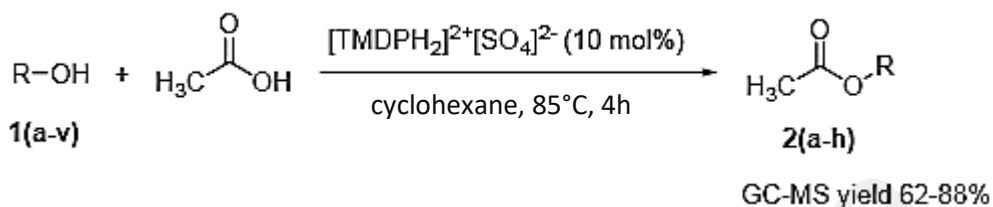
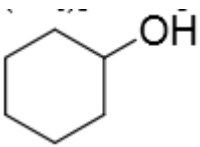
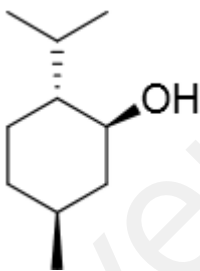
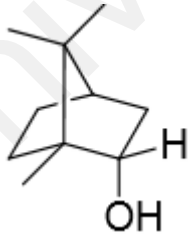
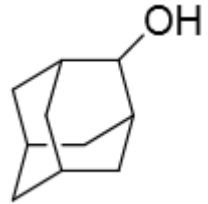


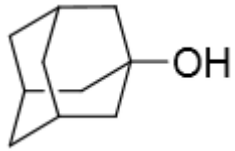
Figure 6.6: Esterification of various alcohols and glacial acetic acid in the presence of $[\text{TMDPH}_2]^{2+}[\text{SO}_4]^{2-}$.

A variety of alcohols were treated with acetic acid under optimized reaction conditions (Table 6.4). The results showed that the primary alcohols gave higher yields than secondary alcohols, which afforded a slightly higher yield than tertiary alcohols, which can be attributed to the acidity of alcohol (Table 6.4, entries 1-14). Moreover, competitive dehydration was observed for the secondary and tertiary alcohols under optimized reaction conditions (Table 6.4, entries 10-14). The substituents at the *ortho*-position of the benzyl alcohols gave lower yields of acetate esters than the same substituents at the *para*-position, which is probably due to the steric effect of the substituents (Table 6.4, entries 15-22), as well as the hydrogen bond formation between $-\text{NO}_2$ and $-\text{Cl}$ and the hydroxyl group of the benzyl alcohols (Table 6.4, entries 21 and 22).

We obtained the **optimal molar ratio** of *n*-butanol to acetic acid is **1.3:1.0** in Table 6.3 at 85 °C for four hours, and we used same ratio for alcohol and HOAc viz. alcohol (0.13 mmol) and glacial acetic acid (0.1 mmol) in Table 6.4.

Table 6.4: Esterification of various alcohols and glacial acetic acid in the presence of $[\text{TMDPH}_2]^{2+}[\text{SO}_4]^{2-}$ under optimized reaction conditions

Entry ^A	Alcohol 1(a-v)	Ester 4(a-v)	Temp. (°C)	Yield (%) ^b
1	CH ₃ OH	4a	75	82 ± 2
2	CH ₃ CH ₂ OH	4b	85	85 ± 2
3	CH ₃ CH ₂ CH ₂ OH	4c	85	88 ± 3
4	(CH ₃) ₂ CHOH	4d	85	85 ± 2
5	CH ₃ CH ₂ CH ₂ CH ₂ OH	4e	85	88 ± 3
6	(CH ₃) ₂ CHCH ₂ OH	4f	85	80 ± 1
7	CH ₃ CH ₂ CH ₂ CH ₂ CH ₂ OH	4g	85	85 ± 2
9	(CH ₃) ₂ CHCH ₂ CH ₂ OH	4h	85	82 ± 2
10		4i	85	75 ± 3
11		4j	85	72 ± 1
12		4k	85	70 ± 1
13		4l	85	76 ± 2

14		4m	85	62 ± 3
15	4-MeO-C ₆ H ₄ -CH ₂ OH	4n	75	82 ± 2
16	4-Me-C ₆ H ₄ -CH ₂ OH	4o	75	83 ± 1
17	4-NO ₂ -C ₆ H ₄ -CH ₂ OH	4p	75	85 ± 3
18	4-Cl-C ₆ H ₄ -CH ₂ OH	4q	75	83 ± 2
19	2-MeO-C ₆ H ₄ -CH ₂ OH	4r	75	78 ± 2
20	2-Me-C ₆ H ₄ -CH ₂ OH	4s	75	76 ± 1
21	2-NO ₂ -C ₆ H ₄ -CH ₂ OH	4t	75	74 ± 1
22	2-Cl-C ₆ H ₄ -CH ₂ OH	4v	75	75 ± 1

^AReaction conditions: alcohol 1a-v (0.13 mmol), glacial acetic acid (0.1 mmol), cyclohexane (1.5 mL), [TMDPH₂]²⁺[SO₄]²⁻ 0.01 mmol, temperature (85 °C), reaction time (4 h).

^BGC-MS yield. The esterification reactions were carried out in triplicate and conducted at least twice on separate days.

The enantioselectivity of the current protocol was investigated through the reaction of glacial acetic acid with (-)-methanol ($[\alpha]_D -50 \pm 1^\circ$, *c* 10% ethanol, $\geq 99\%$ e.e) and (+)-borneol ($[\alpha]_D -37 \pm 2^\circ$, *c* 5% in ethanol, 99% e.e) under optimal conditions, which gave (-)-methyl acetate ($[\alpha]_D -80^\circ$, in benzene, 97% e.e) and (+)-bornyl acetate ($[\alpha]_D -41^\circ$, neat, 96% e.e) with reaction of the configuration at the chiral center in 72 and 70 yield, respectively (Table 6.4, entries 11 and 12). The optical rotation of the desired acetates was recorded and reported based on samples from Sigma-Aldrich.

According to a proposed mechanism, the glacial acetic acid is initially activated by $[\text{TMDPH}_2]^{2+}[\text{SO}_4]^{2-}$ through hydrogen bond formation (Figure 6.7). A nucleophilic attack of the alcohol to the activated acetic acid leads to the formation of intermediate **III**. Hydrogen rearrangement and dehydration of intermediate **III** gives the alkyl acetate. The dehydration step can be promoted by the hygroscopic property of $[\text{TMDPH}_2]^{2+}[\text{SO}_4]^{2-}$. Moreover, the cyclohexane can favor the forward reaction through extraction and separation of the produced alkyl acetate.

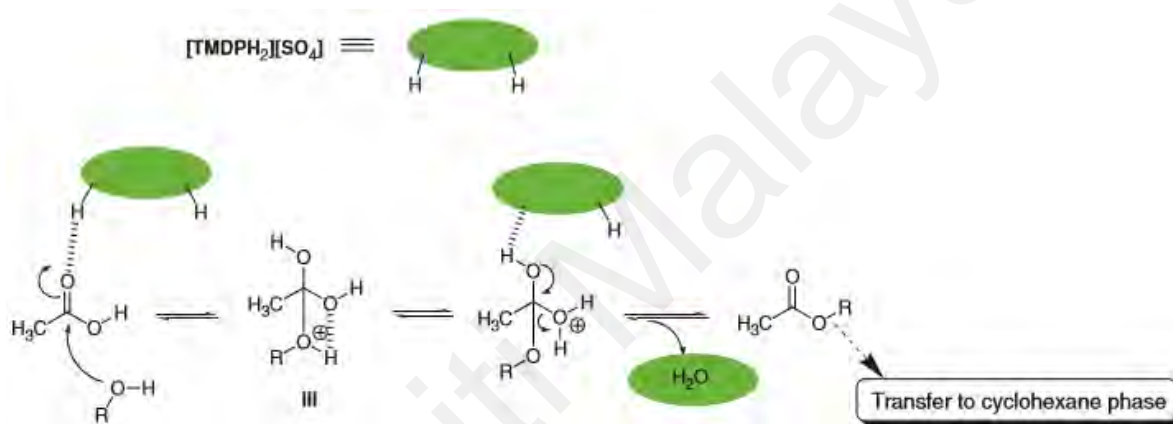


Figure 6.7: A schematic reaction mechanism of the esterification in the presence of $[\text{TMDPH}_2]^{2+}[\text{SO}_4]^{2-}$.

The reusability of $[\text{TMDPH}_2]^{2+}[\text{SO}_4]^{2-}$ was also studied using the model reaction at optimal conditions, which afforded **2e** in 88-82% yield over five catalytic cycles. In another experiment, the model reaction was monitored for a longer reaction time. Aliquots were analyzed by gas chromatography-mass spectrometry (GC-MS) at intervals of 1 h, while the stirring of the reaction mixture continued under optimized reaction conditions. Complete (100%) conversion of glacial acetic acid was observed after 430 ± 10 min.

Finally, the esterification of α -tocopherol (α -TCP) was conducted to show the potential of the current method for a scale-up application. It is well known that tocopherols, an isoform of vitamin E, are sensitive to light and air. Their antioxidant efficiency is rapidly reduced (Prasad et al, 2003), while their ester isoforms exhibited moderate to good stability to light and air (Torres et al, 2008). Large scale acetylation of α -tocopherol (α -TCP) (20 mmol) with glacial acetic acid (30 mmol) was carried out using $[\text{TMDPH}_2]^{2+}[\text{SO}_4]^{2-}$ (10 mol-%) at 60 °C, which gave 8.11 g (88.4% yield) after 4 h incubation in the absence of light under N_2 atmosphere (Figure 6.9=8).

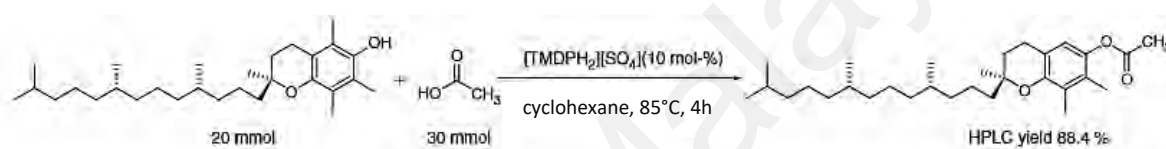


Figure 6.8: Esterification of α -tocopherol (α -TCP) with glacial acetic acid using $[\text{TMDPH}_2]^{2+}[\text{SO}_4]^{2-}$.

Very recently, our group reported the synthesis, characterization, and catalytic application of a low viscous ionic liquid, namely 4,4'-trimethylene- N,N' -sulfonic acid-dipiperidium chloride (TMDPS) (Khaligh et al, 2019). We investigated the structure-activity relationship of the two ionic liquids $[\text{TMDPH}_2]^{2+}[\text{SO}_4]^{2-}$ and TMDPS on the model esterification. The model reaction was also carried out using 10 mol-% of TMDPS, 1,1'-butylenebis-(3-sulfo-3*H*-imidazol-1-ium) chloride ($[\text{Im-C4-Im}(\text{SO}_3\text{H})_2]_2\text{-Cl}$), 1,1'-butylenebis-(3-sulfo-3*H*-imidazol-1-ium) dihydrogensulfate ($[\text{MIm-C4-MIm}][\text{HSO}_4]_2$), and triethylammonium hydrogen sulfate ($[\text{TEA}][\text{HSO}_4]$). The ILs were fabricated according to the literature methods (Keogh et al, 2019; Khaligh et al, 2019; Baker et al, 1991). Although the five ILs can be interchanged under appropriate conditions, the ILs that contained two sulfonic acid moieties or two acidic anions, namely hydrogen sulfate, showed higher yields within shorter reaction times (Table 6.5, entries 1, 3, and 4). The

anion and cation effect for $[\text{TMDPH}_2]^{2+}[\text{SO}_4]^{2-}$ and $[\text{TEA}][\text{HSO}_4]$ on the yield and rate are negligible within experimental error in the measurements (Table 6.5, entries 2 and 5).

Table 6.5: Catalytic efficiency of five ionic liquid catalysts for the esterification of *n*-butanol and glacial acetic acid

Entry ^A	Ionic liquid	Reaction time [min]	Yield ^B [%]
1	TMDPS	230	85 ± 2
2	[TEA][HSO ₄]	240	80 ± 2
3	[MIm-C4-MIm][HSO ₄] ₂	180	88 ± 2
4	Im-C4-Im(SO ₃ H) ₂ -Cl	200	85 ± 2
5	[TMDPH ₂][SO ₄]	240	85 ± 2

^AReaction conditions: *n*-butanol (0.13 mmol), glacial acetic acid (0.1 mmol), cyclohexane (1.5 mL), ionic liquid (0.01 mmol)

^BGC-MS yield.

6.4 Conclusion

In conclusion, a novel bis-core dicationic TMDP salt containing a sulfate counterion was synthesized, and its chemical structure was elucidated by FT-IR, 1D and 2D NMR, and mass analyses. Some physical properties and thermal behavior and thermal stability of the new IL were recorded and investigated. The structure elucidation showed that the IL is a diprotic acid like sulfuric acid, which can be used as a safe alternative of sulfuric acid. The catalytic activity of $[\text{TMDPH}_2]^{2+}[\text{SO}_4]^{2-}$ was employed to promote the esterification process under mild conditions. A simple experimental and sustainable procedure, high yield of the desired product, simple workup, and reusability of catalyst are some of the merits of the current protocol. Another superiority of the new method is avoiding and reducing heavy metal and corrosive waste generation. Further research is being conducted in our group to investigate new applications of TMDP and sulfuric acid at a ratio of 1:1 and 1:2 with promising results.

CHAPTER SEVEN

ARTICLE 5

ARENE DIAZONIUM SACCHARIN INTERMEDIATES: A GREENER AND COST-EFFECTIVE ALTERNATIVE METHOD FOR THE PREPARATION OF ARYL IODIDE**7.1 Introduction**

In the course of our research regarding the synthesis of aromatic iodides through the Sandmeyer reaction or its alternatives. We required an efficient, low cost, and sustainable method for accessing relative stable arene diazonium salts. The most arene diazonium salt are often prepared in situ due to their instability and explosive risk. It is clear that the anion nature influence in situ generation of the arene diazonium salts (Khaligh et al, 2017), and facilitated the preparation of aryl iodides. The preparation of relative stable benzenediazonium tetrafluoroborates was reported in ethanol using HBF_4 and isoamyl nitrite (Beckwith et al, 1987). Most of the reported chemicals and reagents are expensive, toxic, non-biodegradable, unrecoverable, and metal-containing, so we looked for a cheap, nontoxic, recoverable, biodegradable, and biocompatible reagent that show high efficiency under mild conditions.

In the continuation of our previous work and application of saccharin (Khaligh et al, 2018), we encouraged to investigate the potential of saccharin for the synthesis of aryl iodides through in situ formation the arene diazonium saccharin salts which to the best of our knowledge has not been presented to date. According to the current strategy, aryl iodides are formed from diazotization of in situ generated arene diazonium salt which are in turn formed from aniline derivatives and *tert*-butyl nitrite (TBN) in the presence of saccharin. The intermediates are not isolated and purified in the current protocol which

lead to minimizing the solvent waste, and energy efficiency is enhanced by the reaction performance at room temperature and shorter reaction times.

7.2 Methodology

7.2.1 Material and Method

The analytical grade chemicals were provided from Merck, Sigma Aldrich, and Fluka Chemical Companies. The chemicals were used without further purification. Products were characterized by their physical constants such as melting point and ^1H NMR spectrum. The purity determination of the substrates and reaction monitoring were accompanied by TLC using silica gel SIL G/UV 254 plates of colour test of azo coupling with 2-naphthol. The ^1H NMR spectra and melting points were recorded with Bruker Avance 400 MHz instrument and Buchi B-545 apparatus in open capillary tubes, respectively.

7.2.2 Typical procedure for the synthesis of aryl iodide

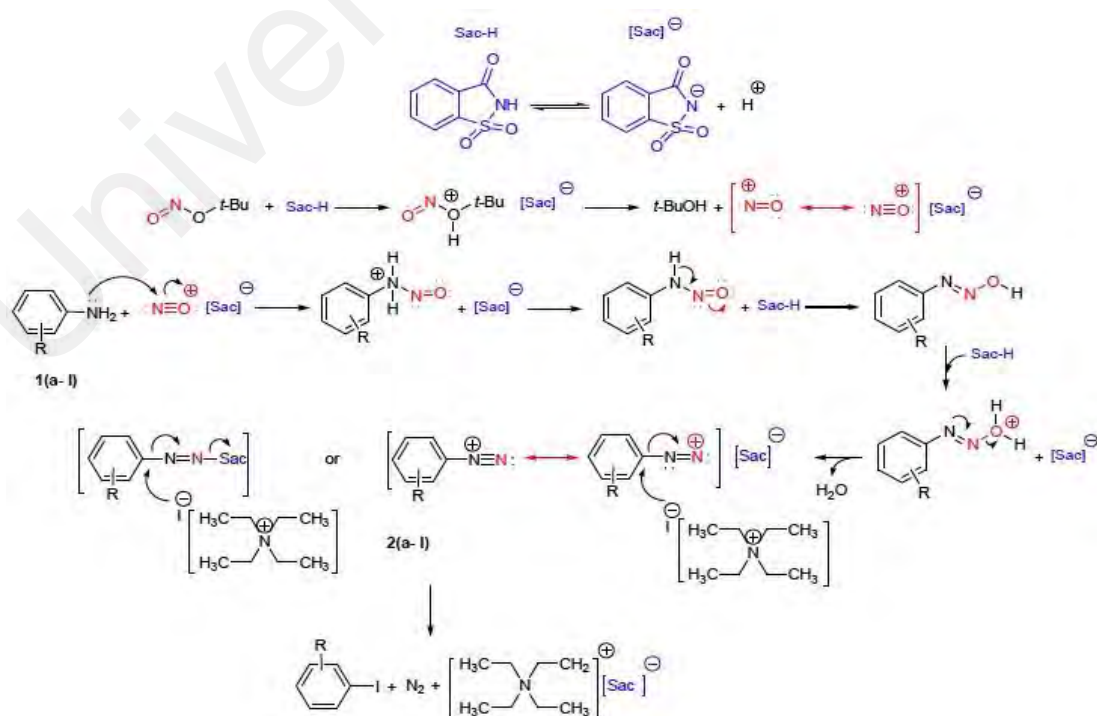


Figure 7.1: The proposed mechanisms for the preparation of aryl iodides using TBN and saccharine.

To a stirring mixture of glacial acetic acid (0.12 mL, 2.1 mmol) and TBN (0.30 mL, -2.3 mmol) in ethanol (10 mL), Sac-H(0.37g, 2.0 mmol) was slowly added at low temperature (an ice bath). After 5 min, aniline derivative 1(a-1) (2.0 mmol) was added dropwise over 5 minutes into the mixture. The solvent, *t*-BuOH, and residue TBN were removed under reduced pressure after consuming of aniline derivatives (monitored by a color test of azo coupling with 2-naphtanol). Then, 5 mL of 4.0 M TEAI solution was added into stirring as-obtained intermediate 2(a-1) in one portion at low temperature. After confirmation of substrate consumption by a negative test of azo coupling with 2-naphthol, the boiling was added to the reaction mixture (15 mL) and the aqueous layer was separated. The organic layer was washed with eq. 10% sodium sulphite (3 x 5 mL), then dried over Na₂SO₄, filtered, and dried under reduced pressure in a rotary evaporator. The purification was conducted by flash chromatography with n-hexane-EtOAc (9:1, v/v) as eluent.

The recovery of reagents was conducted by adding the concentrated hydrochloric acid into the aqueous layer, and the water evaporated under reduced pressure. Then, the residue was extracted 5 times with EtOAc (5 mL), and the collected extracts were dried over anhydrous Na₂SO₄ and filtrated. The evaporation of solvent afforded Sac-H in 72% yield. The tetraethylammonium chloride (TEAC) was isolated in a yield of 0.25 g from the residue of the above procedure (68%). The melting points and FTIR spectra of recovered saccharin and TEAC were identical to the authentic compound (sigma Aldrich $\geq 98\%$).

Table 7.1. Some reported reagents and methods for the diazotization-iodination of 2-nitro aniline 1k.^a

No.	mmol of aryl	Nitrating agent	Reagents	conditions	Time (min)	Yield (%)	Ref.
1	2	TBN (2.3 mmol)	TFSI-H (2 mmol) HOAc (2.1 mmol) TEAI (2.0 mmol)	EtOH:H ₂ O (1:1)/0-5 °C	110	82	Khali gh
2	10	IPN (11 mmol)	<i>o</i> -BDSI (12 mmol) glacial AcOH (60 mL) TBAI (10 mmol)	Two steps: Step 1: 0-5 °C; Step 2: CH ₃ CN/r.t. °C	45	92	Yu
3	2	NaNO ₂ (5 mmol)	<i>p</i> -TsOH (6 mmol) KI (5 mmol)	Water-paste form	20-30	72	Serjeant
4	2	NaNO ₂ (4 mmol)	sulfonated-resin (5 g) KI (5 mmol)	H ₂ O/r.t.	90	71	Larsen
5	5.25	resin-NO ₂ (5.25 mmol)	<i>p</i> -TsOH (5.25 mmol) glacial AcOH (8 mL) KI (13.125 mmol)	Two steps: Step 1: H ₂ O/r.t.; Step 2: H ₂ O/r.t.	30	34	Weihrauch
6	2	Resin-NO ₂ (6 mmol)	<i>p</i> -TsOH (6 mmol) KI (5 mmol)	H ₂ O/r.t.	90	91	Jakopin
7	5	KNO ₂ (20 mmol)	HI (20 mmol)	DMSO/35 °C	15	89	Whitehead
8	3	NaNO ₂ (6 mmol)	<i>p</i> -TsOH (9 mmol) KI (7.5 mmol)	MeCN/10-20 °C	50	81	Rode

9	1	NaNO ₂ (2.5 mmol)	[H-NMP]HSO ₄ (4 mmol) NaI (2.5 mmol)	Solvent-free/r.t.	20–30	85	Baik
10	2	NaNO ₂ (4 mmol)	Wet CSA (1.5 g) KI (5 mmol)	Solvent-free/r.t.	12	82	Krasnokutskaya
11	1	[P4-VP]NO ₂ (0.54 g)	H ₂ SO ₄ (2 mmol) KI (2.5 mmol)	Two steps: Step 1: 0–5 °C; Step 2: r.t. or 60 °C	100	74	Hajipour
12	10	IPN (30 mmol)	diiodomethane (10 mL)	80 °C	240	65	Nemati
13	2	TBN (2.3 mmol)	Sac-H (2 mmol) HOAc (2.1 mmol) TEAI (2.0 mmol)	EtOH:H ₂ O (1:1)/0-r.t. °C	120	78	This work

^aReaction conditions: TBN (0.30 mL, 2.3 mmol), aniline derivatives 1(a-1) (2.0 mmol), glacial acetic acid (0.12 mL, 2.1 mmol), Sac-H (0.37 g, 2.0 mmol), TEAI (0.52 g, 2.0 mmol), solvent (H₂O/EtOH 1:1 v/v, mL); total reaction time (2 h).

Physical and ¹H NMR spectrum data of 4-methoxybenzenediazonium saccharine (2b): ¹H NMR (400 MHz, DMSO-*d*₆) δ 8.41-8.48 (m, 1H), 8.32-8.39 (m, 2H, ArH), 7.87-7.94 (m, 1H, ArH), 7.29 (d, J = 8.8 Hz, 2H, ArH), 7.03 (d, J = 8.8 Hz, 2H, ArH), 3.80 (s, 3H, OCH₃) ppm [6].

Spectra data of the aryl iodides 3a-3l [6].

iodobenzene (3a): ^1H NMR (400 MHz, CDCl_3) δ 7.75 (d, $J = 8.2$ Hz, 2H, ArH), 7.34 (t, $J = 7.2$ Hz, 1H, ArH), 7.13 (t, $J = 7.2$ Hz, 2H, ArH) ppm; ^{13}C NMR (100 MHz, CDCl_3) δ 137.7, 130.4, 127.8, 95.0 ppm; EI-MS: M^+ m/z 204.

1-iodo-4-methoxybenzene (3b): ^1H NMR (400 MHz, CDCl_3) δ 7.56 (d, $J = 8.2$ Hz, 2H, ArH), 6.65 (t, $J = 8.2$ Hz, 1H, ArH), 3.76 (s, 3H, OCH_3) ppm; ^{13}C NMR (100 MHz, CDCl_3) δ 159.6, 138.4, 116.5, 82.8, 55.5 ppm; EI-MS: M^+ m/z 234.

1-iodo-4-methylbenzene (3c): ^1H NMR (400 MHz, CDCl_3) δ 7.59 (d, $J = 8.2$ Hz, 2H, ArH), 6.94 (t, $J = 8.2$ Hz, 2H, ArH), 2.32 (s, 3H, CH_3) ppm; ^{13}C NMR (100 MHz, CDCl_3) δ 136.9, 136.5, 131.4, 91.2, 21.1 ppm; EI-MS: M^+ m/z 218.

1,3-dimethyl-2-iodobenzene (3d): ^1H NMR (400 MHz, CDCl_3) δ 7.20-6.92 (m, 3H, ArH), 2.42 (s, 6H, 2 x CH_3) ppm; ^{13}C NMR (100 MHz, CDCl_3) δ 141.7, 126.4, 126.2, 123.3, 21.8 ppm; EI-MS: M^+ m/z 232.

1,3-diethyl-2-iodobenzene (3e): ^1H NMR (400 MHz, CDCl_3) δ 7.21 (t, $J = 8.0$ Hz, 1H, ArH), 7.06 (d, $J = 8.0$ Hz, 2H, ArH), 2.81 (q, $J = 7.0$ Hz, 4H, 2 x CH_2), 1.23 (t, $J = 7.0$ Hz, 6H, 2 x CH_3) ppm; ^{13}C NMR (100 MHz, CDCl_3) δ 147.3, 128.1, 125.9, 107.2, 35.5, 14.7 ppm; EI-MS: M^+ m/z 260.

1,3-diisopropyl-2-iodobenzene (3f): ^1H NMR (400 MHz, CDCl_3) δ 7.23 (t, $J = 8.0$ Hz, 1H, ArH), 7.05 (d, $J = 8.0$ Hz, 2H, ArH), 3.39 (sept, $J = 7.0$ Hz, 2H, 2 x CH), 1.23 (d, $J = 7.0$ Hz, 12H, 4 x CH_3) ppm; ^{13}C NMR (100 MHz, CDCl_3) δ 151.0, 128.3, 123.8, 109.2, 39.4, 23.4 ppm; EI-MS: M^+ m/z 288.

1-chlorol-4-iodobenzene (3g): ^1H NMR (400 MHz, CDCl_3) δ 7.59 (d, $J = 8.2$ Hz, 2H, ArH), 7.40 (d, $J = 8.2$ Hz, 2H, ArH), ^{13}C NMR (100 MHz, CDCl_3) δ 138.0, 133.8, 130.4, 91.2 ppm; EI-MS: M^+ m/z 238.0.

1-chlorol-2-iodobenzene (3h): ^1H NMR (400 MHz, CDCl_3) δ 7.82 (d, $J = 7.8$ Hz, 1H, ArH), 7.44 (d, $J = 7.8$ Hz, 1H, ArH), 7.28 (t, $J = 7.2$ Hz, 1H, ArH), 6.97 (t, $J = 7.8$ Hz, 1H, ArH) ppm; ^{13}C NMR (100 MHz, CDCl_3) δ 141.1, 138.8, 129.6, 128.0, 98.6 ppm; EI-MS: M^+ m/z 238.0.

1-bromo-4-iodobenzene (3i): ^1H NMR (400 MHz, CDCl_3) δ 7.53 (d, $J = 8.2$ Hz, 2H, ArH), 7.20 (d, $J = 8.2$ Hz, 2H, ArH) ppm; ^{13}C NMR (100 MHz, CDCl_3) δ 139.1, 133.4, 122.0, 92.2 ppm; EI-MS: M^+ m/z 238.0.

1-iodo-4-nitrobenzene (3j): ^1H NMR (400 MHz, CDCl_3) δ 7.97 (d, $J = 8.2$ Hz, 2H, ArH), 7.89 (d, $J = 8.2$ Hz, 2H, ArH) ppm; ^{13}C NMR (100 MHz, CDCl_3) δ 147.6, 138.8, 125.2, 102.8 ppm; EI-MS: M^+ m/z 294.

1-iodo-2-nitrobenzene (3k): ^1H NMR (400 MHz, CDCl_3) δ 7.91 (d, $J = 7.8$ Hz, 1H, ArH), 7.84 (d, $J = 8.2$ Hz, 1H, ArH), 7.49 (t, $J = 7.8$ Hz, 1H, ArH), 7.30 (t, $J = 8.2$ Hz, 1H, ArH) ppm; ^{13}C NMR (100 MHz, CDCl_3) δ 153.1, 142.0, 133.5, 129.2, 125.5, 86.3 ppm; EI-MS: M^+ m/z 249.

4-(4-iodophenyl)morpholine (3l): ^1H NMR (400 MHz, CDCl_3) δ 7.56 (d, $J = 9.0$ Hz, 2H, ArH), 6.70 (d, $J = 9.0$ Hz, 2H, ArH), 3.88-3.83 (m, 4H, 2 x $\text{CH}_2(\text{eq})$), 3.13-3.09 (m, 4H, 2 x $\text{CH}_2(\text{ex})$) ppm; ^{13}C NMR (100 MHz, CDCl_3) δ 151.0, 138.0, 177.8, 81.9, 66.9, 50.2 ppm; EI-MS: M^+ m/z 289.

Caution! The arene diazonium salts are known potentially explosive in the dry state, thus, they must be cautiously stored and handled in the laboratories. Avoid unnecessary heating and mechanical impact, especially when working on a large scale.

7.3 Results and Discussion

TBN and tetraethylammonium iodide (TEAI) were preferred as a nitrating agent and iodide precursors due to their unique properties like safe handling, metal-free, inexpensive, and commercial availability (Khaligh et al, 2018).

Based on our previous work (Khaligh et al, 2019), the glacial acetic acid and TBN together with Sac-H were slowly stirred in ethanol at low temperature (an ice bath). After 5 minutes, aniline 1a was slowly added at the same temperature. After completion of the first step (monitoring by a color test of azo coupling with 2-naphthol), the generated *t*-BuOH and unreacted TBN were removed under vacuum by rotary evaporator. Then, the TEAI solution was added into the stirring intermediate 2a at one time and final product 3a was purified by the flash chromatography (Figure 7.2).

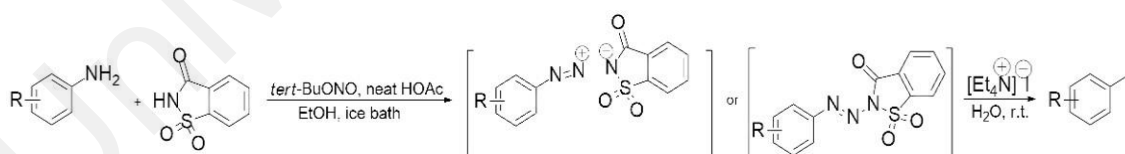


Figure 7.2. Preparation of aryl iodides using TBN = saccharine, and TEAI.

The scope and generality of current methodology was evaluated through transformation of a variety of aniline derivatives into the corresponding iodides using the current protocol. The aryl iodides bearing electron-donating and electron-withdrawing groups were obtained from the corresponding anilines in good to excellent yield (Table

7.2). However, the steric hindered anilines viz. 2,6-dimethylaniline, 2,6-diethylaniline, and 2,6-diisopropylaniline 3(d-f) were isolated in 67%, 40%, 42% yields, respectively as expected (Table 7.2, entry 4-6). All known products showed an identical melting point and NMR spectra to those in the literature (Khaligh et al, 2019).

Table 7.2. Synthesis of aryl iodides through in situ formation of the arene diaonium saccharin intermediates.^a

Entry	Ar-NH ₂ 1(a-l)	Product	Yield (%) ^b	Melting point (°C)	
				Found	Reported [4]
1	C ₆ H ₅ -	3a	80	Oil	Oil
2	4-CH ₃ O-C ₆ H ₄ -	3b	72	50–51	52–54
3	4-CH ₃ -C ₆ H ₄ -	3c	78	Oil	Oil
4	2,6-(CH ₃) ₂ -C ₆ H ₃ -	3d	67	Oil	Oil
5	2,6-(CH ₃ CH ₂) ₂ -C ₆ H ₃ -	3e	40	Oil	Oil
6	2,6-[(CH ₃) ₂ CH] ₂ -C ₆ H ₃ -	3f	42	Oil	Oil
7	4-Cl-C ₆ H ₄ -	3g	79	54–55	55–56
8	2-Cl-C ₆ H ₄ -	3h	77	Oil	Oil
9	4-Br-C ₆ H ₄ -	3i	80	88–90	87–88
10	4-NO ₂ -C ₆ H ₄ -	3j	82	168–169	170–172
11	2-NO ₂ -C ₆ H ₄ -	3k	78	51–52	51–53
12	4-morpholinoaniline (4-(4-Morpholinyl)aniline)	3l	70	158–159	159–161

^aReaction conditions: TBN (0.30 mL, 2.3 mmol), aniline derivatives **1(a-l)** (2.0 mmol), glacial acetic acid (0.12 mL, 2.1 mmol), Sac-H (0.37 g, 2.0 mmol), TEAI (0.52 g, 2.0 mmol), solvent (H₂O/EtOH 1:1 v/v, mL); total reaction time (2 h).

^bIsolated yield.

¹H NMR spectra copies of the aryl iodides (400 MHz, CDCl₃)

Caution! The arene diazonium salts are known potentially explosive in the dry state, thus, they must be cautiously stored and handled in the laboratories. Avoid unnecessary heating and mechanical impact, especially when working on a large scale (Figure A.42 – A.53)

Complete or partial recovering of the catalyst and reagents are very important in the industrial processes due to minimizing the waste, as well as lower raw material, energy, and waste disposal cost. According to the reported procedure in the literature (Khaligh et al, 2018), the saccharin and tetraethylammonium chloride (TEAC) could be recovered in the range of 77%-72% and 68%-64% yield, respectively.

The possible reaction of aniline and saccharin was investigated by a control experiment under optimal conditions. No 3-amino-1, 2-benzisothiazole-1, 1-dioxide were detected by LC-MS analysis.

Another experiment was performed to study the stability of the arene diazonium intermediate. After the first step, the intermediate 2a can be isolated by removing the excess TBN and *t*-BuOH under vacuum and stored in refrigerator (4°C). After four days, the stored arene diazonium 2a was treated with a TEAI solution which afforded iodobenzene (3a) in a 74% yield.

A proposed mechanism is illustrated in Figure 7.1. Saccharin and *tert*-butyl nitrite generated the nitroso ($^+N=O \leftrightarrow N\equiv O^+$) in the first step, which can act as a mild electrophile. The reaction of nitroso and arylamine will form arene diazonium saccharinate $[ArN_2]^+ [Sac]^-$ salt or Ar-N=N-Sac adduct will participate in an electrophilic

substitution reaction with TEAI, which finally affords the corresponding aryl iodides. Our group is working to investigate the detailed processes of reaction mechanism based on 2 routes A.

A large scale of the current protocol was also conducted for 1.9 g of 1a under optimal conditions, which afforded 3.12 g of 3a (ca.75%). Table 9.1 showed some the reported methods and their conditions for the preparation of 2-nitro-1-iodobenzene 2k. the previously reported method have their own merits and limitations, for example, the use of metal-containing nitrites and iodide (Table 7.1 entries 1, 3-11) low yield and slow rate (Table 7.1, entries 5, 12), 2 steps performance (Table 7.1, entries 2, 5), use of expensive reagent or strong acids (Table 7.1, entries 1, 9-11), generation of waste for the preparation of nitrating reagent (Table 7.1, entries 5, 11), tedious workup (Table 7.1, entries 12), the performance of toxic and hazard by-products, and incomplete conversions (Table 7.1, entries 5, 7, 11). *o*-BDSI: *o*-benzenedisulfonimide, CSA: cellulose sulphuric acid, NMP: N-methyl-2-pyrrolidone, P4-VP: poly(4-vinylpyridine), IPN: *i*-pentyl nitrite, Sac-H: Saccharin, *p*-SSA: silica sulphuric acid, TBAI: tetrabutyl ammonium iodide, TsOH: *p*-toluenesulfonic acid, TFSI-H: bis(trifluoromethylsulfonyl) imide.

7.4 Conclusion

In summary, a telescopic reaction developed for the synthesis of aryl iodides in the presence of TBN, Sac-H, glacial acetic acid, and TEAI. The arene diazonium intermediates could be stored for relatively long periods with little reduce of activity. The current methodology is safe, cost-effective, broad substrate scope, and metal-free. All used reagents are commercially available and inert to moisture and air. Also, the saccharine and tetraethylammonium cation were easily isolated from the reaction mixture which reduces the cost and waste of the current protocol.

CHAPTER EIGHT

CONCLUSION

In conclusion, a novel bis-core dicationic TMDP salt containing a sulfate counterion was synthesized, and its chemical structure was elucidated by FTIR, ID, and 2D NMR, and mass analyses. Some physical properties and thermal behavior and thermal stability of the new IL were recorded and investigated. The structure elucidation showed that the new IL is a diprotic acid like sulfuric acid, which can be used as a safe alternative to sulfuric acid.

The chemical structure of novel bis-core dicationic TMDP salt-containing chlorosulfonate counterion was elucidated by 1D and 2D and COSY analysis. Further supports of the corrected structure were obtained by the detailed FTIR and Raman analysis. The lowest bands in the Raman spectrum of new ionic liquid were found at 440 and 193 cm^{-1} , which are assigned to S-Cl stretch and wag, respectively. Our results showed that the nucleophilic attack of the nitrogen atom of the piperidine rings of TMDP to the central atom of chlorosulfonic acid seems unlikely due to more steric hindrance of the sulfur atom by chlorine and oxygen atoms.; thus, the TMDP and chlorosulfonic acid participate in an acid-base reaction to form $[\text{TMDPH}_2]^{2+}2[\text{ClSO}_3]^-$. Furthermore, $[\text{TMDPH}_2]^{2+}2[\text{ClSO}_3]^-$ was employed to promote the one-pot three-component reaction under mild conditions, which afforded the desired products in 73-94% isolated yield within 120-150 min. the current work approved the dual solvent-catalyst efficiency of $[\text{TMDPH}_2]^{2+}2[\text{ClSO}_3]^-$ as a recyclable ionic liquid. Furthermore, the current protocol has the advantages such as simple experimental and sustainable procedure, high yield of the desired products within short reaction times at room temperature; avoid the use of toxic and volatile organic solvent, simple workup, and recyclability of ionic liquid which all

as-mentioned merits will cause to minimize the generation of heavy metal and corrosive waste.

A novel mono-core dicationic salt-containing chlorosulfonate counterion was prepared in a pure solid and liquid state and its structure was characterized by 1D and 2D NMR, Mass spectra. The physical properties such as density and viscosity and pH of the aqueous solution of new ionic liquid were determined. The correct structure was elucidated by COSY analysis, which was supported by Raman study. The FTIR and Raman spectra of pure liquid and solid state of 1*H*,4*H*-piperazine-dium dichlorosulfonate were studied and our assignments for IR and Raman peaks were compared with previous reports in the literature for chlorosulfonate anion. The lowest band in Raman spectrum of $[\text{PZH}_2]^{2+}2[\text{ClSO}_3]^-$ solid- or liquid-state was found at 418 cm^{-1} frequency which is assigned to S-Cl stretch. The band S-Cl wag is depolarized and was weakly observed at 206 and 203 cm^{-1} frequencies in Raman spectra of both solid- and liquid-state of 1*H*,4*H*-piperazine-dium dichlorosulfonate. A combination of the S-Cl stretch and the S-Cl wag was attributed to 675 cm^{-1} frequency in FTIR. Furthermore, The dual-solvent-catalyst efficiency of $[\text{PZH}_2]^{2+}2[\text{ClSO}_3]^-$ was demonstrated to promote a one-pot three-component reaction under mild conditions.

The catalytic activity of $[\text{TMDPH}_2]^{2+}[\text{SO}_4]^{2-}$ was employed to promote the esterification process under mild conditions. A simple experimental and sustainable procedure, high yield of the desired product, simple workup, and reusability of catalyst are some of merits of the current protocol. Another superiority of the new method is avoiding and reducing heavy metal and corrosive waste generation. A new application of $[\text{TMDPH}_2]^{2+}[\text{SO}_4]^{2-}$ was demonstrated to promote a one-pot three-component reaction as a) a dual solvent-catalyst in its liquid state and b) a catalyst in a mixture of green solvents.

The pyrano[2,3-*d*]pyrimidinones were isolated in high to excellent yields. The advantages of the current methodologies are (a) safe and greener conditions, (b) simple separation of catalyst or solvent/catalyst and desired products, (c) minimize the hazardous waste generation and (d) high recyclability of organocatalyst. The unique features of [TMDPH₂]²⁺[SO₄]²⁻, such as commercially available, wide liquid range, bearing Lewis base sites and hydrogen bond acceptor-donor groups, safe handling, and storage make it a promising organocatalyst for organic synthesis. Furthermore, the [TMDPH₂]²⁺[SO₄]²⁻ can be a safe alternative for toxic, flammable, and volatile organic base catalysts.

A telescopic reaction is developed for the synthesis of aryl iodides in the presence of TBN, Sac-H, glacial acetic acid, and TEAI. The arene diazonium intermediates could be stored for relatively long periods with little reduction activity. The current methodology is safe, cost-effective, broad substrate scope, and metal-free. All used reagents are commercially available and inert to moisture and air. Also, the saccharine and tetraethylammonium cation could be partially recovered from the reaction residue, which reduces waste generation, energy consumption, raw material and waste disposal costs.

REFERENCES

- Abd El-Aleam, R. H., George, R. F., Hassan, G. S., & Abdel-Rahman, H. M. (2019). Synthesis of 1,2,4-triazolo[1,5-a]pyrimidine derivatives: antimicrobial activity, dna gyrase inhibition and molecular docking. *Bioorganic Chemistry*, 103411. doi:10.1016/j.bioorg.2019.103411
- Akbarzadeh, O., Khaligh, N. G., Johan, M. R. (2020). Novel zwitterionic and ionic structure of imidazolium propane sulfonate salts on basis of NMR analysis. *Journal of Molecular Structure*. 1202, 127335. doi: 10.1016/j.molstruc.2019.127335.
- Baik, W., Luan, W., Lee, H. J., Yoon, C. H., Koo, S., & Kim, B. H. (2005). Efficient one-pot transformation of aminoarenes to haloarenes using halodimethylsulfonium halides generated in situ. *Canadian Journal of Chemistry*, 83(3), 213–219. doi:10.1139/v05-026
- Baker, J. K., & Myers, C. W. (1991). *Pharmaceutical Research*, 08(6), 763–770. doi:10.1023/a:1015810303089
- Ball, P. (2015). Catalysis: facing the future. *National Science Review*. 2(2), 202-204. doi: 10.1093/nsr/nwv022.
- Beckwith, A. L. J., & Meijs, G. F. (1987). Iododediazoniating of arenediazonium salts accompanied by aryl radical ring closure. *The Journal of Organic Chemistry*, 52(10), 1922–1930. doi:10.1021/jo00386a007
- Belhocine, T., Forsyth, S. A., Gunaratne, H. Q. N., Nieuwenhuyzen, M., Nockemann, P., Puga, A. V., ... Whiston, K. (2015). 3-Methylpiperidinium ionic liquids. *Physical Chemistry Chemical Physics*, 17(16), 10398–10416. doi:10.1039/c4cp05936k
- Chiappe, C., Rajamani, S., & D'Andrea, F. (2013). A dramatic effect of the ionic liquid structure in esterification reactions in protic ionic media. *Green Chemistry*, 15(1), 137–143. doi:10.1039/c2gc35941c
- Cosmas, S., Ekpo, D. E., Asomadu, R. O., Assor, J. O., Nnamani, V. I., Durojaye, O. A. (2018). Review on structure-activity relationship (SAR) using antimalarial drug design as a Case Study. *International Journal of Scientific & Engineering Research*, 9(6), ISSN 2229-5518, 1743-1752.
- Chen, Q., Zhu, X.-L., Jiang, L.-L., Liu, Z.-M., & Yang, G.-F. (2008). Synthesis, antifungal activity and CoMFA analysis of novel 1,2,4-triazolo[1,5-a]pyrimidine derivatives. *European Journal of Medicinal Chemistry*, 43(3), 595–603. doi:10.1016/j.ejmech.2007.04.021
- Dorosz, U., Barteczko, N., Latos, P., Erfurt, K., Pankalla, E., Chrobok, A. (2019). Highly efficient biphasic system for the synthesis of alkyl lactates in the presence of acidic ionic liquids. *Catalysts*, 10(1), 37. doi: 10.3390/CATAL10010037.
- Erben, M. F., Della Védova, C. O., Boese, R., Willner, H., Leibold, C., & Oberhammer, H. (2003). Trifluoromethyl chlorosulfonate, cf₃oso₂cl: gas phase and crystal structure,

- conformation and vibrational analysis studied by experimental and theoretical methods. *Inorganic Chemistry*, 42(22), 7297–7303. doi:10.1021/ic034531a
- Ertl, G. (2009). Wilhelm ostwald: founder of physical chemistry and nobel laureate 1909. *Angewandte Chemmie International Edition*, 48(36), 6600–6606. doi:10.1002/anie.200901193.
- Esteban-Parra, G. M., Méndez-Arriaga, J. M., Rodríguez-Diéguez, A., Quirós, M., Salas, J. M., & Sánchez-Moreno, M. (2019). High antiparasitic activity of silver complexes of 5,7-dimethyl-1,2,4-triazolo[1,5-a]pyrimidine. *Journal of Inorganic Biochemistry*, 110810. doi:10.1016/j.jinorgbio.2019.110810
- Fisches, G. (2007). Recent progress in 1,2,4-triazolo[1,5-a]pyrimidine chemistry. *Advanced Heterocyclic Chemistry*, 95, 143-219. doi: 10.1016/s0065-2725(07)95003-5.
- Fizer, M., & Slivka, M. (2016). Synthesis of [1,2,4]triazolo[1,5-a]pyrimidine (microreview). *Chemistry of Heterocyclic Compounds*, 52(3), 155–157. doi:10.1007/s10593-016-1851-5.
- Gillespie, R. J., & Robinson, E. A. (1962). The raman spectra of sulphuric, deuteriosulphuric, fluorosulphuric, chlorosulphuric, and methanesulphonic acids and their anions. *Canadian Journal of Chemistry*, 40(4), 644–657. doi:10.1139/v62-100
- Guan, R., Zou, H., Lu, D., Gong, C., & Liu, Y. (2005). Polyethersulfone sulfonated by chlorosulfonic acid and its membrane characteristics. *European Polymer Journal*, 41(7), 1554–1560. doi:10.1016/j.eurpolymj.2005.01.018
- Hallett, J. P., & Welton, T. (2011). Room-temperature ionic liquids: solvents for synthesis and catalysis. *Chemical Reviews*, 111(5), 3508–3576. doi:10.1021/cr1003248
- Hernández Fernández, F. J., Pérez de los Ríos, A., Quesada-Medina, J., & Sánchez-Segado, S. (2015). Ionic liquids as extractor agents and reaction media in ester synthesis. *ChemBioEng Reviews*, 2(1), 44–53. doi:10.1002/cben.201400019
- Heacock, R. A., & Marion, L. (1956). The infrared spectra of secondary amines and their salts. *Canadian Journal of Chemistry*, 34(12), 1782–1795. doi:10.1139/v56-231
- Huang, B., Li, C., Chen, W., Liu, T., Yu, M., Fu, L., ... Liu, X. (2015). Fused heterocycles bearing bridgehead nitrogen as potent hiv-1 nrtis. Part 3: optimization of [1,2,4]triazolo[1,5-a]pyrimidine core via structure-based and physicochemical property-driven approaches. *European Journal of Medicinal Chemistry*, 92, 754–765. doi:10.1016/j.ejmech.2015.01.042
- Janosik, T., Shirani, H., Wahlström, N., Malky, I., Stensland, B., & Bergman, J. (2006). Efficient sulfonation of 1-phenylsulfonyl-1H-pyrroles and 1-phenylsulfonyl-1H-indoles using chlorosulfonic acid in acetonitrile. *Tetrahedron*, 62(8), 1699–1707. doi:10.1016/j.tet.2005.11.062
- Jakopin, Z., & Dolenc, M. (2010). Advances in the chemistry of saccharins: from synthetic novelties towards biologically active compounds. *Current Medicinal Chemistry*, 17(7), 651–671. doi:10.2174/092986710790416236

- Kartika, T., Shimizu, N., & Yoshimura, T. (2015). Identification of esters as novel aggregation pheromone components produced by the male powder-post beetle, *lyctus africanus* lesne (coleoptera: lyctinae). *PLOS ONE*, 10(11), 0141799. doi:10.1371/journal.pone.0141799
- Keogh, J., Tiwari, M. S., Manyar, H. (2019). Esterification of glyserol with acetic acid using nitrogen-based bronsted-acidic ionic liquid. *Ind. Eng. Chem.*, 58, 17235-17243. doi: 10.1021/acs.iecr.9b01223
- Kerru, N., Gummidi, L., Maddila, S. N., Bhaskaruni, S. V. H. S., & Jonnalagadda, S. B. (2020). Bi 2 O 3 /FAp, a sustainable catalyst for synthesis of dihydro-[1,2,4]triazolo[1,5-a]pyrimidine derivatives through green strategy. *Applied Organometallic Chemistry*. doi:10.1002/aoc.5590
- Khaligh, N. G., Mihankhah, T., & Rafie Johan, M. (2019). 4,4'-trimethylenedipiperidine (tmdp): an efficient organocatalyst for the mechanosynthesis of pyrano[4,3-b]pyrans under solid-state conditions. *Polycyclic Aromatic Compounds*, 1–10. doi:10.1080/10406638.2018.1564679
- Khaligh, N. G., Chong, K. F., Mihankhah, T., Titinchi, S., Johan, M. R., & Ching, J. J. (2018). An efficient synthesis of pyrrolidinone derivatives in the presence of 1,1'-butylenebis(3-sulfo-3h-imidazol-1-ium) chloride. *Australian Journal of Chemistry*. doi:10.1071/ch18246
- Khaligh, N. G., Ling, O. C., Mihankhah, T., Johan, M. R., Ching, J. J. (2019). Mechanosynthesis of n-methyl imines using recyclable imidazole-based acid-scavenger: in situ formed ionic liquid as catalyst and dehydrating agent. *Australian Journal of Chemistry*, 72, 194-199. doi: 10.1071/CH18408.
- Khaligh, N. G., Johan, M. R., Ching, J. J. (2019). Saccharin: a cheap and mild acidic agent for the synthesis of azo dyes via telescoped dediazotization. *Green Process Synthesis*, 8, 24-29. doi: 10.1515/gps-2017-0133.
- Khaligh, N. G., Mihankhah, T., Johan, M. R. (2019). One-pot synthesis of coumarins using 1,1'-butylenebis (3-sulfo-3h-imidazol-1-ium) chloride as an efficient task-specific ionic liquid. *Polycyclic Aromatic Compounds*, 1-10. doi: 10.1080/10406638.2019.1695215.
- Khaligh, N. G. (2018). A facile and sustainable protocol to the preparation of aryl iodides using stable arenediazonium bis(trifluoromethylsulfonyl) imide salts via the telescopic process. *Heteroatom Chemistry*, 29(2), 2-7, e21418. doi: 10.1002/hc.21418.
- Khaligh, N. G., Mihankhah, T., Johan, M. R. (2019). Synthesis of new low-viscous sulfonic acid-functionalized ionic liquid and its application as a bronsted liquid acid catalyst for the one-pot mechanosynthesis of 4H-pyans through the ball milling process. *Journal of Molecular Liquids*, 277, 794-804. doi: 10.1016/j.molliq.2019.01.024.
- Khaligh, N. G. (2018). Synthesis and characterization of novel binuclear task-specific ionic liquid: an efficient and sustainable sulfonic-functionalized ionic liquid for one-pot synthesis of xanthenes. *Research on Chemical Intermediates*, 44(7), 4045-4062. doi: 10.1007/s11164-018-3354-8.

- Khaligh, N. G., Mihankhah, T., Johan, M. R., Titinchi, S. J. J. (2019). Microwave-assisted synthesis of pyrrolidinone derivatives using 1,1'-butylenebis(3-sulfo-3H-imidazol-1-ium) chloride in ethylene glycol. *Green Process Synthesis*, 8, 373-383. doi: 10.1515/gps-2019-0004.
- Khaligh, N. G., Teng, L. S., Ling, O. C., Johan, M. R., Ching, J. J. (2019). 4-imidazole-1-yl-butane-1-sulfonic acid or a novel liquid salt? The nmr analysis and dual solvent-catalytic efficiency for one-pot synthesis of xanthenes. *Journal Molecular Liquid*, 278, 19-32. doi: 10.1016/j.molliq.2019.01.041.
- Khaligh, N. G., Chong, K. F., Mihankhah, T., Titinchi, S., T., Johan, M. R., Ching, J. J. (2018). Efficient synthesis of pyrrolidinone derivatives in the presence of 1,1'-butylenebis(3-sulfo-3h-imidazol-1-ium) chloride. *Australian Journal Chemistry*, 71, 566-572. doi: 10.1071/CH18246.
- Khaligh, N. G. (2017). Telescopic synthesis of azo compounds via stable arenediazonium bis(trifluoromethane)sulfonimide salts by using tert -butyl nitrite. *Dyes and Pigments*, 139, 556–560. doi:10.1016/j.dyepig.2016.11.058
- Khaligh, N. G., Mihankhah, T., Johan, M. R. (2019). Green one-pot multicomponent synthesis of pyrrolidinones using planetary ball milling process under solvent-free conditions. *Synthesis Communication*, 49, 1-9. doi: 10.1080/00397911.2019.1601225.
- Khaligh, N. G., Johan, M. R., & Ching, J. J. (2018). Saccharin and tert-butyl nitrite: cheap and efficient reagents for the synthesis of 1,2,3-benzotriazine-4-(3h)-ones from 2-aminobenzamides under metal-free conditions. *Australian Journal of Chemistry*, 71(3), 186. doi:10.1071/ch17590
- Khaligh, N. G., Mihankhah, T., Johan, M. R., & Ching, J. J. (2018). Saccharin: an efficient organocatalyst for the one-pot synthesis of 4-amidocinnolines under metal and halogen-free conditions. *Monatshefte Für Chemie - Chemical Monthly*, 149(6), 1083–1087. doi:10.1007/s00706-018-2174-2
- Kotharkar, S. A., Bahekar, S. S., & Shinde, D. B. (2006). Chlorosulfonic acid-catalysed one-pot synthesis of coumarin. *Mendeleev Communications*, 16(4), 241–242. doi:10.1070/mc2006v016n04abeh002256
- Krasnokutskaya, E., Semenischeva, N., Filimonov, V., & Knochel, P. (2007). A new, one-step, effective protocol for the iodination of aromatic and heterocyclic compounds via aprotic diazotization of amines. *Synthesis*, 2007(1), 81–84. doi:10.1055/s-2006-958936
- Larsen, J. C. (2012). Artificial sweeteners. *Nutrafoods*, 11(1), 3–9. doi:10.1007/s13749-012-0003-5
- Laube, T. (2004). X-ray crystal structures of a benzonorbornenyl cation and of a protonated benzonorbornenol. *Journal of the American Chemical Society*, 126(35), 10904–10912. doi:10.1021/ja040115t
- Liew, S. K., Malagobadan, S., Arshad, N. M., Nagoor, N. H. (2020). A review of the structure activity relationship of natural and synthetic antimetastatic compounds. *Biomolecules*. 10(1), 138. doi: 10.3390/biom10010138.

- Linares-Palomino, P. J., Salido, S., Altarejos, J., & Sánchez, A. (2003). Chlorosulfonic acid as a convenient electrophilic olefin cyclization agent. *Tetrahedron Letters*, 44(35), 6651–6655. doi:10.1016/s0040-4039(03)01635-6
- Malherbe, R. R. (2019). Heterogeneous catalysis in zeolites and related materials. *Inglomayor. Section A Volume 16*, 51 of 71. ISSN 0719 7578.
- Luna, O., Gomez, J., Cárdenas, C., Albericio, F., Marshall, S., & Guzmán, F. (2016). Deprotection reagents in fmoc solid phase peptide synthesis: moving away from piperidine. *Molecules*, 21(11), 1542. doi:10.3390/molecules21111542
- Malkar, R. S., Yadav, G. D. (2020). Development of green and clean processes for perfumes and flavors using heterogeneous chemical catalysis. *Current Catalysis*. 9, 32-58. doi: 10.2174/2211544708666190613163523.
- Matuszek, K., Chrobok, A., Coleman, F., Seddon, K. R., & Swadźba-Kwaśny, M. (2014). Tailoring ionic liquid catalysts: structure, acidity and catalytic activity of protonic ionic liquids based on anionic clusters, $[(\text{HSO}_4)(\text{H}_2\text{SO}_4)_x]^-$ ($x = 0, 1, \text{ or } 2$). *Green Chemistry*, 16(7), 3463–3471. doi:10.1039/c4gc00415a
- Mihankhah, T., Johan, M. R., Ching, J. J., Khaligh, N. G. (2019). 4-imidazole-1-yl-butane-1-sulfonic acid ionic liquid: synthesis, structural analysis, physical properties and catalytic application as dual solvent-catalyst. *Phosphorus, Sulfur, Silicon and the Related Elements*. 194, 866-878. doi: 10.1080/10426507.2018.1487426.
- Muhammad, U., Uzairu, A., Arthur, D. E. (2018). Review on: quantitative structure activity relationship (QSAR) modeling. *Analytical Pharmacy*, 7(2), 240-242. doi: 10.15406/japlr.2018.07.00232.
- Nageswara Rao, R., & Kumar Talluri, M. V. N. (2007). An overview of recent applications of inductively coupled plasma-mass spectrometry (ICP-MS) in determination of inorganic impurities in drugs and pharmaceuticals. *Journal of Pharmaceutical and Biomedical Analysis*, 43(1), 1–13. doi:10.1016/j.jpba.2006.07.004
- Nemati, F., & Elhampour, A. (2012). Green and efficient diazotization-iodination of aryl amines using cellulose sulfuric acid as a biodegradable and recyclable proton source under solvent-free condition. *Scientia Iranica*, 19(6), 1594–1596. doi:10.1016/j.scient.2012.10.015
- Oukoloff, K., Lucero, B., Francisco, K. R., Brunden, K. R., & Ballatore, C. (2019). 1,2,4-Triazolo[1,5-a]pyrimidines in drug design. *European Journal of Medicinal Chemistry*. doi:10.1016/j.ejmech.2019.01.027
- Paul, R., Paul, K., & Malhotra, K. (1969). Nature of the complexes of tellurium tetrachloride. *Australian Journal of Chemistry*, 22(4), 847. doi:10.1071/ch9690847
- Prasad, K. N., Kumar, B., Yan, X.-D., Hanson, A. J., & Cole, W. C. (2003). A-tocopheryl succinate, the most effective form of vitamin e for adjuvant cancer treatment: a review. *Journal of the American College of Nutrition*, 22(2), 108–117. doi:10.1080/07315724.2003.10719283

- Przypis, M., Matuszek, K., Chrobok, A., Swadźba-Kwaśny, M., & Gillner, D. (2020). Inexpensive and tuneable protic ionic liquids based on sulfuric acid for the biphasic synthesis of alkyl levulinates. *Journal of Molecular Liquids*, 113166. doi:10.1016/j.molliq.2020.113166
- Qureshi, Z., Deshmukh, K., Jagtap, S., Nandurkar, N., & Bhanage, B. (2009). Ultrasound assisted regioselective sulfonation of aromatic compounds with sulfuric acid. *Ultrasonics Sonochemistry*, 16(3), 308–311. doi:10.1016/j.ultsonch.2008.10.001
- Rad-Moghadam, K., Hassani, S. A. R. M., & Roudsari, S. T. (2016). N-methyl-2-pyrrolidonium chlorosulfonate: An efficient ionic-liquid catalyst and mild sulfonating agent for one-pot synthesis of δ -sultones. *Journal of Molecular Liquids*, 218, 275–280. doi:10.1016/j.molliq.2016.02.082
- Roduner, E. (2014). Understanding Catalysis. *Chemical Society Review*, 43(24), 8226–8239. doi: 10.1039/c4cs00210e.
- Rode, H. B., Sprang, T., Besch, A., Loose, J., & Otto, H.-H. (2006). Pseudosaccharin amine derivatives: synthesis and elastase inhibitory activity. *ChemInform*, 37(5). doi:10.1002/chin.200605119
- Siddiqui, M. A., Khan, A., Zaka, M. (2016). A review of structure activity relationship of amiodarone and its derivatives. *Medicinal Chemistry*, 6, 37-42. doi: 10.4236/ojmc.2016.62003.
- Stufkens, D. J., & Gerding, H. (2010). The assignment of the vibrational frequencies of the SO_3Cl^- Ion. *Recueil Des Travaux Chimiques Des Pays-Bas*, 89(4), 417–422. doi:10.1002/recl.19700890412
- Steger, E., Ciurea, I. C., & Fadini, A. (1967). Das infrarotspektrum von natriumchlorosulfat und die kraftkonstanten der ionen $[\text{SO}_3\text{Cl}]^-$, $[\text{SO}_3\text{F}]^-$ and $[\text{SO}_3\text{S}]^{2-}$. *Zeitschrift für anorganische und allgemeine chemie*, 350(5-6), 225–230. doi:10.1002/zaac.19673500502
- Tanaka, K., & Toda, F. (2000). Solvent-free organic synthesis. *Chemical Reviews*, 100(3), 1025–1074. doi:10.1021/cr940089p
- Torres, P., Reyes-Duarte, D., López-Cortés, N., Ferrer, M., Ballesteros, A., & Plou, F. J. (2008). Acetylation of vitamin E by *Candida antarctica* lipase B immobilized on different carriers. *Process Biochemistry*, 43(2), 145–153. doi:10.1016/j.procbio.2007.11.008
- Valdés, H., Eleno, M. A. G., Gonzalez, D. C., Morales, D. (2019). Recent advances in catalysis with transition metal pincer compounds. *Chemical Catalysis Chemistry*, doi: 10.1002/cctc.201702019.
- Waddington, T. C., & Klanberg, F. (1960). 467. The infrared spectra of some new compounds of boron trifluoride, boron trichloride, and sulphur trioxide. *Journal of the Chemical Society (Resumed)*, 2339. doi:10.1039/jr9600002339
- Wang, H., Lee, M., Peng, Z., Blázquez, B., Lastochkin, E., Kumarasiri, M., ... Mobashery, S. (2015). Synthesis and evaluation of 1,2,4-triazolo[1,5-a]pyrimidines as

antibacterial agents against enterococcus faecium. *Journal of Medicinal Chemistry*, 58(10), 4194–4203. doi:10.1021/jm501831g

Weihrauch, M. R., & Diehl, V. (2004). Artificial sweeteners—do they bear a carcinogenic risk. *Annals of Oncology*, 15(10), 1460–1465. doi:10.1093/annonc/mdh256

Wenda, S., Illner, S., Mell, A., & Kragl, U. (2011). Industrial biotechnology—the future of green chemistry. *Green Chemistry*, 13(11), 3007. doi:10.1039/c1gc15579b

WHITEHEAD, C. W., & TRAVERSO, J. J. (1960). The reaction of saccharin with amines. N-substituted-3-amino-1,2-benzisothiazole-1,1-dioxides. *The Journal of Organic Chemistry*, 25(3), 413–416. doi:10.1021/jo01073a027

Yadav, G. D., & Murkute, A. D. (2004). Preparation of a novel catalyst UDCaT-5: enhancement in activity of acid-treated zirconia-effect of treatment with chlorosulfonic acid vis-à-vis sulfuric acid. *Journal of Catalysis*, 224(1), 218–223. doi:10.1016/j.jcat.2004.02.021

Yang, F., Yu, L.-Z., Diao, P.-C., Jian, X.-E., Zhou, M.-F., Jiang, C.-S., ... Zhao, P.-L. (2019). Novel [1,2,4]triazolo[1,5-a]pyrimidine derivatives as potent antitubulin agents: design, multicomponent synthesis and antiproliferative activities. *Bioorganic Chemistry*, 103260. doi:10.1016/j.bioorg.2019.103260

Yu, S.-B., & Watson, A. D. (1999). Metal-based x-ray contrast media. *Chemical Reviews*, 99(9), 2353–2378. doi:10.1021/cr980441p

Zaijun, L. (2016). Recent development in green synthesis. *Synth. Catal.*, 1, 1-2.

Zhang, Y., Wong, W.-T., & Yung, K.-F. (2014). Biodiesel production via esterification of oleic acid catalyzed by chlorosulfonic acid modified zirconia. *Applied Energy*, 116, 191–198. doi:10.1016/j.apenergy.2013.11.044

Zhang, N., Ayril-Kaloustian, S., Nguyen, T., Afragola, J., Hernandez, R., Lucas, J., ... Beyer, C. (2007). Synthesis and SAR of [1,2,4]triazolo[1,5-a]pyrimidines, a class of anticancer agents with a unique mechanism of tubulin inhibition. *Journal of Medicinal Chemistry*, 50(2), 319–327. doi:10.1021/jm060717i

LIST OF PUBLICATION

1. Zaharani, L., Gorjian, H., Johan, M. R., Khaligh, N. G. (2021). Synthesis and characterization of two new molten acid salts: Safe and greener alternatives to sulfuric acid for the hydrolytic conversion of 1,1,1,3-tetrachloro-3-phenylpropane to cinnamic acid. *Journal of Molecular Structure*, 1245. doi: 10.1016/j.molstruc.2021.130977.
2. Zaharani, L., Shahnavaaz, Z., Johan, M. R., Khaligh, N. G. (2021). Synthesis, characterization, and a study of the influence of $[\text{HSO}_4]^-$ and $[\text{SO}_4]^{2-}$ on thermal phase transition and thermal stability of two new organic acid salts containing dication cyclic amine. *Journal of Molecular Liquid*, 336. 116856. doi: 10.1016/j.molliq.2021.116856.
3. Zaharani, L., Khaligh, N. G., Johan, M. R., Gorjian, H. (2021). Synthesis and characterization of a new acid molten salt and the study of its thermal behavior and catalytic activity in Fischer esterification. *New Journal of Chemistry*, 45, 7081-7088. doi: 10.1039/D0NJ06273A (ISI-Indexed)
4. Zaharani, L., Khaligh, N. G., Gorjian, H., Johan, M. R. (2021). 4,4'-trimethylenedipiperidine as a nitrogen heterocycle solvents or/and catalyst: liquid phase tandem Knoevenagel-Michael condensation. *Turkish Journal of Chemistry*, 45(1), 261-268. doi: 10.3906/kim-2010-41 (ISI-Indexed)
5. Zaharani, L., Khaligh, N. G., Johan, M. R. (2021). Synthesis, structure elucidation, vibrational and thermal behavior study of new one-core dication molten-salt. *Journal of Molecular Structure*, 1235, 130-134. doi:10.1016/j.molstruc.2021.130134 (ISI-Indexed)
6. Zaharani, L., Khaligh, N. G., Mihankhah, T., Johan, M. R., Hamizi, N. A. (2020). Facile and green synthesis of a series of dihydro-[1,2,4]triazolo[1,5-a]pyrimidine scaffolds. *Canadian Journal of Chemistry*, 98(10), 1-5. doi:10.1139/cjc-2020-0145 (ISI-Indexed)
7. Shahnavaaz, Z., Khaligh, N. G., Zaharani, L., Johan, M. R., Hamizi, N. A. (2020). The structure elucidation of new ionic liquid and its application for the synthesis of a series of novel triazolo[1,5-a]pyrimidine scaffolds. *Journal of Molecular Structure*, 1219, 128592, 1-7. doi: 10.1016/j.molstruc.2020.128592 (ISI-Indexed)
8. Zaharani, L., Khaligh, N. G., Mihankhah, T., Johan, M. R. (2020). Application of nitrogen-rich porous organic polymer for the solid-phase synthesis of 2-amino-4H-benzo[b]pyran scaffolds using ball milling process. *Molecular Diversity*. 25(1), 323-332. doi:10.1007/s11030-020-10092-4 (ISI-Indexed)
9. Zaharani, L., Khaligh, N. G., Taraneh Mihankhah, T., Shahnavaaz, Z., Johan, M. R. (2020). Synthesis of a series of novel dihydro-[1,2,4]triazolo[1,5-a]pyrimidine scaffolds: Dual solvent-catalyst activity of a low viscous and acid-functionalized ionic liquid. *Synthetic Communications*, 50(11), 1633-1640. doi: 10.1080/00397911.2020.1749281 (ISI-Indexed)

10. Zaharani, L., Khaligh, N. G., Shahnava, Z., Johan, M. R. (2020). The structure elucidation of new mono-core dicationic salt-containing chlorosulfonate counterion: raman study of a pure sample of chlorosulfonate anion in the solid and liquid state. *Journal of Molecular Structure*, 1216, 128182, 1-6. doi: 10.1016/j.molstruc.2020.128182 (ISI-Indexed)
11. Shahnava, Z., Zaharani, L., Johan, M. R., Khaligh, N. G., (2020). A green alternative for aryl iodide preparation from aromatic amines. *Current Organic Synthesis*, 17(2), 131-135. doi: 10.2174/1570179417666200203121437 (ISI-Indexed)
12. Zaharani, L., Khaligh, N. G., Shahnava, Z., Johan, M. R. (2020). Arene diazonium saccharin intermediates: a greener and cost-effective alternative method for the preparation of aryl iodide. *Turkish Journal of Chemistry*, 44(2020) 535-542. doi:10.3906/kim-2002-26 (ISI-Indexed)
13. Zaharani, L., Khaligh, N. G., Mihankhah, T., Johan, M. R. (2020). 1H,4H-Piperazine-dium dichlorosulfonate: Structure elucidation and its dual solvent-catalyst activity for the synthesis of new dihydro-[1,2,4]triazolo[1,5-a]pyrimidine scaffolds. *Australian Journal of Chemistry*, 73(11), 1118-1124. doi:10.1071/CH20022 (ISI-Indexed)
14. Shahnava, Z., Zaharani, L., Khaligh, N. G., Mihankhah, T., Johan, M. R. (2020). Synthesis, Characterisation, and Determination of Physical Properties of New Two-Protonic Acid Ionic Liquid and its Catalytic Application in the Esterification. *Australian Journal of Chemistry*. 74(3), 165-172. doi: 10.1071/CH20153 (ISI-Indexed)
15. Khaligh, N. G., Mihankhah T., Shahnava, Z., Zaharani, L., Johan, M. R. (2020). Solar energy and TiO₂ nanotubes: Biodiesel production from waste cooking olive oil. *Environmental Progress & Sustainable Energy*, 40(2), e13537. doi: 10.1002/ep.13537 (ISI-Indexed)